NATIONAL AND KAPODISTRIAN UNIVERSITY OF ATHENS

School of Health Sciences

M.SC. IN NANOMEDICINE

Dissertation Thesis

Plasmonic photothermal therapy of oral squamous cell carcinoma using gold nanoparticles

Grigorios Loukas

s.n. 7450642100014

Supervisor

Prof. Efstathios P. Efstathopoulos

Athens, February 2023

“Everything is theoretically impossible until it is done.” –

Robert A. Heinlein

science fiction author, aeronautical engineer

with regards to my professors

Contents

CHAPTER 3 – Plasmonic Photothermal Therapy of Cancer using Gold nanoparticles

INTRODUCTION

Photothermal therapy (PTT) is a promising alternative treatment for cancer that utilizes the absorption of near-infrared (NIR) light by nanoparticles to generate heat and destroy cancer cells. One of the most common types of cancer affecting the oral cavity is squamous cell carcinoma (OSCC), which can be challenging to treat due to its proximity to vital structures such as the tongue and jawbone. In recent years, the use of gold nanoparticles (GNPs) in PTT for OSCC has emerged as a promising strategy due to their unique optical and thermal properties.

The use of GNPs in PTT for OSCC is based on their ability to absorb NIR light and convert it into heat, causing thermal damage to the cancer cells. GNPs are particularly attractive for this application due to their high stability, biocompatibility, and strong NIR absorption. In addition, GNPs can be functionalized with targeting moieties such as antibodies, peptides, or small molecules to selectively target cancer cells, improving the specificity and efficacy of PTT.

The use of GNPs in PTT for OSCC has shown promising results in preclinical studies, demonstrating high efficacy in killing cancer cells and reducing tumor size. Furthermore, the use of GNPs in PTT has been found to be well-tolerated with minimal side effects in animal models, making it a promising option for clinical translation.

Despite the promising results of preclinical studies, several challenges remain to be addressed in the development of GNP-based PTT for OSCC. One of the main challenges is the efficient and uniform distribution of GNPs within the tumor, which is essential for optimal efficacy. Another challenge is the need to minimize the uptake of GNPs by normal tissues, which can lead to unwanted side effects.

In this Diploma Essay for the Master in Nanomedicine of Kapodistrian University of Athens, Greece, there will be presented essential information to understand the mechanics and pathology of Oral Squamous Cell Carcinoma, the basis of Phototermal Treatment and resent studies on the subject will be analyzed to identify the current state of treatment and research about the use of PTT on OSCC.

In conclusion, the use of GNPs in PTT for OSCC holds great promise as a safe and effective alternative to traditional cancer therapies. Further studies are needed to optimize the delivery and efficacy of GNPs in PTT for OSCC and to translate these results to the clinic. With the rapid advancement in nanotechnology and the growing understanding of the underlying mechanisms of PTT, it is likely that GNP-based PTT will play an increasingly important role in the treatment of OSCC and other types of cancer in the future.

CHAPTER 1

The Oral Mucosa

It is mandatory for the better understanding of the mechanisms of carcinogenesis of oral cancer and the suggested treatments, to describe the histological anatomy of the main area of interest of this study which is the oral mucosa. The oral mucosa, also known as the mucous membrane, is a delicate and important structure that lines the inside of the mouth. It plays a crucial role in various oral functions such as speech, chewing, swallowing, and the sense of taste. The oral mucosa is also responsible for protecting the underlying structures of the mouth from physical, chemical, and biological insults. In this chapter, we will delve deeper into the anatomy and physiology of the oral mucosa and understand the various mechanisms that it uses to maintain oral health and prevent disease. We will also examine the different types of oral mucosal tissues and discuss the common conditions that affect this important structure. Ultimately, this chapter will provide a comprehensive overview of the oral mucosa and its significance in oral health and disease.

1.1 General Information

Oral mucosa is the mucous membrane that covers the structures inside the boundaries of the oral cavity. It is a moist soft tissue membrane that stretches from the palatopharyngeal folds to the vermilion border of the lips' labial mucosa junction in the front. (Brizuela et al, 2021) Histologically, the oral mucosa is composed of three layers. The first component is the oral epithelium, a surface squamous stratified epithelium whose thickness and degree of keratinization depend on the location and functional needs (Meyle et al,2019). Lamina propria, the underlying connective tissue, and submucosa, the deepest level of connective tissue, are both present beneath. In some areas of the oral cavity, where the lamina propria is firmly attached to bone or muscle, the latter is absent. (Wang et al, 2019)

The three types of oral mucosa, lining, masticatory and specialized, can be distinguished by their distinct histological, clinical, and functional characteristics. The oral mucosa develops a number of roles, but the primary ones are sensory function, which allows the detection of temperature, touch, pain, and taste, and protection of the underlying tissues from mechanical, chemical, and biological stimuli. Junctional epithelium (JE) is the specific part of the epithelium of oral mucosa that maintains the direct attachment to the tooth surface. The basal cells of the JE are attached to the connective tissue by the external basal lamina while the suprabasal cells are anchored to the tooth surface by an internal basal lamina that is produced by the JE. JE contains

fewer celljunctions as the oral gingival epithelium, but well developed gap junctions and some small adherens junctions can be detected (Garant, 2023). The JE has wide intercellular spaces, is highly permeable for water-soluble substances and serves as the primary pathway for the transmigration of polymorph nuclear leukocytes (Schroeder, 1997). JE does not exhibit phenotypic stratification, but the outermost cells appear elongated and align with their long axis parallel to tooth surface (Squier, 2001).

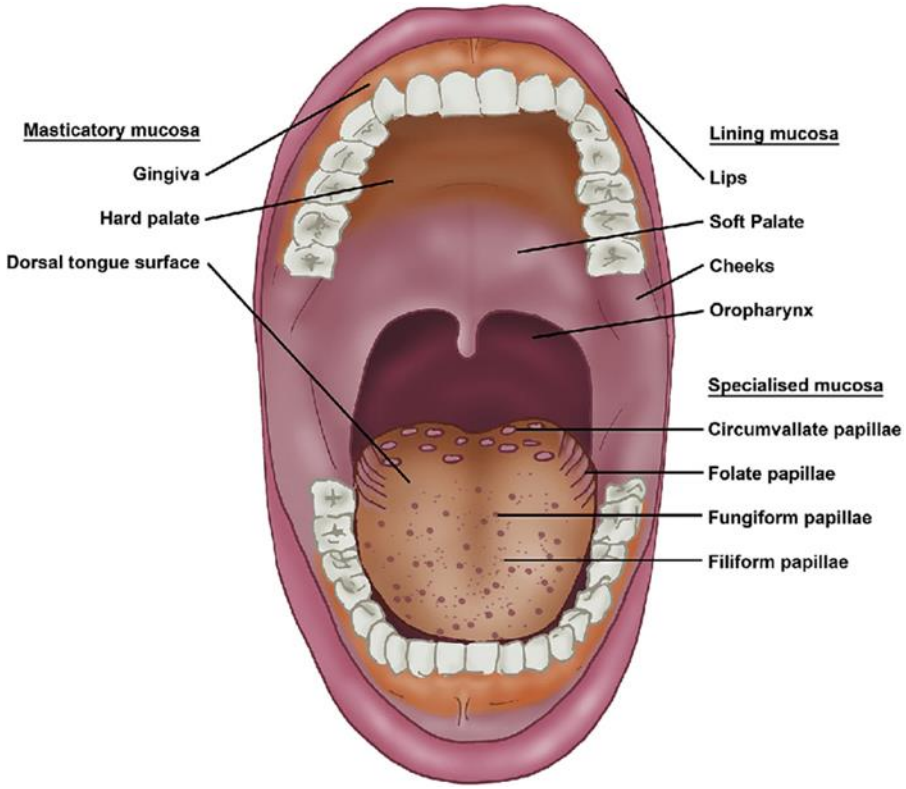

Figure 1. Lingual papillae and oral mucosa. The gingiva, hard palate, and dorsum of the tongue are all covered in keratinized masticatory mucosa. The rest of the mouth's surface, including the lips, cheeks, and soft palate, is covered by the non-keratinized lining mucosa. In the lingual papillae, the taste buds are covered by an unique mucosa that has nerve endings that allow for sensory awareness. The four types of lingual papillae are: Large, dome-shaped papillae called circumvallate papillae are found in the back of the tongue, and they are surrounded by a serous fluid made by nearby Von Ebner's glands; Taste buds are located in foliate papillae, folds on the sides of the tongue's back, which are covered in non-keratinized mucosa; fungiform papillae, which are coated in non-keratinized mucosa and include taste buds, are primarily found on the front of the tongue; The most common papillae type, filiform papillae are very small, keratinized, and cover the majority of the dorsal surface. They do not, however, possess taste buds. (Sarah et al., 2017)

1.2 Structural Description of Oral Mucosa

Oral Epithelium: The oral mucosa is entirely coated in squamous stratified epithelium. The thickness and level of keratinization of this highly structured, avascular, semipermeable tissue varies depending on where in the oral cavity it is located as well as the functional and mechanical needs of the region. The epithelium and lamina propria are connected by an interdigitated interface. The papillary

projections of the lamina propria, which are beneath the undulating rete pegs of the deeper layer of epithelium, serve as a point of attachment. A noncellular basement membrane separates these two tissues, to which the epithelium is firmly attached. The epithelium is supported by the basement membrane, which also connects it to the connective tissue. On light microscopy, it appears as a boundary between the lamina propria's connective tissue and epithelium. However, electron microscopy allows for a clearer observation of the basal lamina, which is further separated into lamina lucida and lamina densa. (Brizuela et al, 2021)

Three forms of oral mucosa that vary histologically, clinically, and functionally can be identified. The lining, also known as "moveable mucosa," refers to the mucosa that covers the soft palate, cheeks, lips, alveolar mucosa, the floor of the mouth, and the vestibular fornix. The lining mucosa is covered with a non-keratinized stratified squamous epithelium (Groeger et al, 2019). Masticatory mucosa refers to the inflexible mucosa that is firmly linked to the underlying bone in the associated gingiva and hard palate. A keratinized or para-keratinized stratified squamous epithelium, which covers these surfaces, gives the masticatory mucosa the ability to better withstand the stress that is placed on it during mastication. The dorsum of the tongue has a specific mucosa that displays a squamous stratified epithelium that can either be keratinized or not. (Otsuka-Tanaka, 2013) Its distinctive characteristic of possessing many kinds of lingual papillae and taste buds that enable taste perception gives it this name. This mucosa is occasionally referred to as masticatory mucosa since the dorsum of the tongue actively engages in mastication.

Squamous epithelial cells are known as keratinocytes since they are mostly composed of cytokeratins (Brizuela et al, 2021). In keratinized oral mucosa, such as the masticatory mucosa, the oral epithelium is composed of four layers. We discovered the stratum basale at the bottom, followed by the stratum spinosum, stratum granulosum, and stratum corneum. When the epithelium is nonkeratinized, such as in the lining mucosa there are stratum filamentosum and stratum distendum above the stratum basale (Groeger, 2019). Furthermore, the spinous layer is known to be generally thinner, and the non-keratinized epithelium, visible on the lining mucosa, lacks the granular layer (Pollanen et all, 2003). Desmosomes connect the cells that make up the epithelium, which gradually flatten from the stratum basale to the stratum corneum, where they take on a scaly or squamous look. Above the basement membrane, where hemidesmosomes attach them, the stratum basale has a layer of cuboidal or columnar cells. These cells are renowned for their propensity for mitosis. The stratum spinosum is made up of many layers of bigger cells that are known as prickle cells because of their morphology just above the stratum basale (Wang et al, 2019). Afterwards, the stratum granulosum forms; these cells have tiny cytoplasmatic keratohyalin granules that exhibit a strong hematoxylin stain. The stratum superficiale or stratum corneum, the last and most superficial layer, is keratinized and made up of very flat cells that lack nuclei and are stained pink by eosin (Adams, 1976).

Every 14 to 21 days, cell division frequently replaces the oral epithelial cells. This is due to the fact that the mouth cavity is constantly subjected to severe functional demands. The process of replenishment begins in the stratum basale, which

is primarily made up of mitotic cells that first go through a proliferation process before differentiating and migrating (Wang et al, 2019). The moveable mucosa is known to spin over more quickly than the masticatory one. Desquamation and differentiation at the surface, which balance cell division, are necessary for preserving the epithelium's homeostasis. A hyperplastic or atrophic epithelium may develop when the homeostasis is affected by causes like aging or pathological situations (Squier, 2006).

Other specialized cells, known as nonkeratinocyte cells, such as melanocytes, Langerhan cells, and Merkel cells, as well as keratinocytes, are permanently housed within the oral epithelium. Additionally, different inflammatory cells may momentarily move to the oral epithelium. (Barrett et al, 1994)

Melanocytes are elongated, melanin-producing dendritic cells that originate from the neural crest and migrate to the skin and oral mucosa, where they are found in the basal layer of the oral epithelium (Thomas et al, 2006). These cells include the proteins necessary for melanosome maturation and melanin synthesis. A measure of the melanocyte to the ratio of keratinocytes in the stratum basale of the oral epithelium is 1:10–1:15 (Yamaguchi et al, 2007). Although their exact role in the human body is unknown, melanocytes are known to produce the pigment melanin, which helps to determine the color of the skin, mucous membranes, hair, and eyes. Melanin shields these tissues from the damaging effects of UV light, reactive oxygen species, and free radicals found in the environment at the same time (Feller et al, 2014). The amount and intensity of oral pigmentations that are considered physiological increase with age because there are more oral melanocytes (Eisen, 2001). This increase may be brought on by a combination of melanogenic triggers, including smoking, medicines, repeated and mild functional injuries, and inflammatory diseases (Meleti et al, 2008).

Dendritic cells called Langerhans cells, which migrate to the oral epithelium and live in the stratum spinosum, are derived from bone marrow. Since they act as antigen-presenting cells by phagocytosing antigens in the epithelium and migrating to the underlying lamina propria, from where they can reach the local lymph nodes, they are crucial in the tissue's immune surveillance. The oral mucosa and the immune system are connected through Langerhans cells. (Brizuela et al, 2021)

The oral mucosa's stratum basale contains sensory touch receptors connected to a neural sensitive ending that are being slowly adapted by Merkel cells (Kingsmill et al, 2005). These receptors are mostly present in the epidermis. They are primarily found in the keratinized epithelium of the hard palate, maxillary and mandibular gingivae, and oral cavity.

Lamina propria: The layer of connective tissue known as the lamina propria is beneath the epithelium and is made up of blood vessels, nerves, fibroblasts, macrophages, mast cells, and inflammatory cells fibers, all of which are submerged in an amorphous substance made of proteoglycans and glycoproteins. The superficial papillary layer and the deeper reticular layer are the two divisions of the lamina propria. The papillary layer, which provides a larger surface area for nutrition delivery,

is made up of thin collagen fibers that are randomly oriented and create undulating papillae ridges that link with the epithelium (Chen et al, 2015). Although the basal collagen fibers gradually arrange to perpendicularly connect to the periosteum, the reticular layer is formed by thicker collagen fibers that orient parallel to the surface and lies between the papillary layer and the underlying structure (submucosa or periosteum depending on the region) (Tungare et al, 2021).

The fibroblast, which performs crucial tasks, is the main cell type in the lamina propria. It takes part in wound healing, where the number of fibroblasts rises, and the synthesis and replenishment of the connective fibers and the amorphous substance. Collagen and elastin are the two main fibers present in the connective tissue of the lamina propria, with collagen fiber types I and III constituting the majority. (Brizuela et al, 2021)

Submucosa: The submucosa, a layer of fibrocollagenous and elastic tissue containing blood vessels and nerves, lies beneath the lamina propria. The submucosa may contain adipose tissue, small salivary glands, lymphoid tissue, and muscle, depending on the region. Except for the connected gingiva and the hard palate covered by masticatory mucosa, where the submucosa layer is absent and the lamina propria is directly attached to the underlying bone, forming a mucoperiosteum, the submucosa is present in all parts of the buccal cavity. (Brizuela et al, 2021)

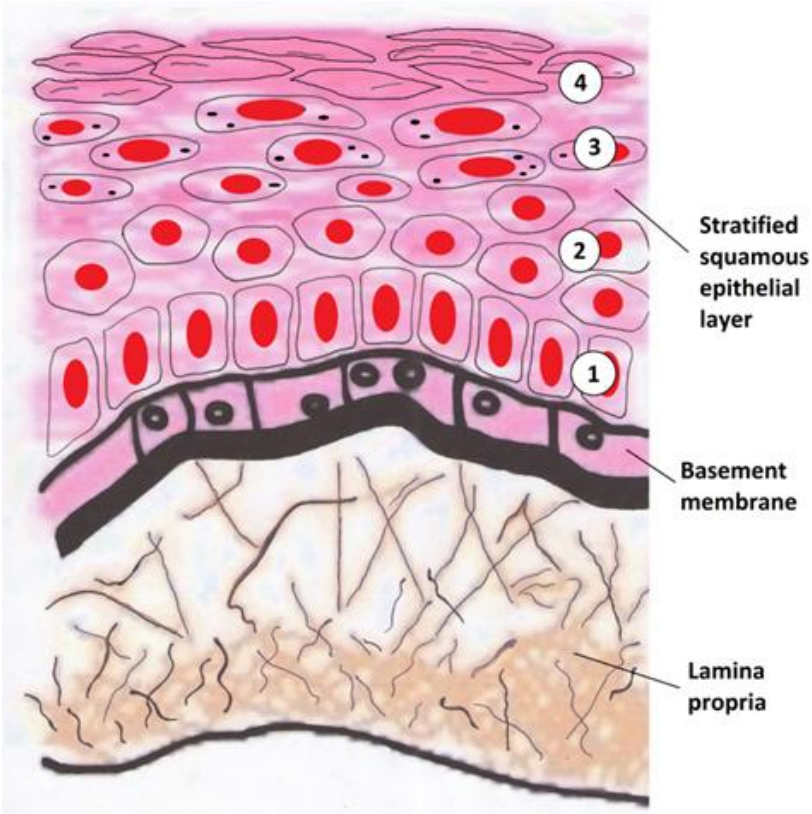

Figure 2 The layers of keratinized oral mucosa are depicted schematically as a series of deeper lamina propria layers with foundation membrane between them, as well as superficial layers of strafied squamous epithelium, from deepest to most superficial: 1: Basal stratum 2: Spinosum stratum 3: Granulosum stratum Fourth: Stratum corneum (Skrypnikova et al., 2022)

1.3 Function of Oral Epithelium

Protective Function: The mechanical, chemical, and biological stressors that come from our daily activities are a persistent threat to the mouth cavity. The oral mucosa is crucial in defending the underlying tissues against external antigens, harmful chemicals from the diet, and mechanical forces associated with mastication (stretching, compression, and abrasion from a hard diet). The gingival epithelium's keratinocytes operate as a barrier against bacterial invasion and infection (Presland et al, 2002). Numerous specialized transmembrane molecular complexes, including cell-cell junctions made up of tight junctions, adherens junctions, and gap junctions, connect them (Groeger et al, 2019). Additionally, carcinogenic chemicals prevalent in some regions' betel nut, cigarette, and alcohol consumption are also exposed to the oral mucosa. To protect against these physiological and pathological stressors, the oral epithelium serves as a barrier. (Wang, 2019).

Secretion: Saliva, which is released via the ducts of the major and minor salivary glands, is the principal material secreted by the oral mucosa. The submucosa includes the small, widely dispersed salivary glands in the oral cavity. Even so, the primary saliva-producing glands are situated outside the boundaries of the mouth mucosa. However, the fact that their excretory ducts extend into the mouth cavity helps to keep the tissue moist. (Wertz, 2018).

Sensory Function: The three branches of the trigeminal nerve supply sensory innervation to the oral cavity. The oral mucosa primarily contains three different sensory ending types: Merkel's disks, Meissner's corpuscles, and free nerve endings. These sensory ends enable the mouth mucosa to sense and react to the stimuli of temperature, touch, and pain. Additionally, it detects the flavors of salty, sweet, sour, bitter, and umami. However, a taste sensation for fat has recently been proposed (Brizuela et al, 2021). Orally, the soft palate and dorsum of the tongue contain taste receptor cells. These receptors are also found in the mucosa of the larynx, pharynx, and upper esophagus. The sensory function of the oral cavity is crucial for item recognition, regulating mastication activities, and triggering the reflex to swallow. The coordination of motions needed by the tongue, lips, and soft palate to properly emit sounds when speaking is made possible by the sensation of touch [Bearelly, 2017].

1.4 Tissue Preparation for Histological Examination

After being properly prepared, a biopsy sample of the oral mucosa can be examined under a microscope. Correct tissue preservation, dehydration, cleaning, paraffin infiltration, sectioning, and staining—most frequently with hematoxylin and eosin—are all possible procedures in the preparation of specimens (H&E). By using contrasting colors to stain the nucleus and cytoplasm, the H&E technique effectively distinguishes the various cellular components (Feldman, 2014).

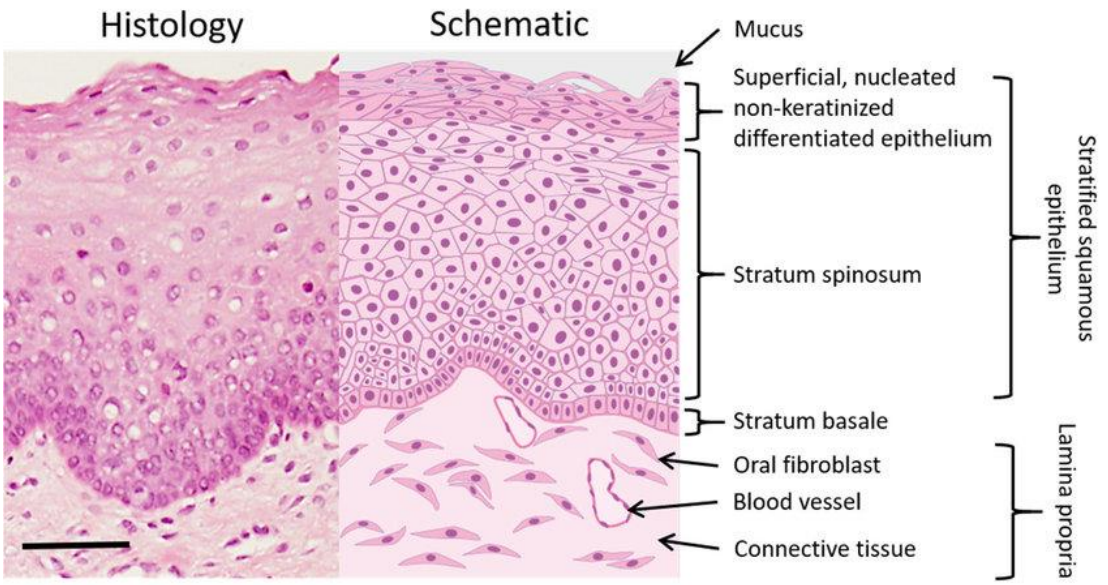

Figure 3 Buccal oral mucosa in a histology (left) and schematic (right) image. Scale bar: 100 millimeters (Edmans et al., 2020)

In conclusion, the oral mucosa plays a vital role in maintaining the overall health and function of the oral cavity. This complex tissue is responsible for a range of functions, including protecting the underlying structures from mechanical and chemical damage, as well as facilitating speech, mastication, and deglutition. The oral mucosa is also the site of many important physiological and pathological processes, including inflammation, wound healing, and the development of oral diseases such as oral cancer. Understanding the structure and function of the oral mucosa is crucial for maintaining oral health and diagnosing and treating oral diseases. Advances in technology have made it possible to explore the oral mucosa at a cellular and molecular level, leading to new insights into the mechanisms of oral disease and the development of more effective treatments. However, there is still much to be learned about the oral mucosa, including its interaction with the microbiome and the impact of systemic diseases on its structure and function. As research in this area continues, it is likely that new insights and therapies will emerge, leading to more effective and personalized treatments for a range of oral diseases.

CHAPTER 2

Oral Squamous Cell Carcinoma

One of the most known proverbs of Chinese general and philosopher Sun Tsu, in his timeless work "The Art of War" is "If you know the enemy, you need not fear the result of a hundred battles." Thus the study of the Squamous Cell Carcinoma of the Oral Cavity (OSCC), which is the target of the presented therapeutic approaches in this dissertation is essential. OSCC is a type of cancer that affects the cells lining the oral cavity, such as the lips, tongue, gums, and floor of the mouth. It is one of the most commonly diagnosed cancers in the world and is a serious public health concern. The development of OSCC is influenced by several risk factors, including tobacco and alcohol use, human papillomavirus (HPV) infection, and exposure to certain chemicals. Early detection and prompt treatment are crucial for improving patient outcomes, but despite advances in medical technology, the prognosis for patients with advanced OSCC remains poor. In this chapter, we will explore the epidemiology, etiology, pathogenesis, and clinical presentation and we will also discuss the current diagnostic and therapeutic approaches.

2.1 Description and General Information

Head and Neck Cancers constitute the category of malignancies that occur on the epithelium of the oral cavity, larynx, pharynx, salivary glands, nasal cavities and the paranasal sinuses. (Argiris et al, 2008) They are the sixth most common type of cancer worldwide. Of them, 40% appears in the oral cavity and nearly 90% of the oral malignant tumors are classified as Oral Squamous Cell Carcinoma (OSCC). (Rothenberg et al, 2012) As a result, Oral Cancer tends to be used interchangeably with OSCC. (Markopoulos, 2012)

According to 2018 statistics from the International Agency for Research on Cancer, over 350,000 cases of OSCC are diagnosed each year. (Almangush et al, 2020) Morbidity and mortality percentages have not improved significantly over the last 30 years (Markopoulos, 2012) and a mean of 170,000 deaths are caused by this type of cancer annually in the world (Chen et al, 2020) , raising the number even in 280,000 if indirect complications are to be taken under consideration. (Liao et al, 2019)

According to the National Cancer Institute of USA, in 2022, 54,000 new cases of Oral Cancer are being expected to be diagnosed in the States, consisting the 2.8% of all Cancer cases. The estimated deaths for the same year, are being calculated to be about 11,000 which is the 2% of all Cancer cases. In the last 30 years, the annual

number of new cases and the number of deaths every year caused by Oral Cancer, remain unaffected which means that neither Prevention programs for avoiding the causing factors (e.g. smoking) had any results nor the therapeutic approached have been improved delivering a more successful outcome. Unfortunately, most Oral Cancer cases are being diagnosed in later stages, about 50% when the Cancer has become regional, meaning that has spread to Regional Lymph Nodes or even worse, 17% of cases are being diagnosed when OSCC has already metastasized (Distant cases). Accordingly the 5 year survival rates drop to even 40% or less for the distant cases and become more disappointing when the area where the cancer appears is the tongue or the mouth floor. According to the same source, Oral Cancer is more common in non – Hispanic white males, in the ages 55-64, while the median age of diagnosis is 64 years. Death rates are higher among males, particularly those of African American descent. The death rate was 2.5 per 100,000 men and women per year based on 2015–2019 deaths. The median age of death was 68 years.

The anatomical structures that are being affected are the lips, tongue, upper and lower gingiva, alveolar mucosa mouth floor, palate, oropharynx and salivary glands. (Abdelaziz et al 2021). Of all these, tongue is the most common subsite and the one with the highest rates of mortality according to an analysis of Surveillance, Epidemiology and End Results (SEER) database. (Farhood et al, 2019) According to the same source, distant Oral Cancer of the Mouth floor in a male patient has the worst prognosis as the 5-Year Relative Survival Rates is only 21%.

Figure 1 Oral squamous cell carcinoma left lateral tongue. (Tsuruoka et al., 2011)

Smoking and Alcohol consumption are considered to be the main risk factors for OSCC development. Biologically, OSCC usually develops from premalignant dysplastic lesions. It occurs as a dysplasia of the squamous cells of the stratified oral epithelium that are keratinocytes. The tumor cells, can deeply invade the sub – epithelial local structures and finally lymph nodes of the neck, leading to further distant metastases. Another characteristic of the OSCC is the “field cancerization” which means that the aerodigestive tract of the patient is susceptible to premalignant

or malignant lesions. (Mohan et al, 2014) It has also a low degree of differentiation and a proclivity for lymph nodes metastasis. (Abdelaziz et al, 2021)

OSCC is usually diagnosed in advanced stages as a result of a wrong differential diagnosis from the attending clinician or ignorance or negligence from the patient. Abscission of the lesion with the neighboring structures, followed by chemotherapy or radiotherapy when is indicated by the stage of the cancer is the most common treatment approach. The life quality of the surviving patient depends on the size and spread of the diagnosed tumor and the followed and appropriate treatment. In some cases, huge parts of facial or jaw bones are being removed creating functioning and aesthetic issues. There also a high-risk disease recurrence. (Montero et al, 2015)

2.2 Risk Factors

The following factors are considered to be highly responsible for the development of the Oral Squamous Cell Carcinoma:

- Tobacco use
-Alcohol Use
- Nut use
- Viral Infections
- Oral Hygiene and Microbiota
- Gene Susceptibility
- Other risk factors

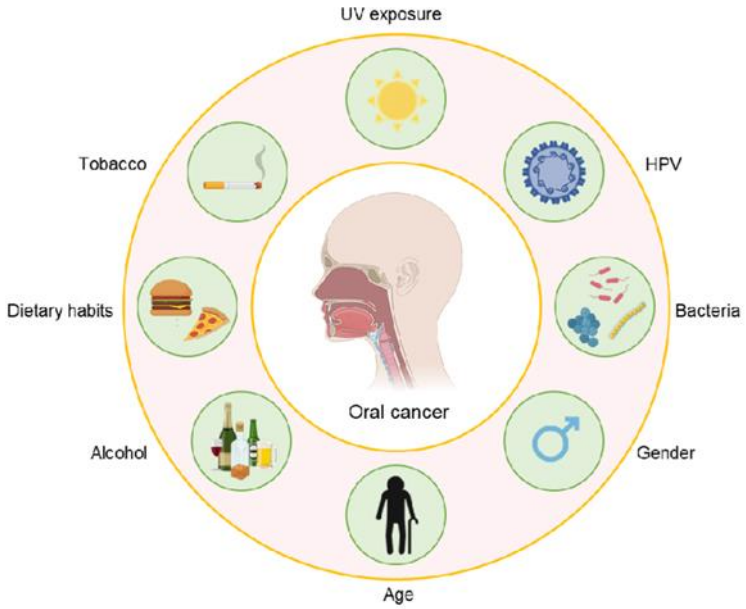

Figure 2 Oral cancer risk factors. (Goldoni et al., 2021)

Tobacco – Alcohol – Nut Use The greatest risk factors for OSCC development are the use of tobacco and alcohol whereas their action seems to be combined (Markopoulos, 2012)

Tobacco use is the greatest carcinogen as it contributes to tumor growth in various cancers. (Sasco et al, 2004) Tobacco smoke is a complex mixture of over 7,000 toxic chemicals, of which are known to induce critical gene mutations that lead in tumorigenesis (Warnakulasuriya et al, 2007). Smoking is associated with 75% of all oral cancer cases. Smokers have a six-fold risk of developing oral cancer compared to non-smokers (Markopoulos, 2012). Nicotine derived nitrosamine ketone is the basic tobacco smoke ingredient that can lead to oral malignant manifestations. (Lee et al, 2015)

Alcohol drinkers are also six times more likely to develop Oral cancer than non-drinkers (Markopoulos, 2012). Acetaldehyde which is the major metabolite of alcohol, is transformed by the enzyme alcohol dehydrogenase and then oxidized to acetate by aldehyde dehydrogenase. Acetaldehyde is a genotoxic substance that can induce DNA damage in mammalian cells (Stornetta et al, 2017). The combination of tobacco and alcohol use rises a fifteen-fold risk of developing oral cancer for users compared to non-users (Markopoulos, 2012).

Betel nut chewing is a common habit in various Asia regions (Chen et al, 2021). It is associated with significant increased risk of developing premalignant and malignant lesions on the oral mucosa, as it is observed in India and Taiwan (Hashim et al, 2019). Specifically in Taiwan, betel nut use has led to an incidence rate of 32.46 per 100,000 persons, which is the highest globally. Betel nut contains chemical components such as arecoline and arecaidine that can cause DNA damage that leads to OSCC formation (Li et al, 2019). Arecoline, as nitrosamine ketone, has been found to increase interleukin-1 expression in the oral mucosa of mice leading to increased cellular proliferation, oncogenic cytokine stimulation and finally malignant transformation (Chen et al, 2021).

Other similar risk factors are areca nuts, narcotics and cannabis that have been found to raise the possibility for OSCC formation. (Markopoulos, 2012)

Viral Infection There are many viruses that can induce carcinogenesis in humans. (Chen et al, 2014) A certain degree of the host cell DNA can be damaged as the viral proliferation process requires the breaking of both the viral and the host DNA leading to protein malfunctions and finally tumorigenesis. Another mechanism is that of the production of oncogenic proteins from the virus replication, that interfere with cell growth regulation (Chen et al, 2021).

The most known virus for causing carcinogenesis in humans is the Human Papilloma Virus (HPV). HPV is an epitheliotropic DNA virus, particularly for keratinocytes, that as we mentioned before are the starting cells of OSCC (Hübbers et al, 2015). The HPV serotypes HPVs 16,18,31,33,35,39 are associated with the development of premalignant and malignant lesions on the oral mucosa, with HPV 16 being the most commonly observed (Chen et al, 2021). The sites where HPV has been

detected the most are the oropharynx and tonsil. There are conflicting hypothesis about the carcinogenetic role of HPV since some research groups suggest that the virous is implicated in the initial stages of carcinogenesis while others propose that it has a short term role. It is believed that two viral proteins, E6 and E7 bind to p53 and retinoblastoma protein (pRb) a tumor suppressor protein respectively, causing their breakdown and inhibiting their function leading to tumorigenesis. HPV infection per se is currently believed that is not enough for malignant transformation of the keratinocytes unless they are exposed to chemical carcinogens such as benzopyrene (Jalouli et al, 2013). The effect of HPV vaccination on oral cancer prevention, although it has the potential to reduce the incidence of oral cancer, has yet to be established in major clinical trials (Ali et al, 2013).

Another virus, the Epstein-Bar Virus, has been hypothesized to have a yet unclear participation on OSCC pathogenesis. It has been proposed that the dominant oncoprotein of the latent phase (LMP-1) is expressed in oral epithelial malignant cells (Gonzalez-Molez et al, 2002).

In a Japanese study, Hepatitis C Virus infection was strongly associated with the development of OSCC (Nagao et al, 2009).

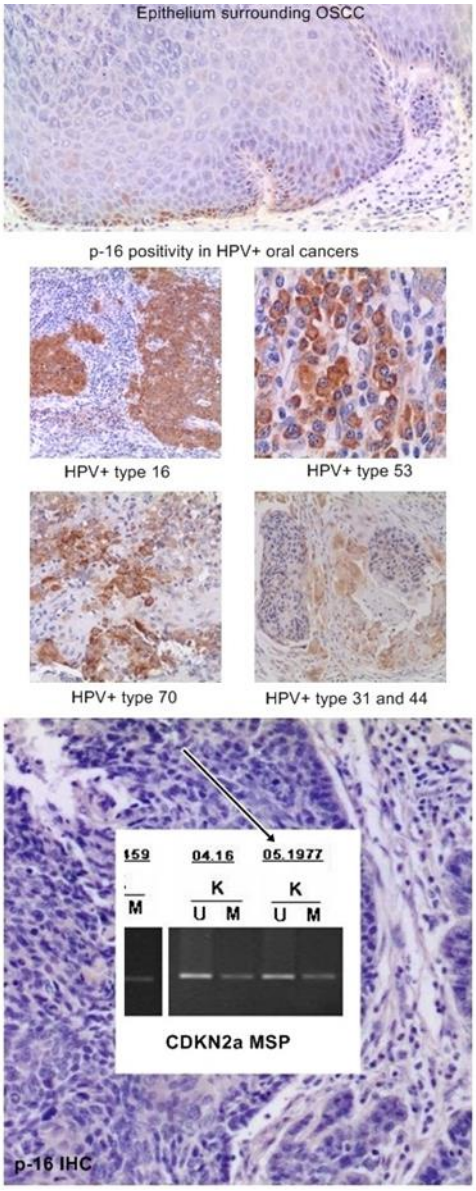

Figure 3 P16 protein is expressed by IHC in typical HPV-positive (DNA type 16) and HPV-negative OSCCs. P16 is overexpressed in OSCC but only at basal-parabasal levels in the epithelium surrounding it. The middle page's figure showed p16 expression in relation to several HR and LR-HPVs. The illustration at the bottom shows an OSCC that lacks p16 expression as a result of CDKN2a's promoter methylation. K stands for cancer samples; M for methylation CDKN2a; and U for unmethylated CDKN2a. (Chi et al., 2020)

Oral Hygiene and Microbiota Infrequent tooth brushing and dentist visits as also missing teeth are associated with oral cancer (Hashim et al, 2016). Poor oral hygiene may interfere with the control of resident microbiota inducing chronic inflammation of the mucosa. Inflammatory cytokines or chemokines produced in this process enable cell proliferation leading to oncogene activation and tumor angiogenesis (Karpinski, 2019). In this microbial imbalance, microorganisms can produce carcinogens, promote carcinogenesis by other

carcinogens or metabolize alcohol to acetaldehyde leading to DNA damage (Chen et al, 2021). Some of the carcinogens produced by oral microorganisms are reactive oxygen species (ROS), reactive nitrogen species, volatile sulfur compounds and organic acids. There also intracellular bacteria that by controlling cell cycle regulation can lead to carcinogenesis. Fusobacterium nucleatum, Porphyromonas gingivalis and Prevotella intermedia have been associated with OSCC (Hsiao et al, 2018). Another three periodontopathogenic bacteria species, Prevotella tannerae, F. nucleatum P. intermedia that were present in the saliva of people with poor oral hygiene, cigarette, alcohol and betel nut use, have been found in a report by Shang-Hung Chen et al. that are correlated with an increased risk of OSCC with patients with all these patients having 2.3 times higher risk for developing OSCC (Chen et al, 2021).

Gene Susceptibility Genetic variations may lead to disparate disease susceptibility among individuals as genetic variations like nucleotide polymorphism (SNP) may influence the transcription efficiency of genes as well as the functionality of the resulting proteins (Chen et al, 2021). Defects in the DNA damage repair network are associated with the induction of oral cancer. XRCC1 and XRCC2 participate in the repair of DNA single strand brake and the SNPs of these genes are related to higher risk for OSCC (Fan et al, 2019)

There are metabolite enzymes which role is to eliminate toxic chemicals in human body. Their malfunction can lead to cancer development. The metabolite enzymes are classified into two categories: Phase I activation enzymes and Phase II neutralization enzymes. The first ones increase the water solubility of lipophilic xenobiotic enzymes, providing sites for conjugation reactions to phase II enzymes. The later, include members of various transferases responsible for the elimination of toxic chemicals. P450 family enzymes that belong to phase I, are being studied for their genetic polymorphism and its role in carcinogenesis of various cancers. CYP41, a member of this family, has been associated with the pathogenesis of oral cancer (Ghosh et al, 2012). GSTT1 and GSTM1 are phase II enzymes that their SNPs are well investigated in the initiation of OSCC (Yadav et al, 2009).

Finally, Tol-like receptors (TLRs) are a critical compound of the human immune system against microbial infection and tissue healing process (Ghosh et al, 2012). OSCC risk is positively correlated with the overexpression of several TLRs (Pisani et al, 2017) as oral bacteria while interacting with them, promote the oral epithelium inflammation (Kauppila et al, 2013). For example, individuals with SNPs of TLR2 and TLR4 have a higher risk to develop bacteria related oral cancer (Chen et al, 2021).

Other Risk Factors OSCC is most common in specific groups like males, in lower socioeconomic groups and in ethnic minority groups (Markopoulos, 2012). The reasons about that are being studied and may be genetic or correlated to poor oral hygiene. There is also an increased risk of developing OSCC in patients under immunosuppressive therapy or conditions like HIV infected patients or individuals submitted to organ transplantation, something connected probably to immune

system defects. Lastly, there may be a significance in hereditary for developing OSCC as the first degree relatives of patients with oral cancer have a relative danger that varies from 1.1-3.8 odds ratios for that disease. (Markopoulos, 2012)

2.3 The Mechanism of OSCC Carcinogenesis

The fundamental characteristic of cancer Formation is the sustained proliferation of the malignant cells (Chen et al, 2021). Carcinogenesis is a complex process during which, specific genetic events alter the regulation of evading growth suppressors, resisting apoptosis, enabling replicative immortality, promoting genomic instability, inducing angiogenesis, activating invasion capacity and escaping immune surveillance (Hanahan et al, 2011). The dysfunction in these critical biological responses results in the malignant transformation of the OSCC (Chen et al, 2021). It is important to understand these molecular processes to provide information not only for the malignant behavior but also for suggesting key elements for potential therapies.

In the development of OSCC there have been identified several anomalies of oncoproteins or proto-oncoproteins, such as: EGFR, K-ras, c-myc, FGF3 and cyclin D1 (Hsieh et al, 2019). EGFR overexpression is observed in almost 90% of all head and neck cancer (HNC) patients and is associated with poor overall prognosis (Barnes et al, 2020). Thus, an anti-EGFR antibody, cetuximab, is approved for the treatment of patients with advanced HNC, succeeding in extending the overall survival of patients under a combined cetuximab / platinum based chemotherapy (Vermorken et al, 2008). Cetuximab is currently considered as a key element in advanced OSCC therapy.

Neoplastic cells must evade the vigorous cell cycle regulation process in order to maintain tumor growth. This process is strictly controlled by the tumor suppression genes products. The most common genetic alteration observed in all human cancers is the inactivation of p53 protein gene (Vermorken et al, 2008). The dysregulation of that gene can be observed in over 50% of oral cancer tissues (NCCN Guidelines for Head and Neck Cancers, 2020).

The second most frequently mutated gene in OSCC is the CDKN2A (Stransky et al, 2011). The product of CDKN2A, namely p16, during the G1 to S phase of the cell cycle, can disrupt the interaction between CDK4/6 and cyclin D1 and promote the cell cycle progression. The loss of CDKN2A as a result of gene mutations, can be identified in approximately 90% of all OSCC. In this case, the combination of cetuximab and Palbociclib, a CDK4/6 inhibitor, achieved significant responses in patients with platinum and cetuximab – resistant HNC, underscoring the significance of tumor suppressor genes in the malignant transformation of OSCC (Chen et al, 2021).

Another important point in OSCC development is the impact of Tumor Microenvironment (TME) as the tumor growth heavily relies on the impact from the complicated ecosystem in the TME (Peltanova et al, 2019). To avoid the immune

system cell attacks, cancer cells have to create in immunosuppressive setting through the complex interaction between tumor cells and their surrounding cells in the TME that incudes loss of tumor neoantigen, polarization of immune cells, dysregulation of inflammatory cytokines and induction of immune checkpoints (Yadav et al, 2009). In patient with oral cancer has been proved that immunosuppressive molecules help to maintain host tolerance by attenuating the cytotoxic T-cell function, which are a major antitumor immunological cell type, resulting in escaping of the immune response for the tumor cells (Kauppila et al, 2013).

Lately a new theory has emerged for Oral Carcinogenesis, that of Field Cancerization. According to this theory, the entire area of oral epithelium is at increased risk for the development of malignant lesions since the epithelium is exposed to carcinogenic factors (Braakhuis et al, 2003). In cancerization field, multiple oral cancers may develop from independent cell clones. A modification of that theory, the patch field carcinoma model, suggests that multiple oral cancers can be delivered from the expansion of an original clone. According to this model, a genetically altered stem cell, located in the oral epithelium, produces daughter cells that expand to a size of several centimeters to the surrounding oral mucosa. This patch of cells is often macroscopically undetectable nut may also appear as a leukoplakia or erythroplakia (Braakhuis et al, 2004).

2.4 Potential Malignant Disorders

Potential Malignant Disorders are mucosa lesions that compared to other oral pathologies have a significantly higher chance of becoming cancerous (Liu et al, 2015). Following the fact that the majority of OSCC cases have resulted from prior “Precancerous Lesions”, WHO recommended changing this term to “Potentially Malignant Disorders” (PMDs) in 2005. PMDs for OSCC are listed bellow:

- Erythroplakia: a clinical term to describe any erythematous (red) area on a mucous membrane, that cannot be attributed to any other pathology.
- Leukoplakia: a condition in which one or more white patches or spots (lesions) forms inside the mouth, particularly:

  Eryhroleukoplakia (nodular or verrucous)

  Proliferative verrucous leukoplakia
- Actinic cheilitis: the lip form of actinic keratosis due to chronic sun exposure.
- Lichen planus: a chronic inflammatory condition affecting the skin and mucosal surfaces. (mainly the erosive and atrophic type)
- Sideropenic dysphagia (Plummer-Vinson syndrome): A disorder marked by anemia caused by iron deficiency, and a web-like growth of membranes in the throat that makes swallowing difficult.
- Submucous fibrosis: a chronic, insidious, scarring disease of the oral cavity, often with involvement of the pharynx and the upper esophagus
- Dyskeratosis congenita: also known as Zinsser-Engman-Cole syndrome is a rare progressive congenital disorder form of bone marrow failure, the inability of the

marrow to produce sufficient blood cells classically defined by the triad of abnormal skin pigmentation, nail dystrophy, and leukoplakia of the oral mucosa
- Discoid lupus erythematosous: the most common type of chronic cutaneous lupus (CCLE), an autoimmune condition, it presents with red, painful, inflamed and coin-shaped patches of skin with a scaly and crusty appearance, most often on the scalp, cheeks, and ears

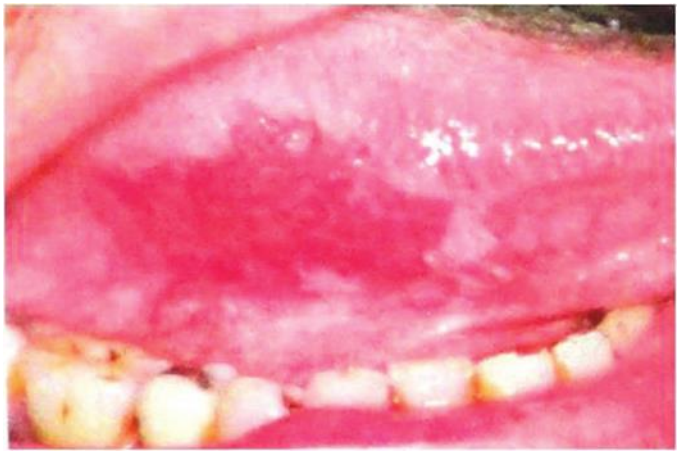

Figure 4 A red patch defined as erythroplakia is one that cannot be clinically or pathologically identified as any other lesion (Shirani et al., 2014).

2.5 Clinical Features

Clinical examination is the first and most important way to detect an OSCC. The traditional oral examination involves clinical assessment and palpation of the oral mucosa under the illumination of the dental chair. The ability to diagnose OSCC at an early stage is critical in order the lower the death probability by locating the malignancy in it's local manifestation stage. (Mascitti et al, 2018)

OSCC in it's early stages can go unnoticed as it is painless or mimics other mucosa lesions. As it advances it may develop a burning sensation or pain, or interfere with mouth functions. (Markopoulos, 2012) It may present as an ulcer with fissuring or raised exophytic margins, as a lump, as a non-healing extraction socket or as a cervical lymph node. OSCC should be considered where any of these futures persists for more than two weeks. (Califano et al, 1996) Another manifestation is that of the known premalignant lesions especially erythroplakia and leukoplakia. These are areas of the mucosa with distinct red or white color and surface morphology that cannot be removed with a simple scratching using a dental probe as in the case of a fungal infection that gives a similar clinical image.

There also staining methods that can aid the clinical evaluation. Toluidine blue (TB), Methylene blue staining, Rose Bangal staining and Lugol's iodine staining are some examples of stains. The usage of TB is a well-established method for detecting

premalignant and malignant lesions and is a recommended part of the clinical examination of high risk patients' oral mucosa. (Abdelaziz et al, 2021)

Therefore, a successful detection of a premalignant or malignant area is of high importance for an effective and complete handling of the OSCC. A well trained clinician and an informed patient that doesn't disregard their oral check scheduled appointments or an insisting anomaly in their mouth, could lead in a well timed diagnosis and a successful treatment.

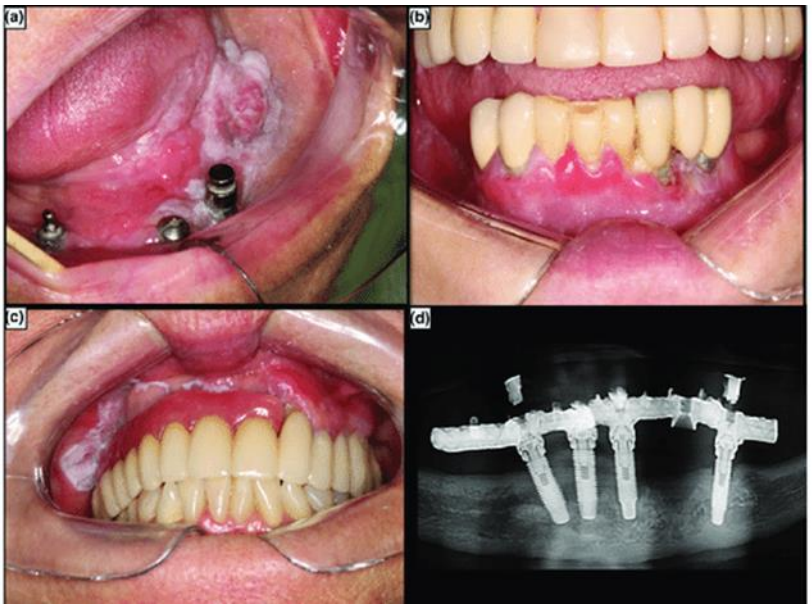

Figure 5 Features of oral squamous cell carcinoma around implants on radiographs. (a) Patient was diagnosed with an exophytic lesion that included the lower left alveolar ridge and extended to the area in front of implants 43, 31 and 33. The lesion had an uneven white surface. (a) Around implants 33 and 34, patient had an erythematous ulcer. (c) Patient's oral examination reveals leukoplakia in the alveolar ridge, a deep groove to the jugal mucosa, and a right hard palate next to overdentures held in place by implants 11, 13, 15, and 17. (d) A radiolucent lesion between implants 33 and 3 was discovered during the radiographic examination of Patient. (Galvis et al., 2020)

2.6 Histopathology Of OSCC

Oral Squamous Cell Carcinoma derives from the stratified squamous epithelium of the oral mucosa (Tumuluri et al, 2002). Histologically, the lesion passes through various phases until the final formation of the neoplasm (Neville, 2002). The main manifestation of the cancer is epithelial dysplasia. Dysplasia is graded as mild, moderate or extreme by the World Health Organization (Abdelaziz et al, 2021). This epithelial dysplasia is characterized by the altered proliferation of dysplastic squamous cells on the surface of the epithelial layer, which subsequently degrades the subepithelial basement membrane (BM). The degradation of BM results in local destruction via the islets and cords of epithelial cells and distant invasion via metastasis (Fuentes et al, 2012).

A study by Bunget et al. in 2018, delivers an analytic histopathological description of the aspects in three types of OSCC: a) well differentiated OSCC, b) moderated OSCC, c) poorly differentiated OSCC. According to them:

a) In well differentiated OSCC, well differentiated squamous cells can be observed, arranged as islands with various shapes and sizes. Keratinous pearls are found inside these islands in which, cells were acidophilic with pyknotic nuclei and karyolysis, while the rest of the cells had nuclei of different shapes and sizes, bigger than normal epithelium nuclei. Many cells had polyhedral aspects with intracellular spines (Bunget et al, 2018).

b) Moderately differentiated OSCC were organized in islands of neoplastic atypical epithelial cells, oval-shaped, oblong, round which infiltrated the tumoral stroma. At the periphery, carcinoma islands were separated by fibrous stromal elements or inflammatory type cells. Nuclei of neoplastic cells had different shapes and sizes, most of them hypochromic with large nucleoli. Tumor cells appeared as atypical cells diffusely scattered in the stroma of oral, lingual or labial mucosa, with rare intercellular bridges. Often tumor cells had large, deformed nuclei, hyperchrome or hypochromic, with pinholes and buddings, and multiple atypical mitosis (Bunget et al, 2018).

c) Poorly differentiated squamous cell carcinomas were designed as cellular cords, islands or epithelioid-like cells of various shapes and sizes, with a different design from the normal epithelium. The various aspects of cancer cells means the malignant tumors are heterogeneous entities, multicellular, containing multiple cell lines whose interactions with each other and with the extracellular matrix through paracrine secreted soluble molecules are dynamic and promote cell proliferation, movement and differentiation of neoplasia (Bunget et al, 2018).

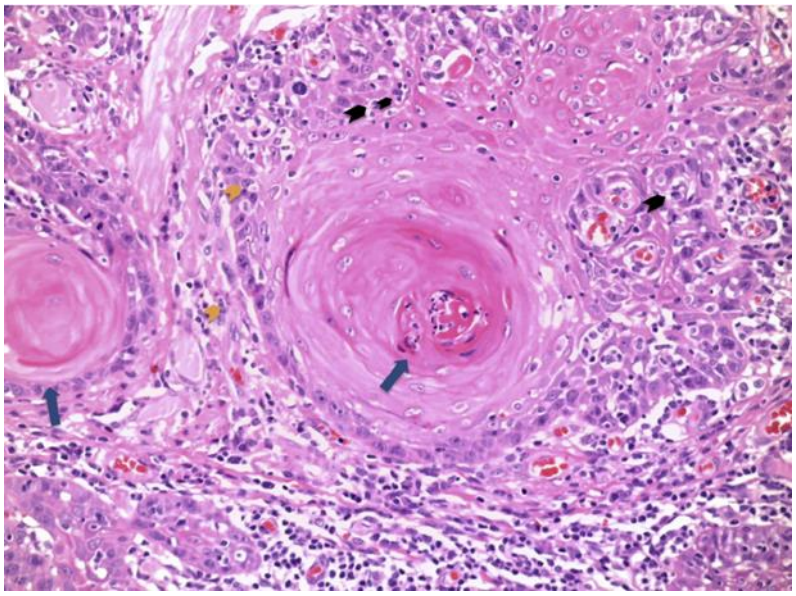

Figure 6 Oral squamous cell carcinoma histological picture (hematoxylin-eosin stain, original magnification = 20). It was determined how much keratinization, nuclear pleomorphism, mitosis, invasion, and response of neighboring tissues had occurred (blue arrows, orange arrowheads, black arrowheads). (Troeltzsch et al. 2014)

There are two systems for histological classification of tumor lesions: the International Classification of Tumors and the Pattern of the Tumor Invasion Front (TIF) (Rivera et al, 2011). The initial classification of lesions is based on the degree of tumor differentiation which is essential to evaluate the tumor's growth rate and ability to metastasize. (Sapp et al, 2004). The TIF describes the most representative area of the tumor as it constitutes the area of the lesion with greatest depth of invasion and is identified by four characteristics: a) the degree of keratinization, b) nuclear polymorphism, c) lymphocytic infiltration and d) the pattern of invasion (PI) which is considered to be a good prognostic factor in OSCC. For evaluating the severity of the invasion, several morphological criteria exist, according to the following categories: a) islet-infiltrating cells with wide fronts of invasion, b) thin infiltrating cords, c) individual infiltrating cells (Dissanayaka et al, 2012).

2.7 Biomarkers Of OSCC

Gene alterations in OSCC lead to reduced expression or overexpression of specific proteins. These changes in oncogenes and tumor suppression genes may lead to oral cancer formation. The critical genes in OSCC include cyclin D1, p53, retinoblastoma, epidermal growth factor receptor, signal transducer and activator of transcription 3 and vascular endothelial growth factor receiver (Choi et al, 2008). Currently, there are almost no definitive therapeutic choices available. A detailed examination of genomic data is also important for the diagnosis and subclassification of cancer based on molecular biology. In addition, the collection of genetic information related to carcinogenesis and the evolution of cancer will immediately lead to the creation of effective new treatments by elucidating mutant genes and the signaling pathways they affect(H2). Attempts to diagnose via liquid biopsy utilizing blood, urine, saliva, pleural fluid, ascites, etc. are gaining popularity at present (h2). The primary goals for biomarker discovery using blood-based liquid biopsy are cell-free DNA (cfDNA), circulating tumor cells (CTC), and microRNA (miR, miRNA). The significance of biomarkers for a nanoparticle-based therapy stems from the fact that they provide a customized report on the progression of the disease and the effectiveness of the treatment.

Ki-67 and p53 are the most commonly studied markers for cell proliferation. P53 protein is one of the basic factors for cell cycle control and apoptosis (Massano et al, 2006). Ki-67 is important in cell division and is expressed primarily during the cell cycle stages of G1, s, G2 and M (Rivera et al, 2014). The quantified detection of these proteins can give information about the development of the malignancy or the succeed of a treatment. Homeobox genes (HOX) in a novel biomarker in the cancer field as it's overexpression has been associated with head and neck neoplasms carcinogenesis (Tucci et al, 2011). These genes may contribute to the onset and progression of tumors (Shah et al, 2010)

Not only tumor growth but also infiltration of the peripheral tissues is an important factor in the prognosis of patients with OSSC as it is a key prerequisite for cancer metastasis (Fan et al,2012). Degradation of the Basement Membrane (BM) must occur for metastasis to appear, between the epithelium and the lamina propria. The most important component of the BM is Collagen Type V (CollV). Its integrity alters after the degradation of the BM via matrix metalloproteinases 2 and 9 of the OSCC allowing to have another prognostic factor for OSCC by monitoring changes in CollV expression (Baba et al, 2008).

2.8 Tumor Microenviroment

Tumor microenvironment (TME) has been proposed as a major aspect in the cancer study field as the malignancy involves a complicated structure and interactions with the surrounding tissues that affect it's functionality in a wider that the cellular level. The TME contains various cells like cancer associated fibroblasts (CAFs), smooth muscle cells, endothelial cells, neutrophils, eosinophils, mast cells, T cells, macrophages and dendritic cells (Rivera et al, 2014). CAFs are the most copious cells of the TME. They may be locally differentiated from normal fibroblasts and they can mechanically reshape the extracellular matrix to facilitate the invasion of cancer cells (Koontongkaew, 2013). CAFs can also progress tumorigenesis by secreting chemokine ligand 7 after their interaction with the tumor cells (Jung et al, 2010). Their increased presence in OSCC is associated with a poor prognosis, as their interactions prepare the environment for tumor invasion and metastasis (Thode et al, 2011).

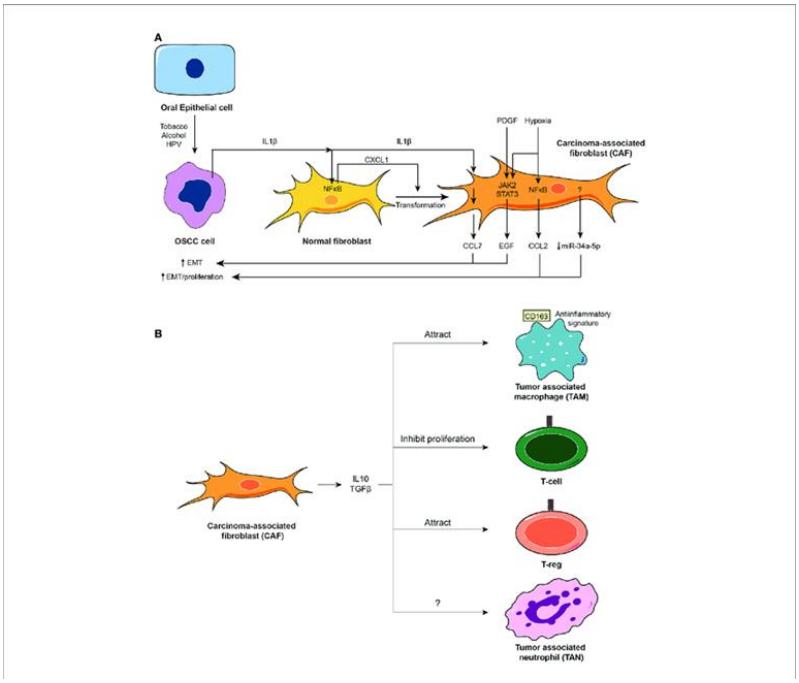

Figure 7 The oral squamous cell carcinoma (OSCC) tumor microenvironment. (A) The OSCC tumor microenvironment is mainly composed of cancer-associated fibroblasts (CAFs). CAFs derive from normal fibroblasts after autocrine stimulation of chemokine (C-X-C motif) ligand (CXCL1) chemokine through a nuclear factor kB (Peña et al., 2020)

2.9 Lymph Node Metastases Of OSCC

A critical stage in the spread of human malignancies is lymphovascular invasion. Lymph node metastases typically develop in individuals with HNC and impact their prognosis and therapeutic approaches as a result of the presence of lymphatic vessels in the cervix (Baik et al, 2019). The major factor affecting tumor lymphovascular invasion is the stimulation of angiogenesis and invasion activity. (Chen et al, 2021)

In human malignancies, such as OSCC, vascular endothelial growth factor C (VEGF-C) is a crucial lymphangiogenic inducer (Naruse et al, 2015). Neoplastic cells can express VEGF-C to stimulate the growth and migration of lymphatic vessels by activating vascular endothelial growth factor receptor 3 on the lymphatic endothelium. Prospero homeobox 1, forkhead box C2, and astrocyte elevated gene-1 are a few proangiogenic factors that have been linked to lymphangiogenesis in oral cancer development (Chen et al, 2020).

Along with the angiogenic switch, the epithelial-mesenchymal transition (EMT) is a well-known dynamic process that enables cancer cells to go through a number of biochemical changes that improve their capability for invasion, migration, and the creation of extracellular matrix components (Ribatti et al, 2020). (A0) Epithelial cancer cells may transform into mesenchymal phenotypes during the EMT stage by losing their intercellular connections and migratory polarity, among other means. Cancer cells have the ability to enter the lymphovascular circulation through the EMT process, travel to nearby lymph nodes, or cause metastases to distant organs. The most significant mediator of the increased invasiveness of oral cancer is the activation of Snail, one of numerous transcription factors linked with EMT. (Chen et al, 2021)

The mesenchymal phenotypes of oral SCC are similarly linked with Twist 1 and Twist 2, two members of the Twist family. Clinical research has shown that Twist overexpression negatively affects oral cancer patients' chances of surviving (Seyedmajidi et al, 2018).

The Wnt signaling system controls important elements of cell fate determination, cell migration, cell polarity, neural patterning, and organogenesis throughout embryonic development. It is a long-established and evolutionarily conserved pathway. (google) The Wnt pathway is thought to have a significant role in controlling the invasiveness and stemness phenotypes of oral cancer, according to a number of findings (Reyes et al, 2020). The Wnt family proteins initiate the -catenin signaling in the nucleus, activate the T-cell/lymphoid-enhancing factor transcription factors, and then bind to their receptors on the cell membrane in the canonical route. 19 proteins from the Wnt family in all have been found to start this signaling pathway (Mikels et al, 2006).

Small non-coding RNAs known as microRNAs (miRNAs) have a role in the development of cancer and other biological processes. They are produced by endogenous genes and belong to the miRNA family (Anastasiadou et al, 2018). Numerous oncogenic or tumor-suppressive miRNAs have been identified in oral

cancer, and studies investigating how these short RNAs control lymph node metastasis have been notable (Fang et al, 2019).

2.10 Characterization Of OSSC

Since they have an impact on risk categorization and are the first step toward individualized treatment, staging and grading of OSCC are established prerequisites for management. Significant changes have been made to the current AJCC/UICC TNM staging (8th edition, 2017) of OSCC by include extracapsular spread/extranodal extension in the N stage and depth of invasion in the T stage. (Almangush et al, 2020)

The TNM system is used for OSCC staging. (Markopoulos, 2012) The TNM system of cancer staging evaluates the size of the primary tumor (T), the involvement of local lymph nodes (N), and distant metastases to determine the amount of tumor progression throughout the body (M). Planning treatments, determining recurrence risk, and assessing overall survival all depend on this classification. The only prognostic feature taken into account by this categorization, however, is the anatomic extent of the disease and not comorbidities or treatment (Patel et al, 2008). cTNM is the stage given after the clinical examination of the patient, while pTNM is the stage after the histopathological examination of the surgical specimen. (Markopoulos, 2012)

Categories	Definitions
Primary tumor (T)	
Tx	Primary tumor cannot be assessed
T0	No evidence of primary tumor
Tis	Carcinoma in situ
T1	Tumor 2 cm or less in greatest dimension
T2	Tumor more than 2 cm but not more than 4 cm in greatest dimension
T3	Tumor more than 4 cm in greatest dimension
T4a	(Lip) Tumor invades through cortical bone, inferior alveolar nerve, floor of mouth, or skin of face
	(Oral Cavity) Tumor invades through cortical bone, into deep (extrinsic) muscle of tongue (genioglossus, hyoglossus, palatoglossus, and styloglossus), maxillary sinus, or skin of face
T4b	Tumor involves masticator space, pterygoid plates, or skull base and/or encases internal carotid artery
Regional Lymph Nodes (N)	
Nx	Regional lymph nodes cannot be assessed
N0	No regional lymph node metastasis
N1	Metastasis in a single ipsilateral lymph node, 3 cm or less in greatest dimension
N2a	Metastasis in a single ipsilateral lymph node, more than 3 cm but not more than 6 cm in greatest dimension
N2b	Metastasis in multiple ipsilateral lymph nodes, none more than 6 cm in greatest dimension
N2c	Metastasis in bilateral or contralateral lymph nodes, none more than 6 cm in greatest dimension
N3	Metastasis in a lymph node, more than 6 cm in greatest dimension
Distant Metastasis (M)	
Mx	Distant metastasis cannot be assessed
M0	No distant metastasis
M1	Distant metastasis

According to the American Joint Committee on Cancer [1].
doi:10.1371/journal.pmed.0050212.t001

Figure 8 TNM Classification System for Oral Squamous Cell Carcinoma (Pastore et al., 2008)

Evaluation of additional neoplasm characteristics, such as differentiation level, infiltration type, and recurrence level facilitate the precise diagnosis and enable the choice of the most effective therapy strategy. (Lacy et al, 1999)

The eighth edition of the staging manual from the American Joint Committee on Cancer (AJCC 8) and the International Union Against Cancer (UICC) was published in 2017. It brought about two significant alterations for OSCC, including the inclusion of extracapsular spread (ECS) in the N stage and the tumor depth of invasion (DOI) in the T stage. Particularly in exophytic and ulcerated lesions, DOI, also known as reconstructed tumor thickness, differs from clinical tumor thickness. (Almangush et al, 2020) Although the UICC Atlas and the AJCC 8 manual both state that DOI can be consistently determined clinically, DOI appears to be difficult to estimate only by palpation. Preoperative imaging, such as magnetic resonance imaging (MRI) or ultrasound (US), to measure the depth of invasion and tumor thickness, might be an approach to overcome these issues. (Almangush et al, 2020) It has been highlighted that a number of cases have been upstaged as a result of the adjustments in AJCC 8 according to recently published studies (Matos et al, 2017). This would have an impact on treatment planning because OSCC cases that were classified as early stage lesions by AJCC 7 are now classified as advanced lesions by AJCC 8. Lowering the T stage threshold has been proposed. To better classify the risk groups of early oral tongue cancer cases, Almangush et al. 2020, advised reducing the cutoff limit (from 5 mm to 2 mm for T1 and from 10 mm to 4 mm for T2). Furthermore, recent research (Rajappa et al, 2019) suggested modifying the N stage by taking the number of positive metastatic nodes into account. Further validation experiments to investigate these recently proposed modifications are still necessary in order to establish the appropriate DOI cutoff point and the quantity of positive nodes used as modifiers of the T and N phases with sufficient risk discrimination. (Almangush et al, 2020) Absence of surrounding intact mucosa, absence or only minimal residual tumor after biopsy, extratumoral perineural or vascular invasion, and a positive deep margin are reported cases where DOI can be underestimated or underestimated (Berdugo et al, 2019).

Although they acknowledge that "Grading alone does not correlate well with prognosis," the current edition of the WHO Classification of Head and Neck Tumors supports a simple grading system (El-Naggar et al, 2017) based on the Broders criteria and only recognizes well-, moderately-, and poorly-differentiated variants of conventional OSCCs. Numerous studies suggest that the WHO grading system has little to no predictive significance (Dik et al, 2018).

A different approach was based on the size of cell nests and tumor budding, although it was unrelated to the level of cell differentiation (Boxberg et al, 2017).
The presence of single tumor cells and tiny tumor cell clusters at the invasive front of carcinomas broadly defines tumor budding. According to some theories, it might be an epithelial-mesenchymal transition (EMT). (Wikipedia) In OSCC, "tumor budding" has gained popularity as a potential prognostic factor (Sakata et al, 2018). This pattern is the result of appealing terminology and support for the idea of tumor budding in other malignancies (Boxberg et al, 2019).

Numerous malignancies have been classified using the so-called immunoscore (Yomoda et al, 2019). This evaluation could be used to select patients who would benefit from immunotherapy (Boxberg et al, 2019). A comprehensive evaluation of the stromal tumor-infiltrating lymphocytes (TILs) may enable risk categorization in early-stage oral tongue SCC, according to Heikkinen et al. Based on HE-stained sections, this assessment can be easily incorporated into standard istopathology reporting.The importance of several lymphocyte subtypes and other immune cell components, such as dendritic cells, in the prediction of overall survival and disease-free survival has been revealed in recent studies using immunohistochemistry (Fanget al, 2017). Specific immunological biomarkers, such as CD57+ and CD163+, have been found recently in meta-analyses for OSCC prognosis (Hadler-Olsen et al, 2019).

In early stage oral tongue SCC, the tumor-stroma ratio (TSR) was also studied and may have predictive value. Compared to stroma-poor tumors, stroma-rich tumors are linked to higher rates of recurrence and mortality (Almangush et al, 2018).

2.11 Therapeutic Approaches

The usual treatment options, continue to include surgery and radiotherapy (Markopoulos, 2012). Surgery is used to eradicate OSCC, either with or without adjuvant therapy (e.g. radiotherapy or chemoradiotherapy). Differentiation, growth pattern, depth of invasion, status of margins, vascular/neural invasion, bone involvement, nodal status (number of lymph nodes involved, size of largest metastasis, extracapsular spread (ECS)/extranodal extension (ENE), and pTNM staging—all of which are described in the standardized histopathology report of the resection—have an impact on the decision to administer adjuvant therapy. (Almangush et al, 2020)

Radiotherapy as neoadjuvant therapy, it can be utilized to shrink the tumor before surgery. Additionally, radiotherapy can be used as adjuvant therapy, which boosts the effectiveness of the first therapy and, as a consequence, improves the symptoms of late-stage oral cancer as well as the likelihood of survival and the danger of recurrence. (Ketabat et al, 2019) When the bone is close to the patient and/or the patient is young, radiotherapy has a number of unfavorable effects that are undesirable, such as xerostomia, osteoradionecrosis, mucositis, and a prolonged treatment period. (Abdelaziz et al, 2021) Oral care and pre-operative dental therapies if needed are especially crucial due to this risks. (Markopoulos, 2012)

Surgery and/or radiotherapy are the primary treatments in the main (I and II) phases since they typically lead to a permanent cure.For the third or fourth stage of OSCC, a combination of surgery, radiation, or chemotherapy is employed. (Markopoulos, 2012)

Nearly 80% of patients who have OSCC metastatic disease will also have cervical lymph nodes involved. In these circumstances, cervical lymphadenectomy (radical neck dissection) is typically used (Shah et al, 2009). To reduce the morbidity

of radical neck dissection, selective neck dissection has been developed (Pagedar et al, 2009).

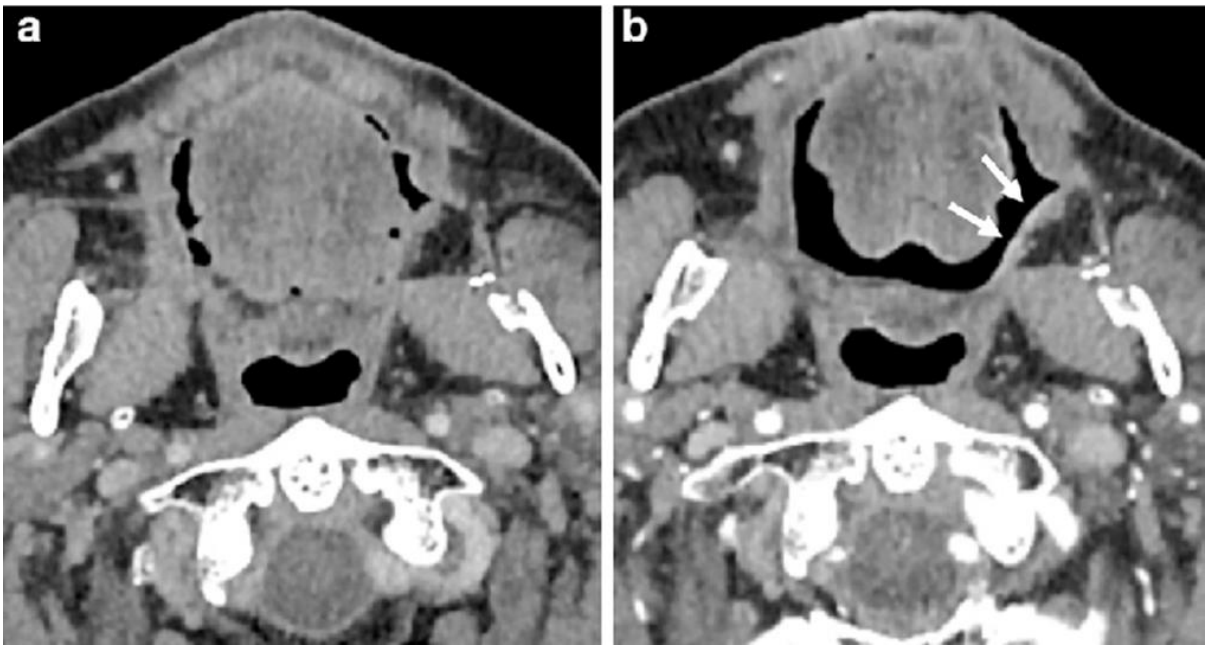

Figure 9 Post-treatment surveillance CT scans were taken 18 months (a) and 24 months (b) after resection and adjuvant radiotherapy on a patient with OSCC that was predominantly in the left mouth floor. The surface of the radialis flap repair has recently been improved (b, indicated by white arrows). The supervising radiologist reduced the primary site's initial NI-RADS category 2a designation to category 1. On the clinical examination and subsequent surveillance CT, there was no indication of a malignant recurrence (Elsholtz et al., 2021).

Alterned fractionated radiation or concomitant chemo-radiotherapy (CT-RT) are two strategies to improve the efficacy of radiotherapy, particularly in cases of local advanced illness (Mazeron et al, 2009).

For locoregionally advanced head and neck SCC, cisplatin-based chemoradiation continues to be the standard of care (Specenier et al, 2009). The most widely utilized medications at the moment have been established to be cisplatin (CDDP), fluorouracil (5-FU), carboplatin, paclitaxel, methotrexate, and others (Marcazzan et al, 2018). The unsatisfactory selectivity of chemical agents between normal cells and malignant cells, despite significant advancements in cancer treatment, could be the cause of numerous side effects (Zhou et al, 2019).

Patients with oral cancer have received targeted molecular therapy, including gene and monoclonal antibody therapy. Epidermal growth factor receptor (EGFR), cyclooxygenase-2 (COX-2), peroxisome proliferator-activated receptor (PPAR), and progesterone receptor are the four molecules that have received the majority of attention in targeted molecular therapy. These therapies can also be used in conjunction with other cancer treatments currently on the market. (Hamakawa et al, 2008)

Due to the location and invasive nature of the treatment, oral cancer treatment methods such surgery, radiation, and chemotherapy are viewed as particularly harsh and have a substantial influence on the patient's quality of life. Treatment for the original tumor using OSCC treatment methods aims to preserve as

much shape and function as possible through appropriate restoration (Marcazzan et al, 2018).

AuroLaseTM gold nanoshells are a noteworthy inorganic nanoparticle-based hyperthermia system that have been tested in clinical studies for prostate, lung, and head and neck malignancies (NCT00848042, NCT01679470) (ID: NCT02680535). (Mapanao et al, 2021)

2.12 Targeted Treatment For OSCC – Nanodelivery Systems

As a result of recent breakthroughs in molecular biology and genetics, researchers are actively working to improve cancer diagnosis and treatment, as well as to better understand the molecular mechanisms behind the disease (Sung et al, 2021). Nano-drug delivery systems are also useful because they help overcome chemotherapy's drawbacks, lessen medication toxicity, and boost the potency of anti-tumor therapies (Sasahira et al, 2022). When it comes to treating tumors, the drug accumulation effect and drug delivery capacity of nano-drug delivery systems are superior (Zhu et al, 2019).

Nano-delivered medications have greater anti-tumor activity, longer blood cycle time, and greater drug solubility compared to conventional chemotherapy. Clinical trials of the nano-drug delivery system for the treatment of ovarian cancer, metastatic breast cancer, and other cancers are now ongoing (Wicki et al, 2015). The system for delivering drugs at the nanoscale is currently evolving at the present time. By boosting active targeting components and improving the release of transported pharmaceuticals, the second generation of nano-drug delivery system has improved tumor targeting effects (Mi et al, 2016). To improve anti-tumor efficacy, the third-generation of nano-drug delivery systems employs multistage nano-carriers, which are comprised of mesoporous silicon particles in the first stage and the drug delivery system embedded in the nano-pores in the second stage. This facilitates interaction between the mesoporous silicon particles and endothelial cells in the blood vessel wall (Mi et al, 2016). Cetuximab, a mouse monoclonal antibody targeting epidermal growth factor receptor (EGFR), and nivolumab, an immune checkpoint inhibitor blocking the programmed death-1 (PD-1) and PD-ligand 1 (PD-L1) pathways, are the primary molecular target medicines available in Japan for oral cancer (Sasahira et al, 2022). In addition, microsatellite instability-high (MSI-H) ovarian, squamous cell carcinoma (OSCC) that is unresectable or metastatic is treated with pembrolizumab (Akagi et al, 2021). Pembrolizumab has a limited usefulness, however, because MSI-H is so uncommon in oral cancer (Hause et al, 2016). However, there are very few molecular targeted therapies available for OSCC compared to other malignancies, despite recent widespread usage of entrectinib, which targets the neurotrophic receptor tyrosine kinase (NTRK) fusion gene (Jiang et al, 2021).

Moreover, despite developments in molecular biology and genomic medicine, it remains uncertain whether or not there are effective diagnostic and treatment

markers for OSCC. Future research into oral cancer must focus on identifying and eliminating potential indicators of the disease, identifying treatment resistance mechanisms, and developing effective, safe, and highly helpful diagnostics.

By definition, nanotechnology is the study of materials having a particle size of 100 nm or less. One nanometer (nm) is equal to one billionth of a meter (m). Nanoparticles and nanosolids are the two main categories of materials at the nanoscale scale in the medical field. (Zhu et al, 2019).

Tumor tissue differs structurally from healthy tissue in obvious ways. When compared to healthy tissue, the capillaries in tumors are porous and lack structural integrity. Therefore, lipid particles and macromolecules that have leaked from the capillary but are unable to flow back into the blood remain in tumor tissue, where they can have certain biological effects upon uptake by tumor cells. The term "increased permeability and retention" (EPR) describes this phenomenon (Spitzbarth et al, 2017). The EPR-based nano-drug delivery system creates a drug carrier transport system at the nanoscale scale, having applications in both general drug delivery and nano-drug carrier-specific targeted therapy. Increased drug concentrations and longer half-lives in the bloodstream are possible thanks to nano-drug delivery systems; the pharmaceuticals they transport can also aggregate preferentially in tumor tissues, where they can do the most good against the disease (Nichols et al, 2014).

The benefits of nano-drug carriers over conventional ones include many advantages. One major benefit is that they improve the durability of medications. When encapsulated in a nano-drug delivery system, the drug is afforded a physical barrier that can prevent some of the normal wear and tear that the medication endures and even slow down the rate at which enzymes can degrade it (Zhu et al, 2019). The second reason is that they improve medicine availability. The blood-brain barrier is an example of a biomembrane that can be altered to increase drug permeability by a nano-drug delivery system, which in turn increases medication bioavailability. Additionally, it may help in enhancing the medicines with low or no solubility for macromolecules. The ability of the nano-drug delivery method to aggregate pharmaceuticals in tumor tissues is yet another benefit. The nanoparticles used in a drug delivery system have a tremendous surface area for their size, allowing them to transport a lot of medicine. Bioavailability and drug uptake is thus benefited by increasing the number of medicines that can bind to tumor tissue and the length of time that they do so. Thirdly, they improve drug targeting. The nano-drug delivery technology allows for precise regulation of drug delivery, preventing harm from unintended side effects. The drug load, kinetic properties, and biocompatibility can all be adjusted by tinkering with nano-carrier materials. This means that nano-carrier medications are more likely to enter tumor tissues than they are to enter normal tissues, resulting in enhanced anti-tumor efficacy (Masoudipour et al, 2018).

By using nanoparticles with sizes between 1 nm and 1000 nm as carriers, therapeutic drugs or agents can be directed to specific organs, cells, or molecules. Carrying drugs or agents in nanoparticles is straightforward via encapsulation, adsorption, or chemical group linkage (Zhu et al, 2019).

Passive Targeting: Based on the increased permeability and EPR in tumor tissue, passive targeting enables medications to reach specific tumor sites by modifying and adjusting nanocarriers, hence extending drug distribution time and retention time. By lowering medication resistance in tumor tissues, passive targeting can also have a greater antitumor effect. Nanoparticles' tiny diameter is mostly responsible for passive targeting functions. In normal tissues, the vascular endothelium is ordered, firmly packed, and uniformly distributed, and macromolecules and lipid particles cannot easily pass through the arterial wall. However, in tumor tissue, neovascular permeability is increased, allowing nano-carriers to easily pass through the vascular wall and reach the tumor tissue. Passive targeted drug delivery system primarily refers to the use of physical and chemical characteristics, such as nanoparticle surface hydrophobicity or hydrophilicity, electrostatic effect, magnetic force effect, nanoparticle diameter size, and surface pH value, to achieve targeted therapy effect (Afifi et al, 2014).

Active Targeting: For active targeting, the surface of the carrier is typically modified with specialized ligands, such as aptamers, peptide chains, and antibodies, in order to find special receptors on tumor cells and in their microenvironment via ligand-receptor interaction. Targeting molecules connect with receptors on the surface of tumor cells to facilitate targeted drug delivery, resulting in increased anti-tumor actions and reduced drug toxicity and side effects in normal tissues (Fan et al, 2014).

Immune Targeting: Active immunity and passive immunity make up immune targeting (Zhu et al, 2019). Currently, vaccinations containing tumor antigens are infused into tumor patients to encourage the body's production of antibodies that can specifically immunize tumor cells. Passive immunity refers to the entry of anti-tumor chemicals into the body to produce an anti-tumor impact. Under the influence of an immune sensitizer, dendritic cells can enhance the proliferation of T cells and increase the recognition of tumor antigenicity, hence strengthening the anti-tumor activity mediated by T cells (Xiao et al, 2011).

Magnetic Targeting refers to the delivery of chemotherapy medications on magnetic nanoparticles to tumor cells in order to boost chemotherapy efficacy. Particles of ferric oxide (Fe_3O_4) have superparamagnetism and can effectively identify malignancies. The particular MENs produced by Oliveira et al.24 deliver paclitaxel to tumor cells and have an antitumor impact without harming normal cells in the surrounding area (Oliveira et al, 2014).

The targeted drug delivery method in oral squamous cell carcinoma can be applied to targeted tumor vessels, interstitial fluid and extracellular matrix, targeted tumor matrix cells, targeted tumor cells, associated dendritic synaptic cells, and targeted tumor stem cells (Zhu et al, 2021).

The primary technique for treating oral squamous cell carcinoma is to target the blood vessels in tumor tissue, as the formation of blood vessels is crucial for tumor nutrition intake, invasion, and metastasis. Numerous growth factors, such as fibroblast growth factor (FGF), VEGF family, platelet-derived growth factor (PDGF)

family, and angiogenin (ANG), contribute to the creation of new blood vessels (Zhu et al, 2021). Extracellular matrix is a collection of numerous big proteins that are produced by cells into the extracellular space and produces a unique structure that can either permit or restrict the passage of specific substances. The nanodrug delivery technology is capable of penetrating the tumor for enhanced efficacy (Liang et al, 2018). Stromal cells in oral squamous cell carcinoma can promote tumor growth by cell adhesion or the paracrine release of related cytokines or growth factor. Current study focuses on improving the therapy of oral squamous cell carcinoma by adjusting the M1/M2 ratio. As oral squamous cell carcinoma deteriorates, tumor stroma will develop an immunosuppressive microenvironment, culminating in tumor immune tolerance (Erez et al, 2010). They can shield antigen from protein breakdown, optimize signal transmission between cells, and activate cells for the purpose of achieving targeted therapy. Current cancer treatments recognize programmed death receptor and ligand (PD-1/PD-L) and cytotoxic T lymphocyte associated antigen (CTLAA) (CTL-4). Currently, tumor-associated dendritic cells (TADC) are regarded as the most promising tumor cells, as they can either activate the host immune system to develop an anti-tumor immune response or induce cytotoxic T cells to destroy tumor cells.

In oral squamous cell carcinoma, nano-drug delivery system may load chemotherapeutic medicines and has chemoprevention potential, including suppression of tumor cells, prevention of malignant tumor precursor cells, and reversal of malignant tumor precursor cells, etc (Iriti et al, 2013). Based on the advancement of nanomedicine, nano-drug delivery systems have additional advantages in the treatment of cancers, however more data is required to determine their efficacy on advanced oral squamous cell carcinoma (Lau et al, 2016).

Zhao et al. developed the 5-fluorouracil-loaded self-assembled nucleotide nanosystem and discovered that the drug delivering nanosystem had a greater in vitro anti-oral squamous cell cancer impact than the nanosystem without 5-fluorouracil (Zhao et al, 2015).

Wang et al. discovered that the cisplatin delivery system produces greater tumor cell death, a more targeted anti-tumor action, and reduced damage to normal cells. In addition, compared to the cisplatin nano-drug delivery system, the polymer micelles of cisplatin encapsulated by the nano-drug delivery system show a higher treatment efficacy on human oral squamous carcinoma cell lines and a lower toxicity to normal cells (Wang et al, 2015).

Doxorubicin is a potent chemotherapeutic agent, but its clinical utility is constrained by its cardiotoxicity. Marcazzan et al. have created a nano-drug delivery system for liposome doxorubicin that can minimize adverse drug responses and cytotoxicity (Marcazzan et al, 2018).

Currently, magnetic nanoparticles containing drugs are also employed as thermal media. Due to their nano-size and the ability for surface modification with antibodies, medicines, and MRI contrast agents38, they are effective theranostic agents for OSCC. In addition, magnetic nanoparticles can induce apoptosis in nearby cells, possibly due to their capacity to convert non-ionizing electromagnetic radiation from therapeutic light sources into heat energy.

Some researchers are investigating the photothermal ablation effect of gold nano-shells in oral squamous cell cancer at present. By reducing Au (gold), colloidal gold nanoparticles were produced. When exposed to near infrared light, the gold nanoparticles converted into heat. In an animal model, some researchers examined the effect of gold nanoparticles and laser therapy on oral squamous cell carcinoma; the gold nanoparticles inhibited tumor development and proliferation by being administered directly into tumor tissues (Jain et al, 2012).

2.13 Prognosis Of OSCC

Early OSCC has the greatest prognosis, particularly when it is well-differentiated and has not metastasized. Unfortunately the majority of OSCC cases receive a late-stage diagnosis. (Markopoulos, 2012) The prognosis for OSCC depends on a variety of tumor-, treatment-, and patient-related variables [de Araújo et al, 2008]. The percentage of cases that survive five years in the advanced stages is less than 12%. Within the first 30 months of their illness, patients with advanced OSCC typically pass away. With a 5-year survival rate of about 50%, the mortality rate has generally remained stable for decades (Marsh et al, 2011). It is still debatable whether or not OSCC patients in different age groups have different prognoses (Zini et al, 2010).

According to the American Cancer Society's (ACS) publication, Cancer Facts & Figures 2022 for the United States, the incidence of oral and oropharyngeal cancer grew by slightly under 1% year from 2009 to 2018. The majority of this rise was seen in non-Hispanic White adults and a subset of oropharynx malignancies connected to HPV infection. 11,230 deaths from oral and oropharyngeal cancer are anticipated in the US in 2022 (7,870 males and 3,360 women). The death rate for these 2 diseases climbed by a little under half a percent annually from 2010 to 2019 after declining for several decades. The increase was brought on by an increase in cancer mortality linked to HPV. The anticipated global death toll from oropharyngeal cancer in 2020 was 225,900. The percentage of persons who survive at least 5 years after their cancer is discovered is shown by the 5-year survival rate. Percentage refers to the number out of 100. Depending on the primary site and the severity of the disease, there are significant differences in the survival rates for oral and oropharyngeal cancer. The overall 5-year survival rate for persons with oral or oropharyngeal cancer in the United States is 67%. Black people have a 5-year survival rate of 51% while White people have a 5-year survival rate of 69%. According to research, White persons are more likely to be diagnosed with HPV-associated cancer, which has greater survival rates. The overall 5-year survival rate for all adults is 85% if cancer is detected early. At this time, 28% of cases of oral and oropharyngeal cancer are discovered. The overall 5-year survival rate is 68% if the cancer has migrated to nearby tissues or organs and/or the local lymph nodes. At this point, almost half of cases are diagnosed. The overall 5-year survival rate is 40% when the cancer has progressed to a distant area of the body. At this point, diagnosis rates for oral and oropharyngeal malignancies are around 18%.

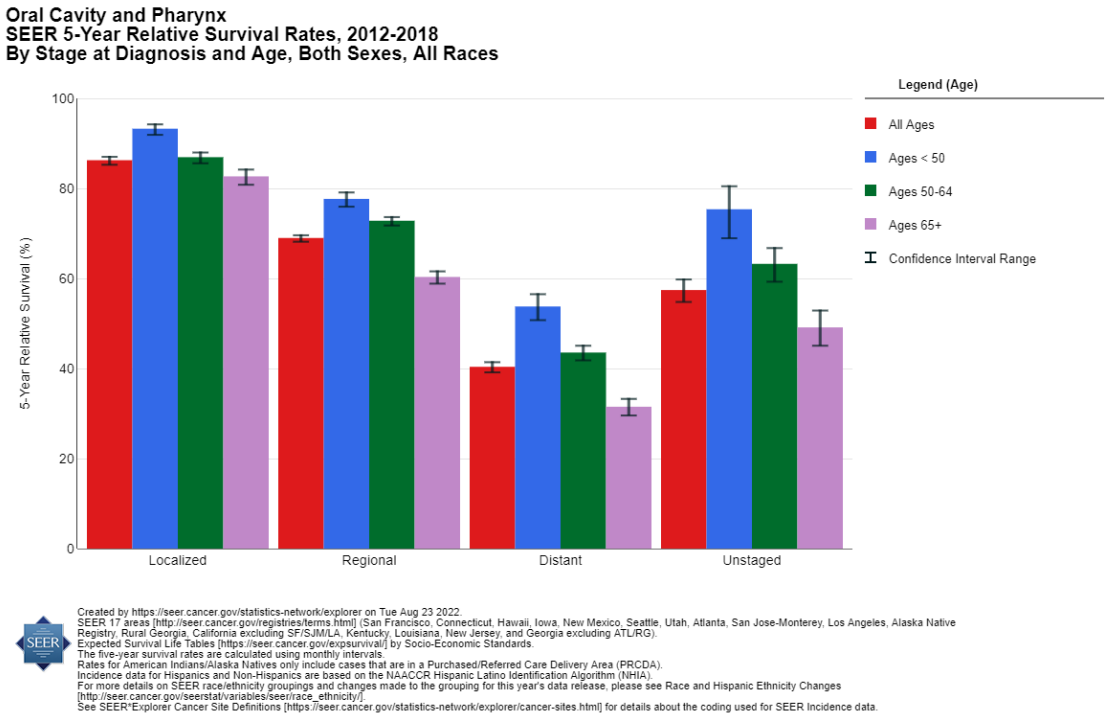

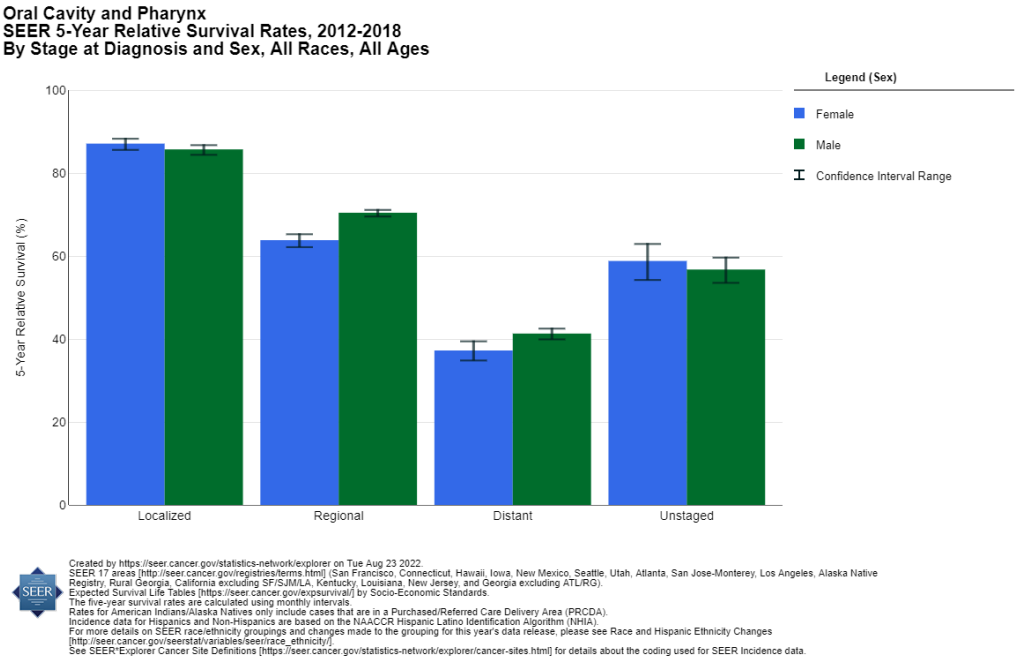

Figure 10 Survival Rates of OSCC (The Surveillance, Epidemiology, and End Results (SEER) Program of the National Cancer Institute (NCI) 2022, https://seer.cancer.gov/)

In conclusion, oral squamous cell carcinoma is a significant and challenging form of cancer that affects millions of people worldwide. While advancements in diagnosis and treatment have improved outcomes, there is still much work to be done to improve survival rates and reduce the morbidity associated with this disease.

Risk factors for oral squamous cell carcinoma include tobacco and alcohol use, as well as infection with high-risk strains of the human papillomavirus. Early detection and diagnosis are critical for successful treatment, and current diagnostic methods include visual examination, biopsy, and imaging.

Treatment for oral squamous cell carcinoma typically involves a combination of surgery, radiation, and chemotherapy, with the specific approach tailored to the individual patient and their cancer stage. In recent years, the use of targeted therapies and immunotherapies has shown promise for improving outcomes, particularly for patients with advanced disease.

Prevention efforts, including education and smoking cessation programs, are also critical in reducing the incidence of oral squamous cell carcinoma. Continued research in this area, including the identification of new biomarkers and the development of novel treatments, will be essential for improving outcomes for patients and reducing the global burden of this disease.

In summary, oral squamous cell carcinoma is a challenging and significant form of cancer that requires a multi-disciplinary approach to diagnosis, treatment, and prevention. As research in this area continues, there is hope for the development of more effective and personalized therapies, ultimately leading to better outcomes for patients with this disease.

CHAPTER 3

Plasmonic Photothermal Therapy of Cancer using Gold nanoparticles

The treatment of cancer remains a major challenge in the field of medicine and continues to demand the development of new and improved therapeutic strategies. Plasmonic photothermal therapy (PPTT) is a type of specialized hyperthermia and a relatively new approach that has shown great promise as a non-invasive and effective treatment for cancer. This innovative therapy uses unique nanoparticles as the primary therapeutic agent and takes advantage of their distinctive optical and thermal properties to destroy cancer cells. As Oral Cancer Plasmonic Photothermal Treatment follows the same main concept with every malignancy confronted with PPTT, in this chapter, we will discuss the principles of how PPTT works, including the incorporated physics, details concerning the strategies used to synthesize and functionalize gold nanoparticles, the results on tumorous environment and the limited but informative outcomes on biological tissues.

3.1 Traditional Hyperthermia

The concept of using heat to treat cancer is not novel. Ancient Egyptians utilized the glowing tip of a firedrill to treat breast cancer tumors at least 3000 years ago (Sullivan, 1996). Based on historical examples in which cancer patients afflicted with erysipelas had high fevers that either reduced cancer symptoms or caused total regression of tumors, hyperthermic cancer therapy was initially devised (Moyer and Delman, 2008). The German physician Wilhelm Busch was the first to report using heat to treat cancer. In 1866, he recorded how a sarcoma disappeared following a patient's erysipelas-caused high fever. (Busch, 1866). A pioneering research conducted by Coley in 1893 (Ahmad et al, 2016). Since the early 1900s, heat has been incorporated into cancer treatment. (Nardine et al, 2016)

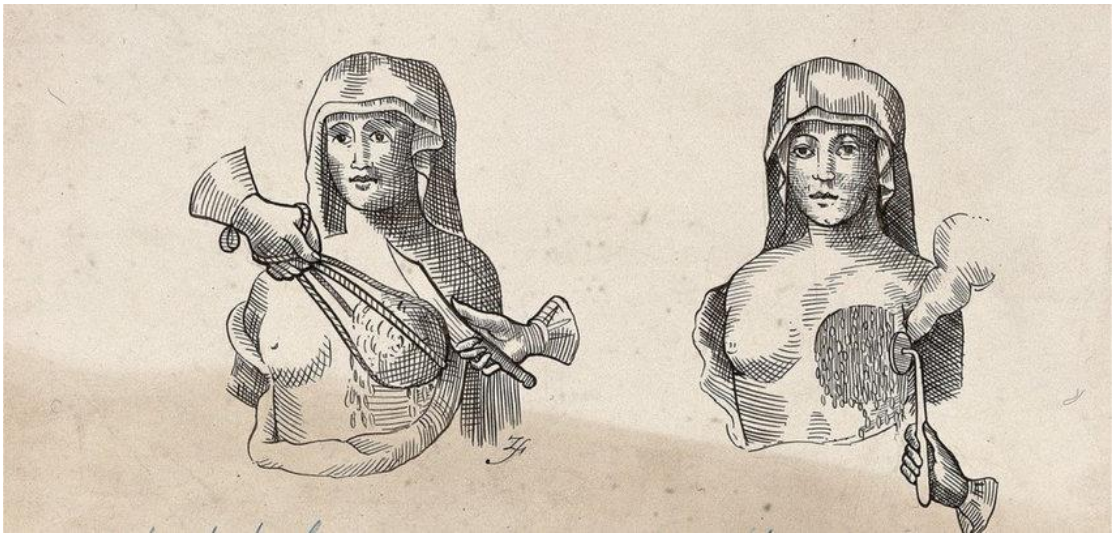

Figure 1 Picture illustrating how to perform a mastectomy and cauterize the wound, ca 1603 (Source: Wellcome Library, London, Tsoucalas et al., 2020).

To treat many malignant tumors, hyperthermia is defined as heating tissue to a temperature between 41 and 47 °C for at least 20 - 30 minutes (Svaasand et al, 1990).

Not only does hyperthermia induce death in cancer cells, but it can also enhance the therapeutic efficacy of radiation and chemotherapy (Kampinga, 2006). In the presence of thermal stress, tumors become radiosensitized, increasing the likelihood that they will respond to radiotherapy, resulting in an increase in cancer survival rates. Similar sensitivity is also observed when chemotherapeutics are combined with heat (Vines et al, 2019).

Among the approaches developed and refined over the past few decades, those employing light absorption have garnered considerable attention due to their superior thermal control and containment within tumor tissue (Cheung et al, 1984). In conventional hyperthermia, the region of the body containing the tumor is heated to 40 - 45 °C, which is several degrees higher than the body's normal temperature (37 °C). Instruments that produce electromagnetic fields (microwaves or radiowaves) or ultrasound are used to generate heat externally (Zagar et al, 2010).

Unfortunately, typical hyperthermia procedures are not optimal since they are not minimally invasive and generate heat across the body in a non-specific manner (Kaur et al., 2016). As a result, major undesired side effects are developed. For instance, whole-body hyperthermia may result in cardiovascular and gastrointestinal adverse effects (Chatterjee et al., 2011) . This method allowed physicians to reach deep-seated targets, but it had one big drawback: the high power density required to properly ablate tumors damages healthy tissue in the beam's path (Hood et al, 2013)

Photodynamic treatment (PDT), which employs a photosensitizer that reacts with tissue oxygen upon exposure to a certain wavelength in the visible or NIR spectrum, is one method used to address this condition. However, because these sensitizers (mostly porphyrin-based) remain in the body for extended periods of time, patients are highly sensitive to light and prone to have problems throughout this

treatment (Huang et al, 2008). Traditional PDT relies on the presence of oxygen to form reactive oxygen species, and its depth of penetration severely restricts its applicability (Wilson and Patterson, 2008). Unfortunately, the depth of penetration of classical photodynamic treatment (PDT) of tissues mediated by laser or visible light is insufficient, limiting its utility for deep tumor therapy (Benov, 2015). However, near-infrared (NIR) light (in the wavelength range of 800–1,100 nm) has substantially greater body transparency, making it preferred for photothermal therapy (PTT) (Vines et al, 2019).

3.2 Plasmonic Photothermal Therapy (PPTT)

Photothermal therapy (PTT) is an alternative to these treatments that uses localized photoabsorbing chromophores to achieve spatially targeted heating. Due to the significant physiological transmissivity observed at these wavelengths. (Hood et al, 2013) PTT typically employs chromophores with absorption peaks within the NIR region, reducing unwanted tissue absorption and associated heating (Bayazitoglu et al, 2013).

Photothermal therapy is based on the conversion of light energy (typically in the near-infrared region) into heat energy to induce necrosis or apoptosis in subsequent cells (Vines et al, 2019). Photothermal therapy is a less invasive method of destroying cancer cells by the conversion of photon energy from light to heat. This avoids the severe infection-related complications that are commonly encountered after surgery (Kemp et al, 2016), as well as the toxic drug-related side effects of chemotherapy (Moustafa et al, 2019).

Plasmonic photothermal therapy (PPTT) is a targeted photothermal therapy form of cancer treatment that uses the photothermal effect of nanoparticles, such as gold or silver nanoparticles, to destroy cancer cells. The nanoparticles are delivered to the site of the cancer and then exposed to laser light of a specific wavelength that excites the electrons in the nanoparticles. This creates plasmons, which are collective oscillations of electrons on the surface of the nanoparticles, and results in the conversion of light energy into heat. The generated heat is then used to destroy the cancer cells, while minimizing damage to surrounding healthy tissue (Sztandera et al, 2019).

The difference between traditional hyperthermia and plasmonic photothermal therapy is that plasmonic photothermal heating occurs only in the immediate vicinity of gold nanoparticles, and local temperatures can rise tens or hundreds of degrees above the body's normal temperature. This suggests that photothermal heating could be more selectively applied to tumors as opposed to healthy tissue in order to lessen the adverse side effects of cancer therapy (Day et al, 2009).

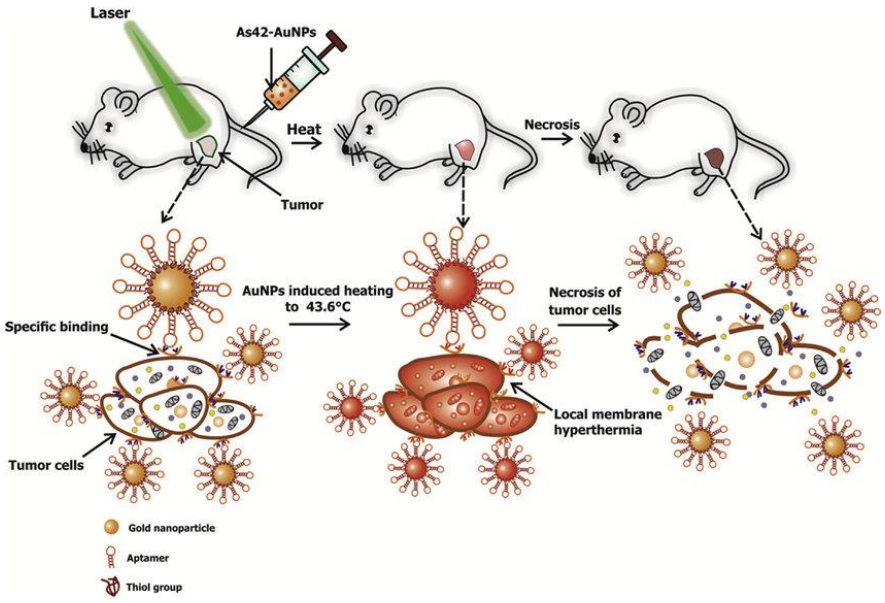

Figure 2 Schematic of Plasmonic Photothermal Treatment for the Selective In Vivo Destruction of Cancer Cells Using As42-AuNPs After being injected into a mouse tail vein, As42-AuNPs become concentrated on the tumor cells. Green laser localization at a tumor site results in nanoparticle heating and cell death, followed by the removal of the tumor. (Kolovskaya et al., 2017)

Heating sources, including NIR or visible light, the magnetic field, radiofrequency waves, microwaves, and ultrasound waves, are used to induce a moderate temperature rise, in a specific target region in order to destroy the cancer cells (Huang et al, 2008). NIR light which is most commonly used because of its ease in clinical application, has wavelengths between 750 and 1700 nm (the first window is between 750 and 1000 nm, and the second window is between 1000 and 1700 nm36), where water absorption is minimal and light can deeply penetrate tissues to reach the tumor site (Moustafa et al, 2019)

In short, a PPTT procedure with gold nanoparticles includes the deployment of synthesized GNPs, modified to specifically target the tumor cells and their irradiation under a NIR source, commonly a laser, in order to produce heat in a controlled area and manner resulting in cancer ablation.

3.3 Laser Configurations used in Photothermal and Plasmonic Photothermal Therapy – Near Infrared Irradiation

Light possesses fundamental physical properties that are important in clinical applications. Light is a type of electromagnetic radiation that has both wave and particle qualities. The wavelength (the distance between two peaks), frequency, and amplitude are all characteristics of light. Light is also distinguished by its energy content. This energy is measured in joules (J). The amount of energy delivered per unit time is measured in watts (W = J/second). Light is commonly reported in terms of wavelength (nm), energy (J), irradiance or power density (W/cm2), and radiant exposure, fluence, or dose (J/cm2) (Jenkins et al, 2011).

A laser configuration is a device that produces a highly collimated, monochromatic, and directional beam of light by amplifying light through a process called stimulated emission. In stimulated emission, a population of atoms or molecules in the gain medium of a laser is excited to a higher energy level by a pumping mechanism, such as a light source or an electrical current (Chen et al, 2011). As the excited atoms or molecules return to their lower energy level, they release photons that are collimated and amplified by the resonant cavity of the laser, producing a laser beam. The term "LASER" is an acronym that stands for "Light Amplification by Stimulated Emission of Radiation." Lasers are widely used in a variety of applications, including medicine, communication, industry, and science, due to their ability to produce a highly focused and intense beam of light (Szymanska et al, 2013).

A NIR (near-infrared) laser is a type of laser that emits light in the near-infrared region of the electromagnetic spectrum. NIR lasers typically operate at wavelengths between 700 nm and 1500 nm and are characterized by their ability to penetrate various materials, including biological tissues, plastics, and liquids. (Frank et al, 2004). NIR lasers are commonly used in a variety of applications, including medical diagnosis, environmental monitoring, food analysis, and industrial process control, among others. In medical diagnostics, NIR lasers are used to monitor the oxygenation levels of blood, measure glucose levels, and monitor blood flow, among other applications (Baffou et al, 2013).

Near-infrared radiation has a unique set of **properties** that make it ideal for use in photothermal treatments. Understanding the physical interactions between tissue and light is crucial. When light strikes the surface, a part (10%) of it is reflected (Steiner et al, 2011). The energy that does pass through the surface is refracted or bent in the direction of a line perpendicular to the surface. This is due to light's particle nature. Of course, these particles are photons. Photons that enter the tissue can be passed through it, dispersed, or absorbed. Scattering increases the volume of tissue that is influenced by light. Photons can switch directions without losing energy. Scattering is especially prevalent at contacts between tissues. At such interactions,

reflection or refraction also occurs. These effects help to shorten the distance that light travels or penetrates into tissue (Wan et al, 1981).

The majority of tissues can absorb light energy. Typically, this occurs when a molecule absorbs a photon. Metal ion-containing molecules have a significant ability to absorb photonic energy, as do DNA and water. The energy absorbed by a molecule can alter its confirmation and/or function (Henderson et al, 2015).

Several parameters impact the depth of NIR tissue penetration: wavelength, energy, attenuation coefficient (consisting of scattering, refraction, and absorption), irradiance area, coherence, and pulsing. Typically, longer wavelengths (up to 1,000 nm) lead to deeper penetration; but, above 1,000 nm, water absorption becomes predominant (Steiner et al, 2011). In general, increases in power density will result in better penetration. The tissue will be traversed by more photons. Due to scattering factors, surface irradiation area also impacts penetration.

When waves of monochromatic light are aligned, a feature known as coherence occurs. This means that each point on the wave has the same amplitude and location as the comparable point in an adjacent wave. The minute changes in the waveform over time are reflected by the temporal coherence. The waveform's temporal coherence increases with waveform consistency. High temporal coherence is generally found in monochromatic light. The deviation of the light from the point of emission causes spatial coherence (Karu et al, 2003). Lasers produce a long, narrow volume of coherent light with almost no spatial divergence. A long, narrow volume of coherent light produced by a laser, in contrast, can reach deeper into tissues (Henderson et al, 2015).

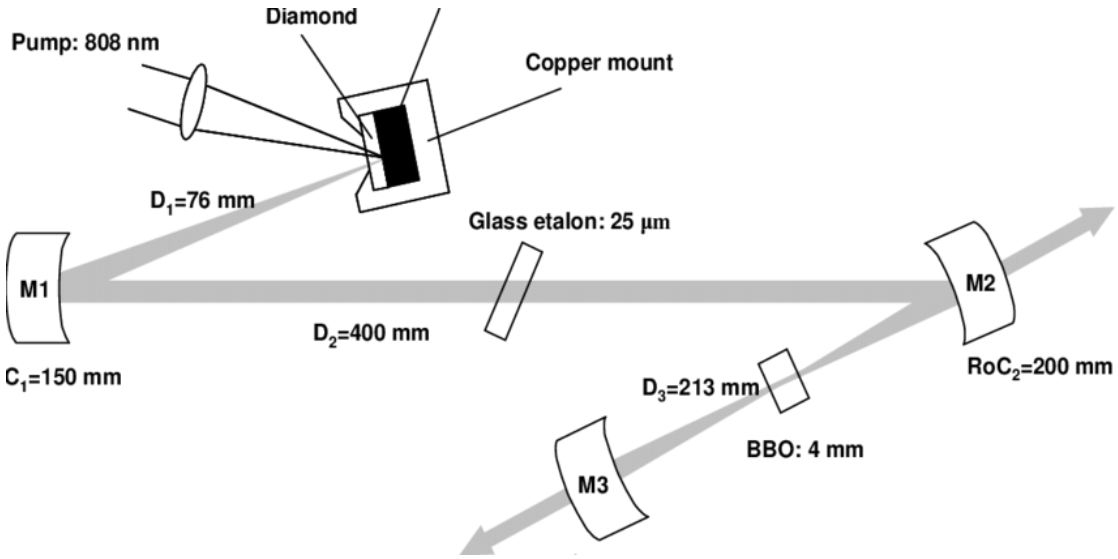

Figure 3 Diagram of a laser setup: A gain mirror and three curved mirrors with high reflective values make up the laser cavity. The outputs of mirrors M2 and M3 showed frequency doubled emission. RoC stands for radius of curvature, D for distance between mirrors, and BBO for barium borate crystal. It was possible to see free flowing laser emission at about 1230 nm without the nonlinear crystal and the glass etalon. The free spectral range of the 300 m thick diamond heat spreader functioning as an intracavity etalon separates a comb of lines in the free running laser spectrum. This characteristic appears as a result of the coated diamond's residual reflection.

The frequency and form of the waves are slightly distorted when coherent light penetrates a tissue. As a result, there may be interference between the waves. Interference is also influenced by polarization that is the angle at which a wave vibrates. When the amplitude of a wave at a particular position differs from that of an adjacent wave and the population of coherent light waves, interference occurs on a single wave basis. The amplitudes at the point of difference may either wipe each other out, be additive, or vary. These interactions produce a speckle intensity pattern, which is a field of unevenly spaced spots with varying light intensities. The effective penetration depth might be significantly impacted by speckles (Hode, 2005). Because of this, high intensity regions will reach deeper or contain energy that is two or three order of magnitude higher at a given depth.

The quantity of energy delivered to any specific spot at the peak of a pulse and the depth of penetration both increase when NIR is pulsed. However, as pulsing allows for energy output troughs, the total amount of energy given to the tissue may be equal to or even lower than that of a continuous emission. In contrast to LEDs, lasers have the ability to pulse (Henderson et al, 2015).

The main advantage of NIR lasers is their non-invasiveness and their ability to penetrate various materials. This makes them ideal for measuring parameters in hard-to-reach or inaccessible areas, such as inside a living organism or in a sealed container. Additionally, NIR lasers are highly sensitive and can be used to detect even small changes in the parameters being measured (Hirsch et al, 2003)

The physics of NIR lasers involves the interaction of light with matter to produce a laser beam. The basic components of an NIR laser include a gain medium, a resonant cavity, and a pumping mechanism (Huang et al, 2014).

1. Gain medium: The gain medium is the material that amplifies the light energy to produce a laser beam. It can be a solid-state material, such as a crystal or a semiconductor, or a gas or a liquid. The gain medium absorbs light from the pumping mechanism and releases it in the form of laser light.
2. Resonant cavity: The resonant cavity is an optical structure that contains the gain medium and provides feedback to the light that is emitted by the gain medium. The cavity is designed to allow only light of a specific wavelength to be amplified, producing a highly collimated, monochromatic, and directional laser beam.
3. Pumping mechanism: The pumping mechanism is used to excite the gain medium and provide the energy required to produce the laser light. It can be a light source, such as a lamp or a flashlamp, or an electrical current, such as a diode or a laser diode.

The laser light produced by the NIR laser passes through the gain medium and is amplified by the resonant cavity, producing a laser beam. The laser light can be focused and directed to a specific target, where it can be used for various medical or industrial applications (Parsons et al, 2010).

Various **NIR laser systems** are used in medicine for different medical applications, including phototherapy, surgery, diagnostics, and imaging (Steiner et al, 2011). Some of the common NIR laser systems used in medicine include:

- Diode lasers: These are solid-state lasers that use a semiconductor material to produce laser light in the NIR spectrum. They are compact, portable, and relatively

inexpensive, making them a popular choice for various medical applications, such as soft tissue surgery, pain management, and phototherapy.

- CO2 lasers: These are gas lasers that produce NIR laser light in the 10600 nm wavelength range. They are commonly used in surgical applications, such as cutaneous, gynecological, and ophthalmological procedures, due to their ability to precisely cut through soft tissues with minimal damage to surrounding tissue.
- YAG lasers: These are solid-state lasers that produce NIR laser light in the 1064 nm wavelength range. They are commonly used in medical applications that require high-energy, such as laser-assisted lipolysis, skin rejuvenation, and tattoo removal.
- Dye lasers: These are liquid lasers that use a laser-active dye as the gain medium to produce laser light in the NIR spectrum. They are widely used in medical applications, such as dermatology, dermatologic surgery, and phototherapy.
- Holmium lasers: These are solid-state lasers that produce NIR laser light in the 2140 nm wavelength range. They are commonly used in urological procedures, such as lithotripsy and prostate surgery, due to their ability to precisely cut and ablate tissues.

In **photothermal therapy**, NIR laser light is used to heat up and destroy abnormal tissues, such as tumors or cancer cells, by converting the laser energy into heat. The NIR laser light is absorbed by chromophores in the target tissues, which leads to an increase in temperature and eventual thermal damage to the target. In order to maximize the effectiveness of photothermal therapy and minimize damage to surrounding healthy tissues, NIR lasers for photothermal therapy may be combined with other technologies such as optical imaging or nanotechnology (Hode et al, 2005). It is particularly suitable for medical applications because NIR light can penetrate deep into biological tissues without causing significant damage or thermal damage. The depth of penetration of an NIR laser into human tissues, particularly oral tissues, depends on several factors, including the wavelength of the laser, the optical properties of the tissues, and the laser power and pulse duration. This depth can vary, but it is typically in the range of a few millimeters to several centimeters, depending on the specific laser system and the tissue optical properties (Jenkins et al, 2011).

The most common NIR laser systems used in photothermal therapy are diode lasers and CO2 lasers (Missert et al, 2016).

- Diode lasers: These are solid-state lasers that use a semiconductor material to produce laser light in the NIR spectrum. They are compact, portable, and relatively inexpensive, making them a popular choice for plasmonic phototherapy. Diode lasers, use a p-n junction semiconductor as the gain medium. In a diode laser, the p-n junction is placed between two mirrors that form a resonant cavity. When an electrical current is applied to the diode, electrons are injected into the p-type material, where they combine with holes in the n-type material to produce a population of excited electrons. As the excited electrons return to their lower energy level, they emit photons that are collimated and amplified by the resonant cavity of the laser. The laser light is then emitted through one of the mirrors, producing a laser beam.
- CO2 lasers: These are gas lasers that produce NIR laser light in the 10600 nm wavelength range. They have a long history of use in medical applications, including surgery and phototherapy. CO2 lasers work by passing an electric current through a

gas mixture of carbon dioxide, nitrogen, and sometimes a small amount of another gas, such as helium or xenon. The current excites the molecules in the gas mixture, causing them to emit light at a specific wavelength. This light is then directed through a resonator, which amplifies the light and focuses it into a coherent, high-intensity beam. The CO2 laser is unique in that it emits light in the infrared part of the spectrum, specifically at a wavelength of 10.6 micrometers. This wavelength is absorbed by many materials, including organic materials, making it useful for a wide range of cutting, welding, and marking applications. In addition to its versatility, the CO2 laser is also notable for its high energy efficiency, as it can convert a significant portion of the electrical energy it consumes into laser energy. CO2 lasers have a high power output and are able to penetrate deep into tissues, making them an effective choice for photothermal therapy.

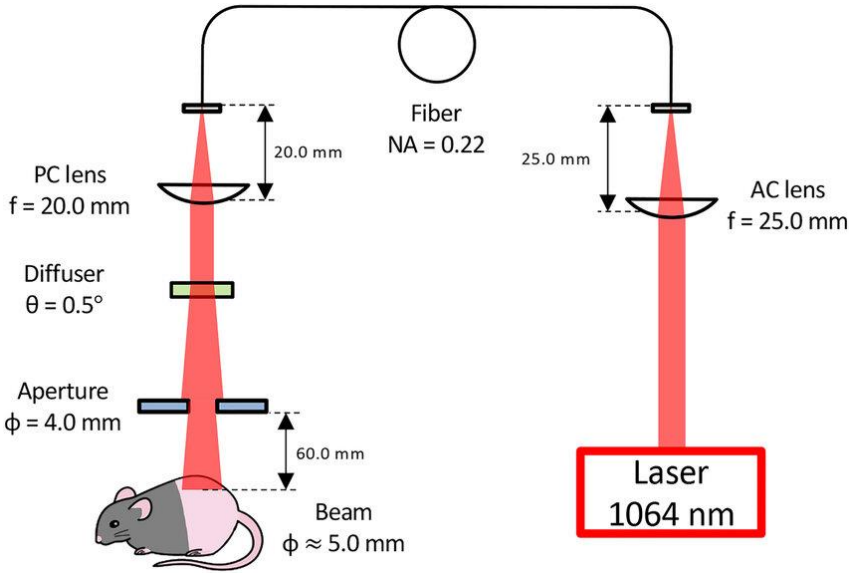

Figure 4 NIR laser irradiation system diagram. NIR light comes from a continuous wave (CW) Nd:YAG laser with a wavelength of 1064 nm. An achromatic lens directs the 1064 nm beam toward the multimode optical fiber. A holographic diffuser is placed in the optical path to spread the beam mode and produce a homogenized flat-top intensity distribution. A plano-convex lens collimates the divergent laser. By altering the aperture's size and the space between an animal's iris and the beam, the beam diameter was set at 5 mm.

Plasmonic photothermal therapy (PPTT) is a higly specialized type of photothermal therapy of cancer that uses plasmonic nanoparticles to convert light into heat and destroy cancer cells. Plasmonic nanoparticles are tiny particles that exhibit plasmonic behavior, meaning they can support surface plasmon resonances (SPRs) (Baffou et al, 2013).

The most common NIR laser wavelengths that are used in PPTT include:

- 808 nm diode laser: This laser is one of the most popular for PPTT due to its ability to penetrate deep into tissues and its relatively low cost.
- 915 nm diode laser: This laser has a slightly longer wavelength than the 808 nm laser, which can improve the thermal efficacy of the therapy by reducing light scattering in tissues.

- 1064 nm Nd:YAG laser: This laser is more expensive than diode lasers, but it has a higher energy output and a longer wavelength that can penetrate even deeper into tissues.
Other NIR lasers that are sometimes used for PPTT include fiber lasers and Er:YAG lasers. The choice of laser for PPTT will depend on factors such as the type of plasmonic nanoparticles being used, the depth of the cancerous tissue, and the size of the treatment area.

3.4 Nanomaterials used for PPTT

Some of the current technologies used for hyperthermic therapy involve nanoparticles, including ferromagnetic nanoparticles such as iron oxide, doped iron oxide, and super-paramagnetic iron oxide nanoparticles (SPION), as well as carbon nanotube (CNT) technologies (Vines et al., 2019).

Ferromagnetic nanoparticles, including SPION, iron oxide, and doped iron oxide, can be stimulated using alternating magnetic fields (AMFs), causing them to rapidly magnetize and demagnetize. This stimulation generates heat suitable for thermal therapy. However, a challenge with magnetic nanoparticle-based therapy is that AMF fields are typically applied to the entire body rather than precisely targeting the tumor as in photothermal techniques, making it difficult to achieve precise and accurate tumor therapy (Dennis et al., 2008).

CNTs are nanomaterials composed of carbon atoms arranged in a honeycomb-like lattice, forming tubes with diameters of a few nanometers and lengths ranging from hundreds of nanometers to microns (Kaur et al., 2016). CNTs can respond to light across a wide spectrum, including visible and near-infrared (NIR) light. However, concerns regarding the long-term biocompatibility of CNTs have been raised due to the development of granulomas similar to asbestos-linked mesothelioma in mice (Poland et al., 2008).

Polymeric materials designed for photothermal therapy (PTT) applications have also been explored. While these polymer-based nanoparticle systems show potential, some, such as polydopamine, exhibit suboptimal mass extinction coefficients and lower photothermal efficiency (Dong et al., 2016). Moreover, the breakdown profiles of many of these polymers are not well understood, raising concerns about their long-term biocompatibility (Cheng et al., 2014). Hence, utilizing nanomaterials with a longer history of proven clinical utilization may be advantageous (Vines et al., 2015).

Metallic nanoparticles, when exposed to light at their resonance wavelength, undergo a collective oscillation of conduction-band electrons known as localized surface

plasmon resonance (LSPR). This phenomenon leads to significant light scattering or absorption, resulting in a fivefold increase in light absorption compared to conventional photoabsorbing dyes (Huang et al., 2008).

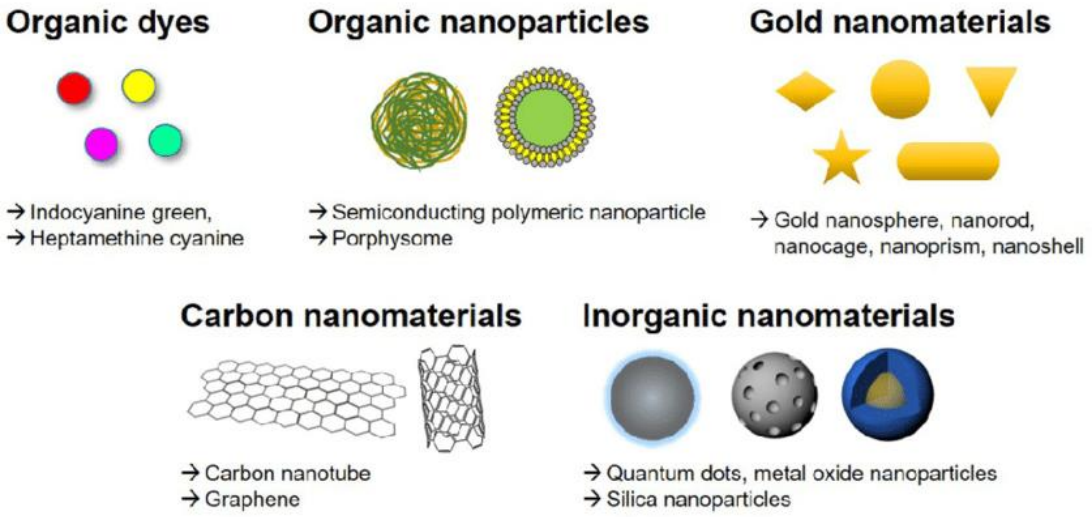

Figure 5 Different types of photothermal agents used for PTT. (Han and Choi, 2021)

3.5 Gold Nanoparticles

3.5.1 Gold In Medicine

Gold, symbolized as Au and with atomic number 79, is a chemical element. It is considered one of the naturally occurring elements with higher atomic numbers. In its pure form, gold is a bright, slightly orange-yellow, dense, soft, malleable, and ductile metal. It falls under the category of transition metals and is classified as a group 11 element. Gold exhibits low reactivity compared to other chemical elements and remains solid under standard conditions. It is commonly found in a free elemental state as nuggets or grains within rocks, veins, and alluvial deposits. Gold can also form solid solutions with silver (as electrum), naturally alloy with metals like copper and palladium, and occur as inclusions within minerals such as pyrite. Additionally, gold can be found in the form of gold compounds, often in association with tellurium (known as gold tellurides) (Hammer et al., 1995).

Due to its chemical inertness, resistance to microorganisms, and biocompatibility, gold has emerged as a valuable substance in improving medical treatments. Historical evidence suggests that gold was utilized over 4,000 years ago to restore teeth affected by decay (Moustafa et al., 2019). It has also been employed in the treatment of syphilis, either alone or in combination with sodium chloride (Pricker et al., 1996). Notably, the presence of gold in compounds, particularly gold cyanide, was found to inhibit the growth of tuberculosis-causing bacteria by German bacteriologist Robert

Koch (Benedek et al., 2004). In 1890, French chemist Jacques Forestier discovered the anti-inflammatory properties of gold compounds, which later led to the development of medications for rheumatoid arthritis treatment in 1929 (Kean et al., 1997).

Gold nanoparticles (AuNPs) have been the subject of scientific study since the initial report by Michael Faraday in the mid-19th century when he created gold colloidal solutions (Edwards et al., 2007). Faraday's lecture titled "Experimental Relations of Gold (and Other Metals) to Light" at the Royal Institution in London in 1852 was the first to highlight the reduction of gold salts, producing solutions containing finely divided particles with a ruby color (Faraday, 1857).

3.5.2 Synthesis of Gold Nanoparticles

Gold nanoparticles (GNPs) can be synthesized using physical or chemical methods, employing either a bottom-up or a top-down approach (Cunningham et al., 2013). The most commonly used bottom-up technique is the Turkevich and Brust approach, where metal salts are reduced to produce spherical and monodisperse GNPs with diameters ranging from 10 to 20 nm. Sodium citrate salts are often used as a reducing agent and stabilizer during synthesis to prevent GNP aggregation (Shah et al., 2014; Zare et al., 2010). Alternative reducing agents such as ascorbic acid, amino acids, and ultraviolet light have been investigated as substitutes for citrate (Mieszawska et al., 2013).

Top-down approaches involve the fabrication of nanoscale materials through the lithographic processing of larger macrostructures (Cunningham et al., 2013). Other physical synthesis techniques include sonochemical, microwave, and photochemical methods (Herizchi et al., 2016). A recent method proposes the use of N-cholyl-L-valine (NaValC) as a self-reducing and stabilizing agent, combined with natural solar irradiation, for GNP synthesis (Annadhasan et al., 2015). Another novel approach involves the irradiation of aqueous [AuCl4] with 532 nm nanosecond laser pulses, resulting in the production of monodisperse 5 nm GNPs without the need for capping agents or additives, thus minimizing the risk of chemical contamination (Rodrigues et al., 2018).

The isolation and synthesis of GNPs from natural sources offer advantages over conventional methods. Green synthesis of GNPs using natural compounds holds potential for improving their medical properties, including antimicrobial and anticancer activities. This approach also reduces the need for residual chemicals, making it cost-effective and potentially resulting in GNPs with minimal to no side effects. Bacteria, fungi, and plants are important sources for green synthesis, with Catharanthus roseus (CR) and Carica papaya (CP) leaf extracts being conjugated with GNPs. The combination of biogenic GNPs and the anticancer properties of plant

extracts has shown consistent inhibitory effects on the viability of HepG2 liver cancer cells and MCF7 breast cancer cells (Kumar et al., 2008; Le Renard et al., 2010; Vines et al., 2019).

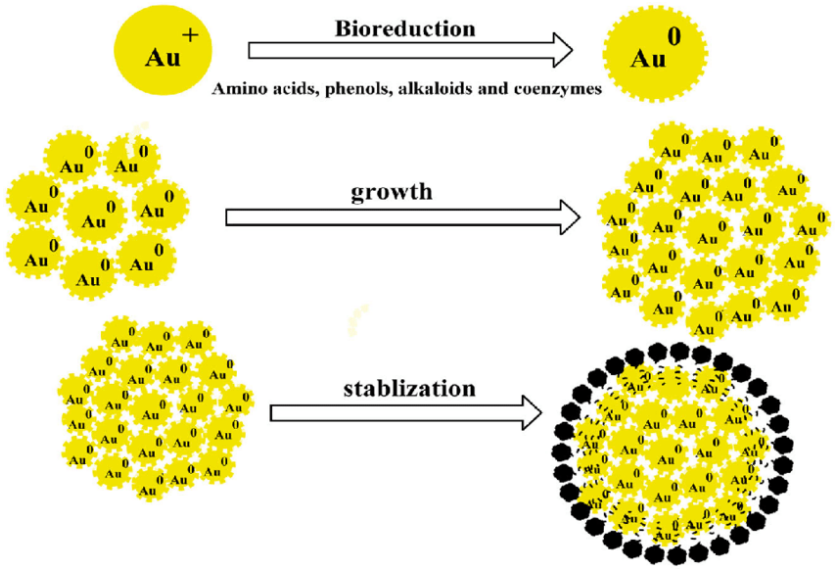

Figure 6 Mechanistic approach for green synthesis of Gold nanoparticles (Nadeem et al., 2017)

Baicalin, an anticancer flavonoid found in Scutellaria baicalensis, was conjugated with gold nanoparticles. Baicalin is an active flavonoid found in Scutellaria baicalensis. Baicalin-produced gold particles exhibited cytotoxicity against the MCF7 cell line (Lee et al., 2016). Croin, which is the primary carotenoid present in the stigma of saffron (Crocus sativus) and possesses antioxidative properties, mediated the reduction reaction of Au 3+ ions, resulting in the creation of gold nanoparticles of regulated sizes. The conjugation of gold nanoparticles with croin significantly inhibited the multiplication of breast cancer cells. (Hoshyar et al., 2016). Against U87 glioblastoma (GNB) cells, gold nanoparticles conjugated with plant extracts obtained from the leaves and stems of Hibiscus sabdariffa exhibited selective cytotoxic action. (Mishra et al., 2016).

Overall, the use of natural derivatives as a supplement to cancer therapy utilizing gold nanoparticles looks to be a viable strategy for the selective targeting of tumors, hence decreasing any adverse effects that may be caused by the use of synthetic therapeutic components. (Vines et al, 2019)

3.5.3 Surface Modification of Gold Nanoparticles for Specific Tumor Targeting

Non-specific targeting of tumor cells, relies on the passive accumulation of therapeutic agents in the tumor due to the enhanced permeability and retention (EPR) effect. This effect is based on the fact that tumors have a leaky and disorganized vasculature, which allows larger molecules, such as gold nanoparticles, to extravasate and accumulate in the tumor. This approach has the advantage of being simple and cost-effective, but can result in lower accumulation of therapeutic agents in the tumor and increased exposure of healthy tissue to the therapeutic agent. Due to EPR, GNPs can passively concentrate in tumor locations, where they are most likely taken up by non-specific receptor-mediated endocytosis (RME) (Chithrani et al., 2006). GNPs may be capable of passive transport to tumor locations to a limited extent, although there are limitations because to the vascular heterogeneity of many types of cancer. In addition, particles and reticuloendothelial system (RES) uptake limit passive drug distribution (Choi et al, 2003)

Specific targeting on the other hand, involves the use of specific molecular moieties, such as antibodies or peptides, to direct the therapeutic agents directly to the cancer cells. These moieties specifically recognize and bind to receptors that are over-expressed on the surface of cancer cells, effectively delivering the therapeutic agent directly to the site of the cancer. This approach has the advantage of increasing the concentration of therapeutic agents at the site of the cancer and minimizing damage to healthy tissue.

GNPs possess distinctive physiochemical features, such as the capacity to bind thiol and amine groups, as well as surface plasmon resonance (SPR), which permits their modification for more targeted cancer therapy (Shukla et al., 2005). Numerous tiny compounds, proteins, and peptides have been designed to attach to particular receptors on tumor cells exhibiting varied degrees of tumor formation. (Khlebtsov et al, 2011).

Targeting ligands may consist of antibodies that bind to an overexpressed protein,48 RNA/DNA aptamers that fold into unique 3-D conformations via intermolecular interactions and bind to target molecules on cellular surfaces, (Huang et al, 2008) or molecules such as folate that facilitate translocation into cancer cells overexpressing folate receptors via receptor-mediated endocytosis. (Tong et al, 2009)

By conjugating tumor-specific recognition molecules such as transferrin, folic acid, epidermal growth factor (EGF), or any number of monoclonal antibodies to the surface of GNPs, more specific tumor targeting can be obtained (Eghtedari et al., 2009). Using this targeted method, it was demonstrated that substantially larger quantities of GNPs can be employed while avoiding significant accumulation of nanoparticles in the liver and kidneys (Patra et al., 2008).

PEGylation, which can be accomplished by employing thiol-terminated methoxypoly (ethylene glycol) to replace the stabilizing surfactant bilayers that ordinarily surround GNPs, is a technique that can be used to modify GNPs (Liao et al, , 2005). By altering the surface of GNPs with polyethylene glycol, the affinity of PEG for cellular membranes may increase cellular absorption (Paciotti et al., 2006).

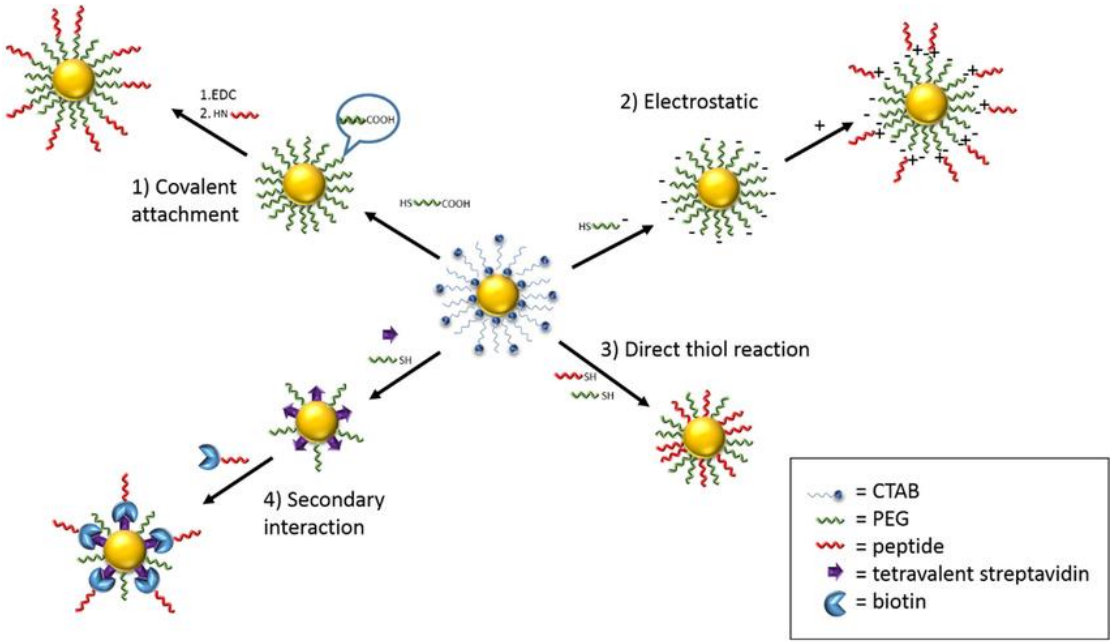

Figure 7 The four main methods for surface modification of a nanoparticle, with PEG serving as the antifouling substance and a peptide serving as an example of a biomolecule. (1) Covalent attachment: Between the antifouling layer and the end groups of biomolecules, covalent interactions like EDC/NHS coupling take place; (2) Electrostatic: Use biomolecules and cationic/anionic antifouling substances to enable charge-charge conjugation; (3) Direct thiol reaction: loading of biomolecules and anti-fouling substances via thiol binding to the surface; (4) Secondary interaction: To enable ligand-receptor-specific conjugation, biomolecules containing a specific receptor are deposited onto the surface before ligands. (Sriram et al., 2015)

3.5.4 PPTT with Gold Nanoparticles

In cancer therapy, the heat emitted by gold nanoparticles can be used to damage/destroy malignant cells and tissues.

The first instance of photothermal cancer therapy mediated by gold nanoparticles was described in 2003 by West, Halas, and colleagues (Calderwood et al., 2008). Gold nanoshells comprised of 110 nm silica cores surrounded by 10 nm gold shells were functionalized with the biocompatible polymer polyethylene glycol (PEG) (PEG). Gold nanoshells were injected directly into the tumors, and NIR irradiation (820 nm, 4 W/cm2, 6 min) caused an average temperature increase of 37.4 +- .6 °C in the irradiated tumor location, compared to 9.4 +-4.7 °C with the laser alone. The histological examination of tumors demonstrated heat damage, including coagulation and cell shrinkage. Due to the rapid diffusion of the nanoshells throughout the tumor and the high tissue absorption, the maximum depth of the injured areas was only 46 mm, indicating a limitation of the treatment 31 (Hirsch et al., 2003).

In 2004, the same team conducted a study demonstrating the in vivo photothermal killing of CT26.WT colon tumors in BALB/ cAnNHsd mice. The tumors disappeared ten days after therapy, and all animals remained healthy and tumor-free for 90 days. In contrast, all controls exhibited considerable tumor growth and

averaged only 10 days of survival. This suggested there was some possibility in photothermal cancer therapy utilizing gold nanoparticles (O'Neal et al, 2004).

El-Sayed and colleagues have enhanced the potential application of photothermal therapy by employing gold nanoparticles. (El-Sayed et al, 2006) in a study with human squamous cell carcinoma cells as well.

Conditions for nanoparticle LSPR and irradiation can be optimized to increase heating efficiency (Link et al., 1999). Since irradiation is targeted to the tumor site, it may be possible to avoid the undesirable side effects of conventional cancer treatments. However, photothermal therapy may also be used in concert with other cancer treatments, such as chemotherapy, to increase tumor killing (Wust et al., 2002).

3.5.5 Advantages of Gold Nanoparticles for PPTT

Gold nanoparticles have several benefits that make them ideal for the photothermal treatment of cancer. Gold nanoparticles have considerable advantages for the following reasons:

(1) Excellent Biocompatibility, **.** Gold is more chemically inert than other metals, which could render the gold nanoparticles biocompatible. Studies of short-term gold nanoparticle exposure to diverse cell types reveal that, at clinically relevant concentrations, they are noncytotoxic and nonimmunogenic.

(2) they can be delivered locally to the tumor while limiting non-target dispersion.

(**3) Ease of Synthesis**. With breakthroughs in synthesig methodsn, scientists have been able to deliver sarrangements of gold nanoparticles of varied sizes and forms **.**

(4) Great capability for Surface Modification. They can be modified to develop complex PTT and medication delivery systems for cancer**.** Since gold nanoparticle size, shape, and surface chemistry are highly modifiable, it may be possible to tailor them for maximum tumor accumulation and actively target tumor locations.

(5) Unique Optical and Physical Properties. They can be activated by near-infrared (NIR) laser light, allowing them to deeply penetrate biological tissues while light absorbed by nanoparticles of specified shapes and sizes can be transformed into nonradiative heat with great efficiency (Huang et al., 2007).

It is important to highlight that cytotoxicity attributed to synthesis techniques has historically been a barrier to the in vivo application of GNPs. Recent developments have shown that the addition of polyethylene glycol (PEG), dense silica (d-SiO2), and titanium dioxide (TiO2) coatings significantly reduces cell damage (Bao et al., 2016).

3.5.6 Commonly Used Gold Nanoparticle Configurations

The transparency of the human body to near-infrared (NIR) light in the range of 800 to 1200 nanometers has led to the utilization of gold nanorods (GNRs) or hollow gold nanoshells to modify the geometry of gold nanoparticles (GNPs) and shift their resonance peak towards the NIR spectrum (Loo et al., 2004). Various shapes of gold nanoparticles, including nanorods, nanoshells, nanocages, and nanostars, have been found to absorb NIR light. Recent studies have also demonstrated the photothermal capacity of alternative shapes of gold nanoparticles such as bipyramids, nanoprisms, nanorings, and caterpillar-like nanoparticle assemblies (Xia et al., 2018). The use of gold nanospheres (GNS) for photothermal therapy (PTT) was first demonstrated by El-Sayed et al., making them one of the earliest investigated GNP shapes (Huang et al., 2008). GNS have gained popularity in PTT applications due to their simple manufacturing process, small size, rapid synthesis, and the ability to conjugate ligands. Modified versions of gold nanospheres have shown therapeutic properties when coupled with antibodies targeting specific proteins overexpressed in malignancies, and they have been combined with other metals to enhance their photoacoustic and photothermal features (Day et al., 2010; Zhang et al., 2015).

Gold nanostars exhibit enhanced NIR light absorption along with reduced toxicity (Chen et al., 2015). Their unique branch-like structure provides tip-enhanced plasmonic characteristics (Ahmad et al., 2016). Numerous studies have demonstrated the effective use of multifunctional gold nanostars in photothermal applications using NIR light to target various types of cancer cells (Li et al., 2016).

Gold nanoshells consist of silica gels encapsulated by a thin, hollow gold shell (O'Neal et al., 2004). By adjusting the thickness of the shell and the diameter of the core, gold nanoshells can be tailored to absorb NIR light, making them suitable for photothermal and photoacoustic applications (Hirsch et al., 2003). Gold nanoshells offer unique flexibility in their preparation, allowing them to mimic the aspect ratios of other nanomaterial configurations such as nanorods, which can enhance attributes like cellular uptake and increase drug loading capabilities due to their larger surface areas (Vines et al., 2019). The synthesis process for gold nanoshells involves growing silica nanoparticles, attaching gold seeds to the silica surface through molecular linkage, and adding gold nanoparticles to the seeds by reducing gold ions in the production medium (Loo et al., 2004).

Gold nanorods (GNRs) were first synthesized by Wang et al. (Chang et al., 1997), and their application in NIR photothermal therapy was reported by El-Sayed et al. in 2006 (Jain et al., 2006). The unique structure of GNRs, which possess longitudinal and transverse plasmons, contributes to their potent photothermal characteristics (Hwang et al., 2014). GNRs have gained significant popularity and are widely utilized in the development of photothermal technologies for cancer therapy, with various designs and modifications being explored (Vines et al., 2019).

Popcorn-like nanostructures of gold were developed by Zhang et al. (2019), while gold nanoflowers (GNFs) were recently introduced by Li et al. (2015). Au nanocages (AuNCs) for photothermal cancer cell destruction were created

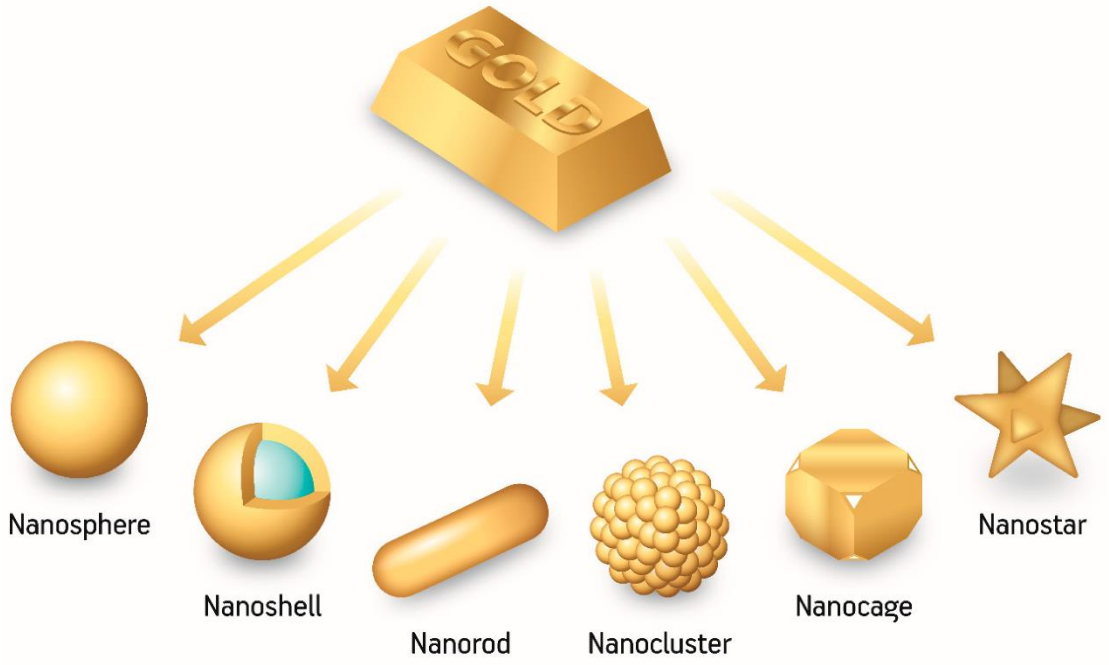

Figure 8 Representative scheme of the most common gold nanoparticle assemblies and morphologies.(Freitas de Freitas et al., 2018)

3.5.7 Limitations Of Gold Nanoparticles For PPTT

The ideal candidate for photothermal therapy (PTT) should possess certain characteristics: (i) an appropriate nanoparticulate size and shape, (ii) good dispersibility in aqueous medium, (iii) responsiveness to near-infrared (NIR) light in the range of 650-950 nm to minimize damage to healthy cells, provide effective photothermal performance, and enable sufficient penetration depth, (iv) adequate photostability to ensure a suitable diffusion time for targeting tumors before losing photosensitivity, and (v) low or no cytotoxicity in organisms (Zhou et al., 2013).

The long-term cytotoxicity of gold nanoparticles (GNPs) is still not fully understood, and the potential effects of nanoparticle accumulation are largely unknown (Yin et al., 2018). In their study, it was observed that after five days, 46% of the initial dose of positively charged gold-dendrimer complex particles with a size of 5 nm were excreted.

Another study indicated that only approximately 10% of the initial dose was excreted for negatively or neutrally charged nanoparticles measuring 5 nm or larger than 11 nm (Balogh et al., 2007).

The liver and spleen appear to have the most accumulation, with one study revealing foreign bodies in 7 out of 8 spleens and 8 out of 8 livers from mice that had intravenous injections of PEG-coated GNRs (Goodrich et al., 2010). It was hypothesized that such foreign bodies formed as a result of GNR aggregation in these tissues. Furthermore, evidence of chronic inflammation described as minimal to mild was found in the areas surrounding these foreign bodies, albeit the study did not reveal the long-term effects of this inflammation (Hao et al., 2004)

Sadly, experiments on GNPs have only been conducted in animal models for up to six months, leaving unsolved issues about how GNPs effect health over longer time periods. There are still uncertainties over whether GNPs eventually leave the body and whether GNP accumulation can have long-term implications (Goodrich et al., 2010).

3.6. Localized Surface Plasmon Resonance (LSPR)

3.6.1 Generating Heat with Gold Nanoparticles

Colloidal Au displays a distinctive localized surface plasmon resonance (LSPR) when a certain wavelength of light collides with electrons on the surface of gold (Vines et al., 2019).

LSPR is defined as an optical phenomenon in which incident light interacts with surface electrons in a conduction band (Petryayeva and Krull, 2011). The light induces a collective coherent oscillation of conduction band electrons, resulting in the light's extinction. Light scattering and absorption is dependent not only on the nanoparticle's physical size but also on the medium of the colloidal Au (Kelly et al., 2003).

These conduction band electrons are highly polarizable, and when received light resonates with the wavelengths of their surface plasmons, the electrons move under the influence of an external field, resulting in a net charge difference at the nanoparticle edges. Gold nanoparticles can absorb/scatter incident light, and photon confinement results in the creation of strong electromagnetic fields at the metal's surface as well as a wide range of optical phenomena (Ghosh et al., 2007).

Due to d–d transitions, this excitation induces collective oscillation (localized plasmon oscillations) in AuNPs in the visible area of the electromagnetic light (Mourdikoudis et al., 2018). The oscillation of surface plasmons can deteriorate nonradiatively by transferring energy to heat (Moustafa et al., 2019).

Small colloidal Au absorbs visible light in the blue-green and red regions of the visible spectrum. In large colloidal Au, however, the LSPR leads in the absorption of longer wavelengths of light along the red section of the VLS, resulting in the reflection of blue-spectrum light. The particle sizes of colloidal Au influence the plasmon bandwidth of the gold nanoparticles. Due to electron oscillations along each axis, the

plasmon resonance band may split into many peaks in anisotropic nanoparticles (Nardine et al., 2016).

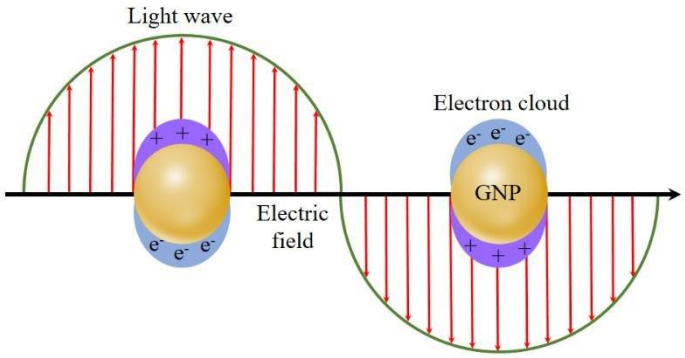

Figure 9 Surface Plasmon Resonance of gold nanoparticles.(Ismail et al., 2019)

Gold nanorods (GNRs) can exhibit both longitudinal and transverse surface plasmon absorption peaks. The length of Au nanorods determines the longitudinal resonance, while the diameter of GNRs determines the transverse resonance. Changing the aspect ratio of GNRs modulates the spectral position of the LSPR, which is well-known (Smitha et al., 2013). Due to variations in their response with light in the visible light spectrum, GNRs with variable aspect ratios (length/width) generate nanorod solutions of varying colour (Pérez-Juste et al., 2005). Two SPR peaks are seen in AuNRs: the transverse peak and the longitudinal peak. The modest transverse SPR peak is around 520 nm in wavelength. Due to a change in the aspect ratio (length of a rod divided by its width), the longitudinal SPR peak of AuNRs moves from the visible to the near-infrared (NIR) spectrum (Moustafa et al., 2019). There are two absorbance peaks in gold nanorods, one associated with the shorter transverse axis near 520 nm and the other with the longer longitudinal axis. The longitudinal peak is more susceptible to aspect ratio (length/width), and when aspect ratio (AR) is increased from 1.1 to 4.4, the max moves from 640 to 850 nm (Nardine et al., 2016).

For normal, **spherical-shaped colloidal Au**, the greatest absorption spectra was between 500 and 530 nm (Vines et al., 2016).

Compared to spherical-shaped gold nanoparticles, three-tipped Au nanoparticles produced by a wet technique exhibited a considerable red-shift (Hao et al., 2004). Between 650 and 700 nm, the branched colloidal Au particles exhibited a plasma band (Vines et al., 2016).

A **gold nanostar**, as specified by a solid core with extending prolate tips, can display hybridized plasmons due to its solid core with projecting tips. The red-shift of gold nanostars ranged from 557 to 700 nm (Chen et al., 2013).

Using colloidal lithography, **Au nanorings** with diameters between 75 and 150 nm were produced. The LSPR of several nanorings ranging in diameter from 75 to 150 nm was between 1,000 and 1,300 nm, demonstrating that the diameter of the ring-like Au structures contributed to their tunability(Larsson et al., 2007).

However, **nanobranches, nanorods, and nanobipyramids** have two primary surface plasmon peaks. There is a consistent LSPR shift toward red light from nanospheres, nanocubes, and nanorods with varied aspect ratios. The greater aspect ratio of the nanorods results in a longer red-spectrum shift. Nanobipyramids with varying aspect ratios also exhibit a red shift in spectrum. Due to their substantial longitudinal electron oscillation, synthesized nanobranches exhibited the greatest red shift in spectrum (Kim et al., 2017).

3.6.2 Explaining the mechanism of LSPR in Gold Nanoparticles

The mean free path of an electron in gold is around 50 nm; accordingly, collisions of conduction band electrons with the surface of a gold nanoparticle are highly dependent on its diameter. Consequently, the LSPR wavelength (max) and extinction cross-section of gold nanoparticle colloids depend on their size and shape (Link et al., 1999). As a result, optical absorbance can be controlled from the visible to the near-infrared (NIR), as demonstrated both experimentally and theoretically . Strong optical absorption and subsequent nonradiative energy dissipation make gold nanoparticles applicable for plasmonic photothermal treatment (Day et al., 2009).

The LSPR oscillation causes a significant temperature increase on the surface of the AuNP when it is exposed to a suitable (resonant) light source, converting the AuNP into a focused nanosource of heat. By using laser radiation with a frequency that greatly overlaps with the AuNPs LSPR band, the intense LSPR absorption, followed by quick energy conversion and dissipation, may be easily utilized band to heat the surrounding area and kill cancer cells (Ali et al. 2019). This effect serves as the foundation for PPTT and offers a potentially beneficial alternative for conventional therapies for localized cancers such chemotherapy, radiation, and surgery.

3.6.2.1 Initiation of LSPR

An essential requirement for interacting with electromagnetic (EM) fields is the presence of a significant number of free conduction and easily polarisable electrons, which are mostly distributed near the surface of AuNPs. Metal nanoparticles produce the surface phenomenon known as LSPR, which causes electrons to collectively oscillate in resonance with incident light. These collective oscillations of free electrons are called Plasmons (Willets et al. 2007). While with increasing distance, the electric field's intensity gradually decreases, it is magnified by several orders of magnitude around the localized plasmons. Along with strong EM fields, these resonances produce a sharp optical absorption or scattering (Kasani et al. 2019).

Resembling the photons in a light wave, Plasmons are quasiparticles formed by oscillating conduction electrons at the interface between a metal and a dielectric and are generated by the electric field vector of incident light (Powell et Swan, 1960). The plasmon of an NP can be regarded as a harmonic oscillator that is light-activated (Guglielmelli et al. 2021). The oscillating electric field generates coherent oscillations of conduction electrons and polarizes the charge on the surface of metal nanoparticles when they are exposed to light (Anker et al. 2008). Resonance is dominated by absorption when the size of the nanoparticles is small (15 nm), and by scattering when the size is bigger (>15 nm) (Kasani et al. 2019).

The cross-section of absorption and scattering by spherical particles whose diameter is less than the wavelength of incident light is explained by the Mie solution which is based on Maxwell's equations (Mie, 1908).

$$\sigma_{\text{ext}} = 9\frac{\omega}{c}\varepsilon_{3/2}V_0\frac{\varepsilon_2(\omega)}{[\varepsilon_1(\omega)+2\varepsilon_m]^2+\varepsilon_2(\omega)^2}$$

where x = 2 for sphere, $V_0 = (4\pi/3)R^3$, ω is the angular frequency of the extinction radiation, ε_m is the dielectric function of the medium surrounding the metal nanoparticles, and ε_1 and ε_2 are the real and imaginary parts of the dielectric function of the metal nanoparticles, respectively.

The application of Mie's theory is restricted to spherical particles. Richard Gans calculated the absorption cross section for the prolate spheroid in 1912, by generalizing Mie's equation based on small particle approximation. (Gans, 1912)

$$\sigma_{\text{abs}} = \frac{\omega}{3c}\varepsilon_m^{3/2}V\frac{\left(\frac{1}{P_j^2}\right)\varepsilon_2}{\left\{\varepsilon_1+\left[\frac{1-P_j}{P_j}\right]\varepsilon_m\right\}^2+\varepsilon_2^2}$$

This provides the extinction spectrum for both the longitudinal and transverse plasmon modes. This equation depicts the connection between shape and LSPR peak wavelength (Kasani et al. 2019).

The singularity condition in LSPR refers to the condition where the frequency of the incident light is equal to the resonance frequency of the plasmonic system. The electric field at the nanoparticle surface is significantly enhanced when this condition is satisfied because the incident light is efficiently coupled to the plasmonic system. The singularity condition can be represented mathematically as:

$R[\varepsilon_1(\omega)] = -2\varepsilon_m$

where ε_m is the dielectric constant of the surrounding medium, ε_1 is the real portion of the metal nanoparticle's dielectric function, and ω is the angular frequency of the incident light. The system's optimal resonance frequency and sensitivity are determined by the singularity condition (Lance, 2002). The singularity condition ($\varepsilon_1 = -2\varepsilon_m$) is met for noble metals like Ag and Au nanoparticles in the visible and near-infrared (NIR) regions, where optoelectronic devices are used and numerous biological applications are carried out.

The resonant frequency in LSPR refers to the frequency at which the collective oscillation of free electrons on the surface of a metal nanoparticle is in resonance with the frequency of the incident light. The light wavelength at which an individual metal nanoparticle exhibits the strongest LSPR effect is known as the LSPR peak. The LSPR peak and the LSPR frequency in general are highly dependent on the material, the dielectric constant of surrounding medium, and the size and shape of the Nanostructure. (Kasani et al. 2019)

3.6.2.2 Optical Results of Gold Nanoparticles' LSPR

Due to the interactions of the nanoparticle with visible light, colloidal gold has been employed by painters for ages. Depending on particle size, shape, local refractive index, and aggregation state, gold nanoparticles absorb and scatter light, producing colors that range from vivid reds (smaller particles) to blues to black to finally clear and colorless (larger particles) (Anderson et al. 1999).

In general, as the size of a symetrical nanoparticles grows, so does the wavelength of light that is absorbed (Link et al. 1999). For instance, the LSPR of 5–10 nm gold nanospheres is 520–580 nm, indicating that they absorb blue light and their colloid appears red as a result. According to Burrows et al. (2016), larger nanospheres have a redshifted LSPR, which means that when they absorb light with longer wavelengths closer to the red, their colloid color takes on more of a purple or blue hue.

The environment in which colloidal gold is suspended can also affect how a gold nanoparticle solution appears to be colored (Underwood et al. 1994). The molecules directly connected to the nanoparticle surface (i.e., nanoparticle ligands) and/or the nanoparticle solvent both may have an impact on the observed optical features since the optical properties of gold nanoparticles depend on the refractive index near the nanoparticle surface. The NP LSPR will switch to longer wavelengths as the refractive index near the gold surface rises. The extinction peak can be adjusted in addition to the solvent environment by coating the nanoparticles with non-conducting shells like silica, biomolecules, or aluminum oxide (Xing et al. 2009).

Finally, as gold nanoparticles aggregate, the effective particle size, shape, and dielectric environment all change, which alters the particle's optical characteristics. (Ghosh and Pal, 2007).

3.6.2.3 Physics of Plasmonic Heating

An AuNP's absorption and scattering cross-sections can be significantly enhanced by efficiently trapping energy within the incredibly small volume of an AuNP using the LSPR (Palpant, 2012). The absorption cross-section indicates the percentage of absorbed light that is re-emitted as heat, whereas the scattering cross-section indicates how much energy is re-radiated by the AuNP in the form of light. As a result, in thermoplasmonics, absorption is what really counts (Baffou, 2017).

It is crucial for us to remember that the optical properties of the nano-objects under investigation are regulated by a series of energy exchanges in order to gain a deeper comprehension of these processes (Guglielmelli et al. 2021). AuNPs can absorb photons via electron transitions when they engage with an impinging short light pulse in the visible-light range. If the incident radiation's frequency fits the LSPR band, a resonant coupling with the EM wave occurs, resulting in excitation at the plasmon resonance. This phenomenon is manifested as a collective, coherent, and dipolar oscillation of electrons in the conduction band. As a result, there is a general nonequilibrium condition. To restore these electrons' internal thermal equilibrium, energy is redistributed inside the quasi-free electronic plasma via electron-electron collisions (e-e). This procedure occurs on a time scale of about 10 fs to 100 fs. Following that, the energy of the hot carriers is redistributed by a relaxation process associated with the electron-phonon-interaction (e-ph) in a time period of 100 fs to 1 ps. The final stage includes the medium surrounding the AuNP and the transmission of thermal energy to the interface via phonon-phonon collisions (ph-ph) on a time scale of 10 ps to 10 ns. This final step (thermal dissipation) causes the AuNP to cool, releasing heat to the surrounding medium and raising its temperature. The heat transfer characteristics of the surrounding medium have an enormous impact on the dynamics of this process (Kim et al. 2019)

As a result of this chain of energy transfers, the internal energy of the electron gas following photon energy absorption passes through:

1) a rapid and resonant enhancement (LSPR)
2) a confined electron gas redistribution (e–e) (athermic regime)
3) a fast decrease (e–ph scattering) and
4) a slow recovery of the initial state of equilibrium (ph–ph) (heat transfer to the surrounding medium). (Guglielmelli et al. 2021)

The electron and lattice temperatures have been mathematically described utilizing the two-temperature model, where Ce and Cl are the electronic and lattice heat capacities; Te is the electron temperature; Tl is the lattice temperature; g is the electron phonon coupling constant; κ’ is the electronic thermal conductivity describing the heat transport away from the excited laser spot; and LP(z,t) is the spatial temporal evolution of the exciting laser pulse (Huang et al., 2014).

$$C_e(T_e)\frac{\partial T_e}{\partial t} = -g(T_e - T_l) + \nabla\cdot(\kappa'\nabla T_e) + \mathrm{LP}(z, t) \quad (1)$$

$$C_l\frac{\partial T_l}{\partial t} = g(T_e - T_l) \quad (2)$$

Due to the requirement of light absorption by the photothermal process, nanoparticle extinction determines the ensuing change in surrounding temperature. The extinction cross-section of gold nanoparticles in the NIR is 108 - 1010 M^{-1} cm^{-1}, which is several orders of magnitude more than the strongest organic chromophores (Huang et al., 2008).

Since there could be millions of atoms in a gold nanoparticle, thus extinction is commonly reported in molarity rather than mass. Absorbance is typically the contributory factor to extinction, and because smaller gold nanoparticles have higher absorbance cross sections over larger nanoparticles (scattering contribution increases

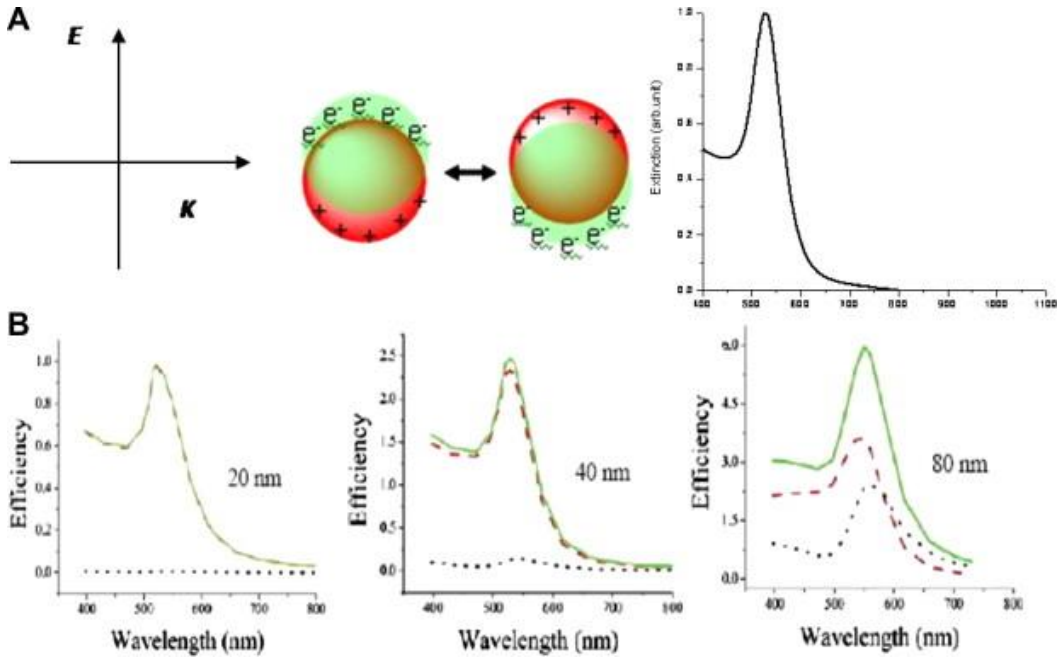

Figure 10 Illustration depicting the predicted absorption and scattering characteristics of gold nanoparticles of various sizes (B) and the localized surface plasmon resonance (A). Conduction band electrons collectively oscillate coherently with regard to the positively charged metallic core as a result of the electric field of incident light. The frequency at which this dipolar oscillation resonates with the incoming light is dependent on the size and form of the particles. The size of the nanoparticles affects the efficiency of absorption and scattering. The contribution of light scattering increases as nanoparticle size increases. (Huang e al., 2011)

with nanoparticle size), they can be utilized as more effective nanoheaters (Nardin et al., 2016).

To enhance light absorption, the LSPR of gold nanoparticles can be adjusted to a specific laser wavelength. This makes it possible to heat gold nanoparticles in vivo in locations where body tissues are more optically transparent (700 - 1200 nm), such as the "water window" (Eustis et al., 2006).

It is achievable to calculate the change in temperature of a nanoparticle solution exposed to laser radiation.

After 20 minutes, a 50 mW, 785 nm laser will deliver 60 J of energy. If the absorbance of 1 mL of gold nanorods at 785 nm is 1, then the light transmittance is 10% and 90% of the incident light will be absorbed/scattered by the particles. Considering that 97% of extinction is attributable to absorption, 52 J would be absorbed. If photothermal efficiency is assumed to be 100 percent, then the change in water temperature may be calculated usingthe equation bellow, where Q is energy (52 J), m is mass (1 g), and c is the specific heat capacity (4.8 J/g°C). Under these conditions, the temperature of the solution would rise by 11 °C (Jain et al., 2006).

$$A = 2 - \log(\%T) \quad (3)$$

$$Q = mc\Delta T \quad (4)$$

3.6.3 Affecting factors of the amount of heat generated in PTT by NIR irradiation of AuNPs

Photothermal heating can be extremely complex. Various studies demonstrate that nanoparticle properties, such as volume, LSPR wavelength, surface ligand, and concentration, influence photothermal heating efficiency and subsequent temperature changes. However, irradiation factors such as irradiation period, laser intensity, and laser wavelength also affect heating.

Theoretically and experimentally, H.-C. Huang et al. (2010) examined the spatiotemporal temperature fluctuations induced by NIR irradiation of PEG-functionalized gold nanorods (max = 800 nm).

To predict temperature distributions in 16 mm well plates containing evenly distributed nanorods, a heat transfer model based on Pennes' bioheat equation was utilized.

Conclusions drawn from this study:

- After 20 minutes of irradiation, both the experimental results and model projections indicated that the temperature attained a stable state.
- The temperature would fall as the distance between the focused laser light and the surface of the fluid increased.
- It was also discovered that NIR laser power affects heating, with 832 W/cm3 laser energy resulting in steady-state temperatures between 36 and 60 °C.

In photothermal therapy, it was demonstrated that models can accurately predict the effects of nanoparticle concentration, laser power, and irradiation length.

It is acceptable to assume that a higher **concentration** of gold nanorods would result in more light absorption and photothermal heating, although this impact is confined in solution.

Other researchers have proven that an increase in the optical density of gold nanorods can reduce light penetration, hence limiting the depth of photothermal heating (Jang et al., 2011).

The **photothermal conversion efficiency (η)** is the ratio of absorption to extinction and is frequently used to define the light-to-heat conversion efficiency. Wang and colleagues (2010) conducted a comprehensive research of the photothermal conversion efficiency of gold nanorods. After 30 minutes of CW (809 nm) laser irradiation, a temperature increase of 55 - 76 °C was detected when the LSPR was at 810 nm and consequently in resonance with the laser wavelength. After 20 min of irradiation, regardless of LSPR, all traces reached a plateau, the same behavior found by H.-C. Huang et al (2010).

Experimentally and theoretically, the **heating efficiency vs volume** of gold nanorods and nanobipyramids with the same max but different absolute dimensions was calculated. The scientists determined that a correlation existed between particle size/volume and photothermal conversion efficiency, and this conclusion has been supported by additional research (Jiang et al., 2013). The absorbance/scattering ratio was highest for nanoparticles with the smallest radii; hence, the nanoparticles with the smallest volume were the most effective light converters. This effect may be restricted, however, as smaller nanoparticles decrease extinction (Mackey et al., 2014).

In general, smaller AuNPs exhibit greater absorbance than bigger AuNPs , leading in more effective heat generation. As the nanoshell size of AuNSs decreases, their absorption contributions relative to their extinction can drop rapidly 60. As for AuNRs, it has been demonstrated that smaller AuNRs generate heat more efficiently (Jaque et al., 2014)

Several experimental studies have studied the photothermal conversion efficiencies of gold nanoparticles of varied **sizes and shapes**. The absorption cross-section and LSPR peak position are dependent on the tumor's shape and may consequently influence the light-to-heat conversion and tumor temperature. Unlike nanoparticle volume, particle shape shows no obvious pattern. Due to the varied experimental settings, it is difficult to assess the efficacy of different investigations. Due to this heterogeneity, it is proposed that it may be advantageous to calculate/estimate the photothermal conversion efficiency of a nanoparticle form in a physiological environment prior to contemplating its usage in photothermal therapy (Ayala-Orozco et al., 2014).

Ligands may impact thermal conductivity as well. A shift in the transient absorption signal of gold nanoparticles can be noticed shortly after laser irradiation (1000 fs) due to a rise in temperature in the nanoparticle's immediate surroundings. J. Huang et al. (2013) examined heat dissipation in gold nanorods produced with varying quantities of CTAB or coated with charged polyelectrolytes using pump-probe transient absorption spectroscopy. Greater water penetration within the CTAB bilayer or polymer layers boosted the thermal conductivity and heat capacity of gold nanorods, which may contribute to the photothermal heating efficiency.

Sometimes, the physical dimensions of gold nanoparticles can be altered by intense **laser irradiation**, resulting in melting and fragmentation. The form of gold nanoparticles can alter their optical characteristics and subsequently their photothermal heating capacity (Link et al., 1999).

Researchers will be required to study and refine these characteristics for optimal heating in any individual physiological setting.

3.7. PPTT and cancer

3.7.1 Types of Tumors for PPTT Treatment.

Site - specific solid tumors respond favorably to treatment. Because of its limitation in light penetration depth, PPTT is more convenient when used to superficial cancers (such as breast, head and neck, and melanoma tumors). We can, however, achieve photothermal therapy of deeply buried malignancies by employing optical fibers to transport light into deep tissues. Breast cancer,head and neck cancer, melanoma, lung cancer (ClinicalTrials.gov Identifiers NCT01679470), prostate cancer (ClinicalTrials.gov Identifiers NCT02680535), liver cancer, have all been studied with PPTT (Mustafa et al., 2019)

3.7.2 Effects of PTT on Tumor Cells and Tumor Microenviroment

Tumor tissue is assumed to be more hypoxic, acidic, and nutrient-deficient than normal tissues. These characteristics may make some cancer cells more sensitive to heat. However, heat shock protein overexpression has been seen in several malignancies. Because these proteins may render cancer cells more resistant to heat-based therapies than expected, the effects of thermal therapy may not be universal in all types of cancer. (Calderwood and Ciocca, 2008)

3.7.2.1 Cancer Cell Death Pathways

When cells are exposed to temperatures higher than 42 °C, they can die. Cell death often occurs via one of two separate pathways: apoptosis or necrosis. Cells are said to undergo apoptosis at 44 °C and necrosis at a higher temperature of 46 °C . Heat breaks the plasma membrane during necrosis, allowing cytoplasmic components to flow out and inflammation to develop. Apoptosis is a finely regulated cell death pathway that does not promote inflammation, making it a "cleaner" option to remove cancer cells. (Samali et al., 1999)

Because apoptosis discourages an inflammatory response, manipulating PPTT to induce apoptosis would be a more advantageous choice in terms of clinical result. Because apoptosis is carefully regulated and does not produce inflammation, moderate PPTT settings can trigger an apoptotic pathway that is preferable to necrosis. (Melamed et al., 2015)

To quantify apoptosis following PPTT, we can look for signs such as mitochondrial damage, cytochrome c release, plasma membrane permeability, DNA fragmentation, immunological detection, and so on. Necrosis and apoptosis can be distinguished using microscopic methods or flow cytometry (Krysko et al., 2008)

Modification of treatment parameters can cause PPTT to elicit apoptosis rather than necrosis. High-dose PPTT (high AuNP concentration, laser intensity, and/or exposure time) can result in necrosis, whereas low-dose PPTT (low AuNP concentration, laser power, and/or exposure time) can result in apoptosis (Davidovich et al., 2014).

In a study, (Banfalvi et al., 2017) 42.7% of the population underwent apoptosis and 2.89% necrosis, respectively, , whereas 5 minute laser irradiation (more than 500 times the dosage of 2 minute irradiation) caused 20.17% of the population to undergo. 2 minutes of irradiation resulted in a mild alteration within the tumor, whereas 5 minutes of irradiation resulted in severe burning.

Several studies have found that the mitochondrial apoptotic pathway is involved in apoptosis. According to Pérez-Hernández et al., apoptosis during PPTT using gold nanoprisms is mediated by proteins Bak and Bax via activating the Bid protein (Pérez-Hernández end al., 2015).

Heat shock proteins are a type of protein that can withstand heat-induced apoptosis. According to Ali et al., (2016) AuNR-assisted PPTT has shown differential responses to different cancer types due to varying amounts of heat shock proteins. Targeting heat shock protein with AuNRs is anticipated to induce apoptosis and increase PPTT efficacy (Dickerson et al., 2008). Ali et al., (2017) discovered that cytochrome c and p53-related apoptotic mechanisms were contributing to the PPTT mechanism by using AuNR-assisted PPTT to treat head and neck tumor-bearing mice. Apoptosis pathways found by proteomics studies include Granzyme B signaling, phosphorylation of the BAD protein (BCL2-associated activator of cell death), caspase cascade, and others.

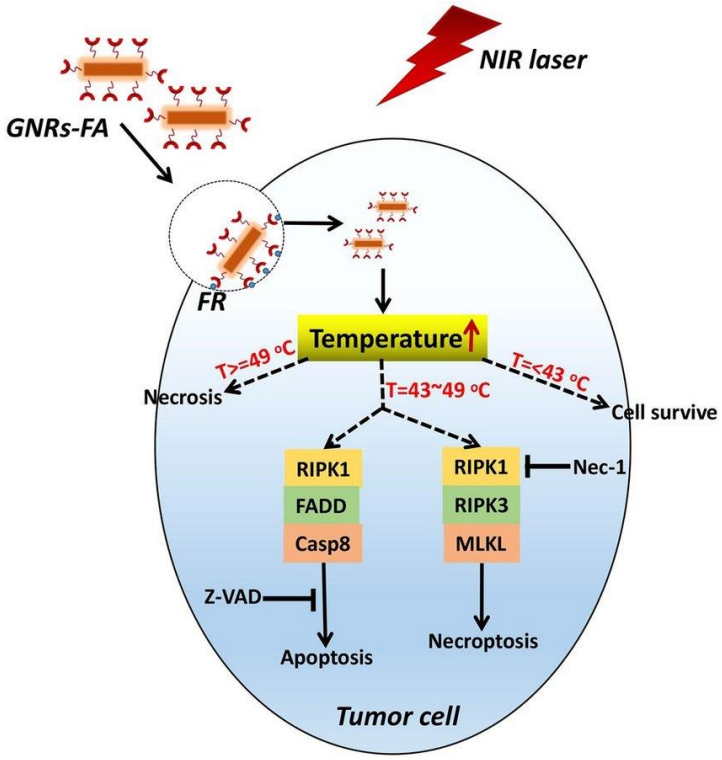

Figure 11 Diagram illustrating the suggested method by which tumor cells are affected by photothermal therapy (PTT). After the induced temperature reaches about 46 °C, PTT mostly causes necroptosis and apoptosis in tumor cells, which destroys them. The primary molecular process via which PTT kills tumor cells at a higher temperature (49 °C) is necrotic. In contrast, when the induced temperature is lower than 43 °C, the majority of tumor cells will survive (Zhang et al., 2018).

3.7.2.2 The Impact of PPTT on Tumor Microenviroment

Emerging evidence suggests that nanomedicine may have a greater influence on the tumor microenvironment (TME). Tumors are increasingly regarded as organs whose behavior can only be understood by examining their particular cellular makeup (Egeblad et al., 2010). The TME is crucial in the development and progression of cancer. Endothelial cells and immunological inflammatory cells (e.g., tumor-associated macrophage (TAM), cancer-associated fibroblasts (CAFs), etc.) are among the many types of cells seen in the TME. The interaction between cancer cells and their TME has a significant impact on cancer progression. Blood arteries, in addition to TME cells, play significant roles in tumor growth and metastasis (Bhowmick et al., 2004). Mukherjee et al. (2005) demonstrated that AuNPs could disrupt the interaction between malignant and stromal cells. Furthermore, many immune cells spontaneously ingest AuNPs, which may aid in the TME immune cells' ability to eradicate malignancies (Saha et al., 2016)

A sufficient heat dosage can successfully elicit an immunological response. Photothermal therapy has been shown to inflame the tumor microenvironment, raise

proinflammatory cytokines, accelerate local DC maturation, induce a "vaccine-like" immunological response, and improve T cell penetration. (Chen et al., 2016)

Furthermore, multiple investigations have shown that PPTT can activate an immunological response that inhibits metastasis. According to Bear et al., PPTT enhances dendritic cell maturation inside tumor-draining lymph nodes, which are thought to be the initial organs of metastasis, hence increasing anticancer T cell responses. Furthermore, Mukherjee et al. (2005)showed that AuNPs had antiangiogenic capabilities, one of which is that they may specifically bind the vascular permeability factor/vascular endothelial growth factor (VPF/VEGF)-165, inhibiting angiogenesis in vivo.

3.7.2.3 GoldNPs PPTT to prevent Cancer Metastasis

Metastasis allows cancer cells to travel to distant secondary sites, accounting for 90% of cancer-related deaths. Metastasis is a multistage process in which initial cancer cells move and locally infiltrate areas near the primary tumor. They then intravasate and circulate in blood or lymphatic channels before extravasating and colonizing in additional places. Cell migration is divided into four stages: protrusion, adhesion, contraction, and retraction. The polarization and expansion of actin protrusions initiates cell migration. Cells develop adhesions that connect the actin cytoskeleton to the extracellular matrix in order to stabilize the protrusions (ECM). The adhesions at the cell's back then dissolve, allowing the cell body to retract forward. (Carmeliet and Jain, 2000)

Several nanotechnology-based techniques for avoiding metastatic cancer have been investigated. In general, there are three approaches to utilize AuNPs to inhibit metastasis:

(1) using an AuNP-based drug delivery system to deliver chemo-drugs, antibodies, or siRNA to invasive cancer cells, cancer stem cells, and TMEs (since metastasis only occurs in "supportive" TMEs, perturbing the TME could be a good strategy for inhibiting metastasis),

(2) using AuNPs alone, and

(3) combining AuNPs with near-infrared light to generate the photothermal effect. (Mustafa et al., 2019)

PPTT can be utilized to destroy primary cancer cells and treat lymph node metastases. Integrin-targeting by influencing Rho GTPase and other pathways AuNP-assisted PPTT, can promote cytoskeleton remodeling, resulting in a decrease in cancer cell motility. (Burke et al., 2012). To avoid metastasis, PPTT can be used with other therapies like as chemotherapy and radiotherapy. Wang et al. (2014) found that doxorubicin-loaded DNA-wrapped AuNRs combined with photothermal ablation suppressed lung metastasis in an orthotropic 4T1 mammary tumor model. According

to Atkinson et al., (2010) gold nanoshells and PPTTs can sensitize breast cancer stem cells (which cause metastasis) to radiation therapy.

3.8. Biological Impact of Gold Nanoparticles

3.8.1 Gold Nanoparticle Administration Strategies: Intravenous vs Intratumoral

As intravenous injection relies on the EPR effect, enough numbers of AuNSs may be difficult to transfer to the tumor location. Several trials have shown that when administered via intravenous injection, fewer than 10% ID/g gets delivered to the tumor. In some circumstances, i.v. injection may be more beneficial, particularly for tumors that are inaccessible via direct injection of AuNPs. (Li et al., 2008)

When an appropriate dose was used, intratumoral injection proved successful. The intratumoral injection could directly introduce AuNPs into the tumor site, resulting in a higher AuNP concentration inside the tumor while reducing the injection dosage.

3.8.2 Distribution And Pharmacokinetics of GNPs in the body

Gold nanoparticles (GNPs) are generally considered non-cytotoxic, with the expectation that they will be eliminated by the kidneys due to their small size (2-4 nm) (Alric et al., 2013). However, studies on localized non-specific cytotoxicity have shown inconsistent results, with some demonstrating cellular toxicity such as the generation of reactive oxygen species, apoptosis, necrosis, and acute mitochondrial toxicity (Balasubramanian et al., 2010). The toxicity of GNPs is highly dependent on their size and design, where smaller GNPs (less than 8 nm) can pass through the renal filtration system, while larger GNPs (greater than 10 nm) are more likely to accumulate in the liver and kidney (Blanco et al., 2015).

The impact of GNPs on the immune system is influenced by their size. For instance, 5 nm nanoparticles dramatically suppressed IL-1B production in macrophages, while 35

nm nanoparticles had no effect (Sumbayev et al., 2013). Similarly, 4 nm GNPs inhibited inflammatory responses in murine macrophages by inhibiting TLR9 responses (Tsai et al., 2012). On the other hand, larger GNPs (ranging from 14 to 100 nm) showed a greater inflammatory response with upregulations in IL-1, IL-6, and TNF-alpha (Yen et al., 2009).

The clearance of nanoparticles administered intravenously primarily occurs through the reticuloendothelial system (RES) via macrophages in the liver and spleen. Nanoparticles with reduced contact with the RES exhibit prolonged blood circulation time, which enhances intratumoral penetration (Ernsting et al., 2013). The enhanced permeation and retention (EPR) effect, resulting from leaky tumor blood capillaries, allows nanoparticles within the size range of 60-400 nm to accumulate passively in solid tumors (Jain and Stylianopoulos, 2010).

The behavior of gold nanoparticles in the body is influenced by their size. Smaller nanoparticles can pass through the blood-brain barrier (20 nm) and achieve renal clearance (Hillyer and Albrecht, 2001). However, larger nanoparticles (>20 nm) are unable to cross the blood-brain barrier and are primarily accumulated in the liver and spleen. Studies have shown that 20 nm nanoparticles had the slowest clearance and longest blood circulation time, while 80 nm nanoparticles cleared the fastest (Zhang et al., 2009). Another study demonstrated that smaller nanoparticles (4 and 13 nm) had longer blood circulation intervals and were removed by day 7, while 100 nm nanoparticles were rapidly cleared in 24 hours (Cho et al., 2010).

In conclusion, the ideal nanoparticle size for optimal behavior appears to be around 20 nm. These nanoparticles are less likely to cross the blood-brain barrier and have a prolonged circulation time compared to larger nanoparticles, increasing the possibility of tumor penetration.

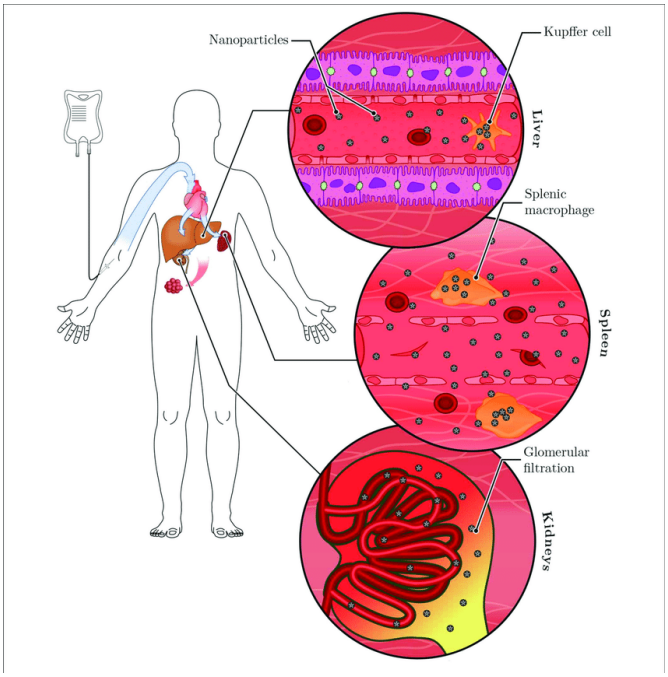

Figure 12 Nanoparticle clearance in the body. Nanoparticles are dispersed systemically throughout the bloodstream after intravenous infusion. They get to the spleen and liver, where tissue-resident macrophages (referred to as Kupffer cells in the liver) sequester a significant amount of the dosage. Urine contains nanoparticles that are too tiny to pass through the glomerular filter (below 5 nm). Any leftover nanoparticles have the potential to gather in tumor tissues (Thomas and Weber, 2019).

3.8.3 Toxicity of GNPs

There are indications that smaller nanoparticles are more harmful than bigger ones, presumably because of their greater likelihood of interacting with their environment and generating greater immunological responses due to their high surface area compared to their mass. Pan Y et al. (2009) discovered that 1.4 nm AuNPs are far more lethal than 15 nm AuNPs of same chemical composition. According to Coradeghini et al., (2013) 5 nm AuNPs display cytotoxicity at concentrations more than 50 M, but 15 nm AuNPs demonstrate no cytotoxicity.
Pattanayak et al. (2016) investigated AuNPs with diameters ranging from 15 to 20 nm in the L929 mouse cell line for 1516 hours and found no toxicity. Murphy et al. (2005)

demonstrate that 18 nm AuNPs have no acute cytotoxicity. Khan et al. (2007) pre-incubated HeLa cells with 18 nm AuNPs for 3 and 6 hours. The AuNPs were discovered to be localized inside the cytoplasmic membranes and did not enter the cellular nucleus, and the expression levels of the majority of the genes remained unchanged. As we can conclude, the 5 nm size is possible that for a nanotoxicity threshold.

Specific surface modifications' architectures, functional groups, and charges result in varied cellular responses to conjugated AuNPs. Surface-chemistry-dependent alterations in cell function have been documented, including gene expression and migration. We also note that chemicals utilized in the creation of nanoparticles (i.e., surfactants) can be hazardous. As a result, before biological exposure, it is critical to assess the influence of a particular surface ligand on cell viability and cell behavior. (Connor et al., 2005). Incomplete purification of AuNRs during production results in free etyltrimethylammonium bromide (CTAB) molecules, which produce the reported cytotoxicity, according to research. Goodman et al. (2004) created cationic and anionic particles and discovered that AuNP toxicity was related to their interactions with the cell membrane. They discovered that cationic AuNPs were more strongly attracted to the negatively charged membrane than anionic AuNPs. Schaeublin et al. (2011) discovered that charged AuNPs were poisonous at relatively low concentrations (10 mg/mL), whereas neutral AuNPs were harmful at a greater dosage of 25 mg/mL. demonstrating that both positively and negatively charged AuNPs were hazardous, with the negatively charged AuNPs having an amplified reaction, resulting in necrosis as the major mode of cell death.

The FDA-approved PEG modification was achieved by adding mPEG-SH to the gold nanoparticles to generate a nearly neutral surface, which demonstrated negligible cytotoxicity in vitro and is now one of the most promising surface modifications of AuNPs for in vivo use. PEG modification provides a nonspecific barrier that inhibits unspecific binds in blood components such as proteins and cells, potentially resulting to prolonged blood retention and greater uptake in the tumor. (Niidome et al., 2006)

As a conclusion, neutrally charged NPs do not induce any toxicity. Positively charged NPs bind strongly on the cell. Negatively charged NPs induce cell death. Finally, PEGilated NPs are neutral and as a consequence non toxic and can escape RES resulting in higher circulation time.

3.9 Advantages, Disadvantages and Concerns of GNP assisted PPTT

Other types of cancer treatments benefit greatly from AuNP-assisted PPTT. For instance, AuNP-assisted PPTT bypasses the systematic adverse effects associated with standard cancer treatments like chemotherapy. The treatment primarily targets

localized solid tumors, with little to no side effects on healthy tissues. Second, because PPTT is a physical treatment, there are no limitations on the types of cancers that can be treated. Different cancer kinds typically have their own therapy medications, and many tumors acquire resistance to specific drugs after a given amount of time. PPTT could thus become a "universal" treatment for various forms of cancer. (Mustafa et al., 2019)

However, AuNP-assisted PPTT has its own set of issues. The first problem is the metabolic destiny of AuNPs, particularly over time. AuNPs have numerous potential applications, but their exerts beneficial in nanomedicine is determined by their toxicity level. Despite the overwhelming evidence that AuNPs are nontoxic and chemically inert, research with contradicting outcomes have been conducted. However, in many cases, the toxicity is caused by either the nonbiocompatible surface ligands, the high power of the laser,56 or the high AuNP treatment dosage.
(Khlebtsov et al., 2011).

The primary concern with AuNP-based PPTT is that AuNPs concentrate largely in the liver and spleen. Many investigations, however, have demonstrated that their harmful impact on the aforementioned organs is minor. The second issue is inconsistency in treatments caused by laboratory variations such as lab personnel, different types of AuNPs, surface changes, laser dosage, varied handling, and so on. These discrepancies will provide different results, which can explain for large variances in PPTT. The third concern is that PPTT is mostly used to treat confined solid tumors. The efficiency of PPTT may be considerably reduced in cases of delocalized or advanced metastatic malignancy. Despite this, recent improvements in PPTT demonstrate its potential for preventing and suppressing cancer recurrence and metastasis. (Zou et al., 2016).

From 2006 to 2016, a thorough assessment of the literature on NP delivery to tumors in vivo demonstrated that just 0.7% of NPs delivered reached the tumor location, independent of the coatings utilized to increase accumulation. This study clearly identifies a barrier that practically all nanoparticle delivery techniques that rely on the EPR effect confront. Once this issue is resolved, PPTT has enormous potential since it will be able to reach tumors that are inaccessible for surgery, it should be applicable to every cancer type, and it should be able to kill cancer stem cells. (Jauffred et al., 2019)

3.10 Examples of the Current Stages of Gold assisted PPTT

In Human medicine, AuroLase treatment, a type of PPTT based on 150 nm silica-gold nanoshells (AuNSs) that absorb NIR light, generate heat, and are covered with polyethylene glycol (PEG), was devised by Nanospectra Biosciences, Inc. and has been in clinical trials (ClinicalTrials.gov Identifiers: NCT00848042 for refractory and/or recurrent tumors of the head and neck). AuroLase clinical studies involve intravenous

(i.v.) injections of AuNSs into the blood, and the concentration of these nanospheres inside malignancies via the increased permeability and retention (EPR) effect is caused by leaky and poorly structured tumoral blood arteries. (Mustafa et al., 2019)

In Veterinary field, since cancer is so widespread in cats and dogs, studies of gold nanorods (AuNRs) have been employed in the treatment of spontaneous tumors in canine and feline patients. Ali et al. (2016) conducted multiple investigations in cats and dogs on the therapy of spontaneous mammary gland cancers by directly injecting AuNRs into solid tumors (intratumoral injection, i.t.), followed by NIR irradiation. In all cases, effective tumor regression was accomplished with no recurrence or metastasis; additionally, there were no toxic effects on the blood profile or a reduction in liver and kidney function subsequently. Similar investigations on dogs and cats with mammary gland cancers were also undertaken by Abdoon et al. (2016). Their findings revealed that the treated animals experienced complete remission (62.5% (10/16), partial remission (25% (4/16), and substantially low remission (12.5% (2/16)). London and colleagues (2017) employed AuNR-PPTT to treat canine spontaneous neoplasia (carcinoma, sarcoma, or mast cell tumors). The AuNRs were given intravenously into seven canines 72 hours before the tumor mass was irradiated with a 30 W, 808 nm

NIR laser. At the end of the research, London and colleagues saw either partial or total

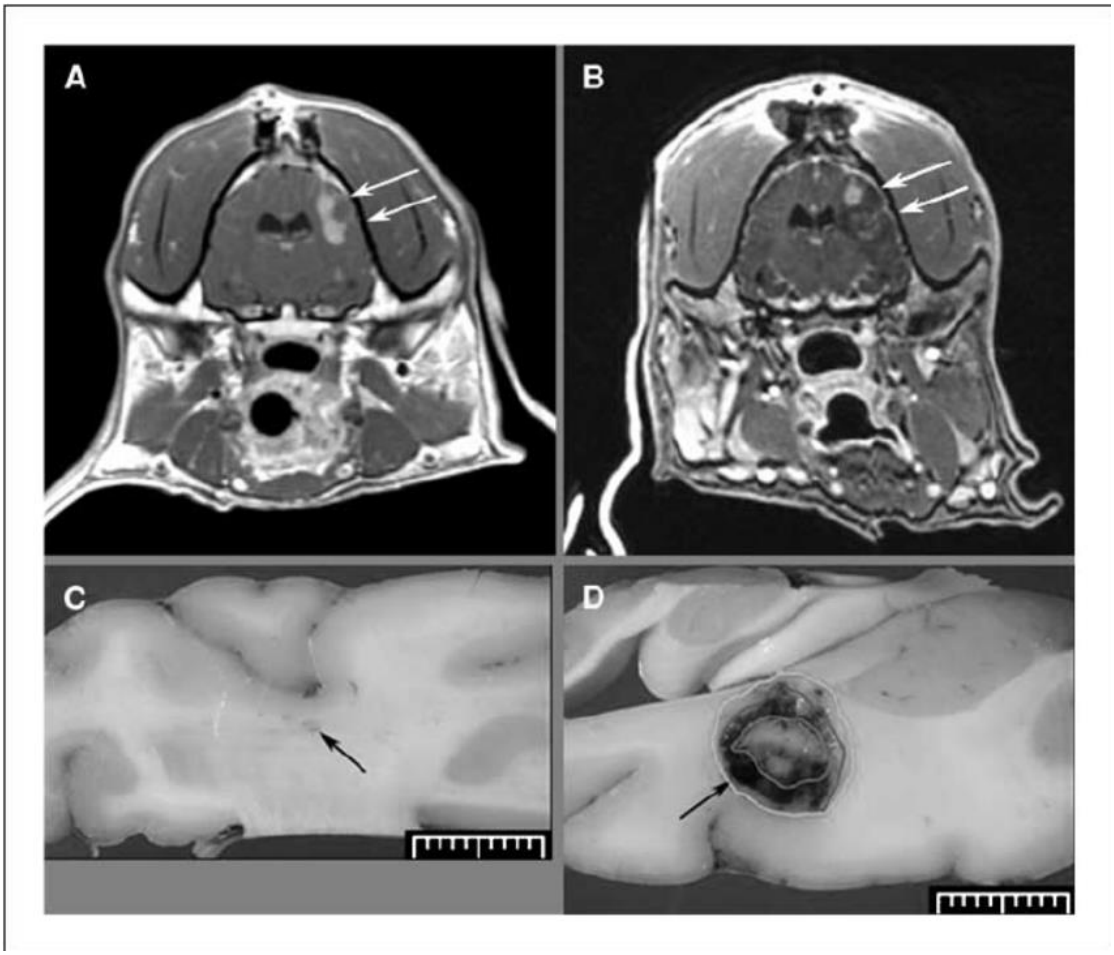

Figure 13 Treatment of canine brain cTVT with AuroLase. The bilobed tumor along the inoculation route is contrast-enhanced in the dog brain MR-DCE axial image (figure A, arrows). After receiving laser therapy, the inferior lobe of the dog's brain is shown to have been abated in image B with arrows. C, the control cerebral hemisphere, which displays a normal brain with no ablation. Fiber insertion point on an arrow. D, ablation zones (inner ring = tumor boundary, middle ring = thermal necrosis boundary, outer ring = zone of edema boundary) (Schwartz et al., 2009)

tumor remission, with an overall response rate of 28.6%.

The use of gold nanoparticles to target and destroy cancer cells has proven to be a promising new approach in the fight against cancer. The results of many studies show that using laser light to excite the plasmonic resonances in the gold nanoparticles, results in generating sufficient heat to destroy the cancer cells while sparing the surrounding healthy tissue which is a unique element of this cancer treatment. The next step is to bring this innovative treatment in more clinical trials. If successful, it has the potential to change the way cancer is treated forever. The development of new and more advanced nanoparticles with enhanced photothermal properties will continue to push the boundaries in medicine. The road ahead may be challenging, but with determination and a commitment to advancing the field, Plasmonic Photothermal Therapy of Cancer using Gold nanoparticles will become a reality and bring hope to those in need.

CHAPTER 4

Approaching the Oral Squamous Cell Carcinoma Plasmonic Photothermal Treatment
A Review of Nine Indicative Studies

In preview chapters, we have set the basic knowledge to understand the pathophysiology of Oral Squamous Cell Carcinoma and the fundamental mechanics of Thermoplasmonic Treatment of Cancer in general using Gold Nanoparticles under near – infrared irradiation. In this chapter, we will review nine indicative papers that propose various approaches to OSCC plasmonic photothermal treatment. These papers present a range of innovative strategies for optimizing the effectiveness of PTT using AuNPs, including the use of targeted nanoparticles, the development of multimodal imaging techniques, and the combination of PTT with other therapeutic modalities.

The analysis of the papers will be presented in a comparative way through specific categories: The nanoparticles used, synergetic treatments, Results of PTT in tumors, Toxicity of nanoparticles.In this way we will be able to have a better understanding of the effectiveness and the results of the proposed methods. During the preparation for the writing of this chapter, analytical and collective tables named as PAPER ID, for each paper have been formed, that can be found in Appendix, and can be used for a quick and further research.

Overall, this chapter aims to provide an overview of the current state of research in OSCC plasmonic photothermal treatment planning, highlighting the most promising approaches and identifying areas for future development. By understanding the latest advances in this field, researchers and clinicians can work towards improving the efficacy and accessibility of PTT for OSCC, ultimately improving outcomes for patients.

4.1 The nanoparticles

Simple Gold Nanoparticles or more complex elaborate nanostructures have been synthetized.

Abdelaziz et al,(2021) synthesized 50 nm PEGylated gold nanospheres. They used a reduction technique with a chloroauricacid (HAuCl) solution. Although they do not mention the method, they prepared a PEGylated amount of gold nanoparticles as

it becomes clear in the Discussion section of the study. PEGylation is a process of covalently attaching polyethylene glycol (PEG) to a nanoparticle. PEG is a hydrophilic, non-toxic, and biocompatible polymer. PEGylation can improve the pharmacokinetic and pharmacodynamic properties of the attached molecule. It can increase the molecule's solubility, stability, and half-life in the bloodstream, as well as reduce its immunogenicity and toxicity. PEGylation can also improve the drug's ability to penetrate biological barriers and target specific tissues or organs. PEGylation can enhance the EPR (Enhanced Permeability and Retention) effect by prolonging the circulation time of nanoparticles in the bloodstream, allowing them to accumulate in the tumor or inflamed tissue for a longer period of time. The hydrophilic PEG chains on the surface of the nanoparticles create a steric barrier that reduces opsonization and uptake by the reticuloendothelial system (RES) and increases circulation time. The attachment of PEG to a molecule can be achieved through various chemical reactions, such as the formation of an amide bond.

The resulted nanoparticle can be used in NIR PTT and as it is covered in PEG, has better biodistribution behavior.

Yang et al, (2021), created a nanoparticle with a size of 100 – 150 nm, consisting of Gold (Au), Chrysin and Extracellular Vesicles (EVs) labeled with PKH26. The EVs were extracted from a culture medium of SCC9 line cancer cells and then were treated with chrysin. By incubating the EVs with $HAuCl_4$, GNPs were self-grown on the surface of EVs - chrysin forming a new nanomaterial, which was Au-EV.

The important in this synthesis method is the use of EVs i.e. extracellular vesicles that are lipid bound vesicles secreted by cells into the extracellular space. EVs are able to specifically accumulate in tongue and squamous cell carcinoma (Li et al., 2018) thus achieving a specific – targeting method of the malignant cells. EVS also contain plenty of miRNAs. Some of them increase the expression of the let-7a family of proteins which are tumor suppressors (Wu et al., 2015).

On the other hand, in several cancer cells, chrysin has been shown to promote cell death and inhibit growth via ncRNAs. Chrysin, like flavonoids, inhibits the development of tumors through controlling the expression of ncRNAs (Zhong et al., 2020).

So in this case we have a polydynamic nanoparticle that can be used for PTT because of the Gold, has specific targeting abilities because of the tumor specific EVs that they also provide tumor suppression and a chemotherapeutic ability because of the chrysin.

El-Sherbiny et al,(2021) synthesized a nanoparticulation composed of Gold nanorods (GNRs) and Thymoquinone Nanoparticles loaded on PLGA and conjugated with targeting agent folate or folic acid (FA) with a final size ranged from 115-180 nm and a morphology spherical in shape.

GNRs display an excellent behavior in NIR applications and they were prepared with the seed-mediated growth method(Zhang et al., 2016).

Thymoquinone (TQ), which is derived from the Nigella sativa plant, has demonstrated potent anticancer properties (Goyal et al., 2017). It has multiple targeting effects, interferes with a variety of tumorigenic actions, including migration

and invasion of angiogenesis, carcinogenesis, and malignant development (Mostofa et al., 2017). Because TQ has a quick elimination and a slow absorption, it also has a poor bioavailability which can be increased in the form of nanoparticles and present nano-chemotherapy or nano-chemoprevention behavior. Thus TQ nanoparticles (NTQ) have a more promising effect than TQ alone due to its improved bioavailability and better focus on cancer hallmarks (Schneider et al., 2014).

One of the most popular nanoparticulate carriers is polylactic co-glycolic acid (PLGA) that is a biodegradable copolymer as it breaks down into water and carbon dioxide (CO2) (Silva et al., 2015). This degradation of the polymer can allow the chemotherapeutic to be released specifically on the tumor.

Folic acid (FA) is a promising active target since cancer cells have a tendency to overexpress the folate-receptor as they so highly depend on folic acid. Its expression is minimal in healthy organs and tissues.

Colorectal, ovarian, epithelial (like OSCC), and cervical cancers all exhibit significant levels of folate receptor expression (Parker et al., 2005). Folic acid is highly stable across a range of temperatures and pH levels.

The resulted nanoparticle has PTT abilities because of the Gold Nanorods, it can specifically target the cancer cells because of the folic acid and can release in a controlled manner because of the PLGA the Thymoquinone, achieving chemotherapeutic results.

Zeng, S. et al, (2021), produced a nanosynthesis composed of Gold nanorods, mesoporous silica, Hyaluronic Acid and Doxorubicin that was labeled as DOX-AuNRs@mSiO2-HA. GNRs were synthesized with the seed growth mediated method and then were coated with mesoporous silica nanoparticles (mSiO2). Then, the anticancer drug doxorubicin (DOX) was loaded into the AuNRs@mSiO2 nanoparticles via electrostatic interaction. Finally, the amine functioned AuNRs@mSiO2 by the post grafting method was attached to hyaluronic acid (HA) through the EDC mediated amidation reaction, forming DOXAuNRs@mSiO2-HA nanoparticles for photothermal and chemotherapy applications.

Doxorubicin hydrochloride (DOX) is the hydrochloride salt of the anthracycline antibiotic Doxorubicin excibiting antitumor action. Doxorubicin is obtained from the Streptomyces peucetius bacteria. DOX intercalates between DNA base pairs, hence reducing DNA replication and, eventually, protein synthesis. In addition, doxorubicin inhibits topoisomerase II, which increases and stabilizes the cleavable enzyme-DNA linked complex during DNA replication and prevents the ligation of the nucleotide strand after double-strand breakage. Doxorubicin hydrochloride, is an effective anti-tumor chemotherapy drug that in a targeted application can be more effective than conventional chemotherapy. (Fong et al., 2017).

Mesoporous silica nanoparticles have been widely used to coat gold nanorods in order to increase their long-term stability, hydrophilicity, and drug delivery capacity. These particles have a high specific surface area, a large pore volume, easy surface modification, good biocompatibility, and convenient drug loading (Ramasamy et al., 2018).

Hyaluronic acid (HA) is a natural, biodegradable, and non-immunogenic polymer with high affinity for the CD44 receptor, which has been shown to be involved in a variety of tumor biological activities, such as tumor proliferation, progression, and metastasis. The HA shell protects the drug, increases the drug's stability, and enables sustained drug release (Ramasamy et al., 2017).

The resulted nanocarrier has PTT abilities due to the Gold nanorods, can specifically target the cancerous cells because of the HA which also releases DOX in a controllable way as it degraded by Hyal-1 only after the nanoparticle has been internalized by receptor-mediated endocytosis, leading to maximum chemotherapeutic results.

Zeng, J. et al, (2020), created a Drug Delivery System (DDS) that included Black Phosphorous nanoparticles, gold nanoparticles and loaded with the chemotherapeutic cisplatin in an analogy of BPNPs to GNPs 5:1. Newly discovered black phosphorus nanoparticles (BPNSs) have facilitated the development of novel electronic and biological devices. Due to their unique electronic structure and layer-dependent energy band, BPNSs have been deemed a highly effective photosensitizer and employed as a photodynamic therapy (PDT) agent to create singlet oxygen. Due to its distinctive puckered lattice shape and physicochemical features, BPNSs could also be used as an effective drug delivery system[KOTCHERLAKOTA et al., 2017].

Cisplatin is a chemotherapeutic drug used to treat numerous types of cancer. It belongs to the family of antineoplastic drugs containing platinum. It functions in part by attaching to DNA to prevent its replication (HIRAISHI et al., 2008).

The paper does not clarify the exact nature of the prepared DDS. It only mentions that the best result occurs from the DDS with a composition of BPNPs-GNPs 5:1/cisplatin and through the described synthesizing methods we can only understand that the DDS consists of BPNPs loaded with cisplatin and GNPs loaded with cisplatin that exist in the same mean in an analogy of 5 to 1. The importance of this paper is that delivers a comparison of the effectiveness of GNPs in the treatment of OSCC against another material that has PTT and drug delivery abilities and that is why it is included in this essay.

The resulted Drug Delivery System displays an excellent PTT ability and drag delivery capability of the chemotherapeutic cisplatin to the OSCC tumor, but concludes that is due to the increased presence of the black phosphorous nanoparticles in the solution.

Sun et al, (2020) managed to synthesize nanostructures consisted of Pegylated Gold Nanorods coated onto KB cancer cell membrane vesicles that they labeled as GNR@MEM. The GNRs were produced using the Growth seed mediation with a final size after the PEGylation of 68 +- 5 nm in length and 11 +- 1 nm in width. Their aim was to develop an agent that can act as a photosensitizer and radiosensitizer simultaneously.

The PEGylated GNRs were coated with the plasma membrane of oral squamous KB cancer cells.

And there was a reason behind that decision. Nanomaterials have been coated with a variety of synthetic and natural tumor-targeting coatings to facilitate their preferential accumulation in tumor tissues and cells. Yet, these artificial coatings are nonetheless

likely to be recognized by the immune system, resulting in rapid removal of the nanoparticles and an undesirable immunological response following repeated administration (Mao et al., 2011). The cell membrane-based cloaking method has shown a viable way to cover nanomaterials with a thin layer of cell membrane. Complex engineering of the inherent advantages of cell membranes permits nanocarriers to concentrate preferentially in the target tissues. Nanoparticles encased in cell membranes can duplicate the biological functions of the cells that supplied their cell membranes, allowing for longer systemic circulation and disease-specific targeting (Fang et al., 2018). Due to its unique membrane protein composition and structure, the membrane of cancer cells possesses immune evasion and homologous binding capabilities, thereby overcoming the problem of immune clearance and nonspecific binding (Lv et al., 2019).

The resulted nanoparticle has a dual PTT and Radiotherapeutic functionality because of the Gold Nanorods and immune evasion and specific targeting capabilities due to oral squamous KB cancer cell membrane coating.

Mapanao et al, (2020) composed gold ultrasmall nanoparticles in silica cover loaded with a Cisplatin prodrug for chemotherapy, labeled as tNAs-cisPt with a mean diameter of the final nanoparticle between 100 and 150 nm.

Their method involves the rapid reduction of gold in aqueous solution with sodium borohydride, resulting in the creation of gold Ultra Small Nanoparticles (USNPs) coated with poly(sodium 4-styrene sulfate) (PSS). To partially aggregate the USNPs for tNAs and tNAs-cisPt, dimercaptostilbene (DMSB) was added. Electrostatic interaction between anionic gold USNPs and poly(L-lysine) (PL) facilitated the development of aggregates under control. The polymeric aggregates of gold USNPs served as a template for the creation of the silica shell via a modified Stober procedure.

To expand the potentials of noble metal nanoparticles in oncology, an ultrasmall-in-nano method for the efficient synthesis of a family of nonpersistent noble metal nano-architectures (NAs) has been developed. NAs vary in diameter from 100 to 150 nm and are typically constructed of biodegradable silica nanocapsules containing gold ultrasmall nanoparticles (USNPs) of around 3 nm that are placed in a polymeric matrix (Cassano et al., 2018) . In this paper, the authors introduce the very first multifunctional NAs (tNAs-cisPt) for synergistic chemo-photothermal therapy. The nano-architectures consist of an endogenously double-controlled cisplatin prodrug for chemotherapy and narrow near-infrared (NIR)-absorbing gold ultrasmall nanoparticles for moderate hyperthermia through photothermal (PT) action.

The various elements of NAs provide several functional properties:

1) Gold USNPs can be used for light-mediated applications such as photothermal treatment (PTT) and as a radiotherapy sensitizer.

2) PL can be covalently changed to accommodate tiny molecules within the nanoarchitectures' cavities. In the case of NAs-cisPt and tNAscisPt, PL was conjugated with an octahedral cisplatin prodrug.

3) the silica shell protects the encapsulated substance until its disintegration and provides an easily changeable surface for the attachment of molecules, such as active targeting or delivery moieties. It has also been demonstrated that the silica shell

enhances ultrasonic (US) signal, making it appropriate for US-based imaging (Armanetti et al., 2018).

The tNAs-cisPt nanoparticle presents functionality for PTT and Radiotherapy, is a capable drug delivery platform because of PL and silica and can be used as of the last, aa an ultrasound imaging contrast agent.

Liao et al, (2019) created a nanoparticle consisting of Gold nanorods, Alginate-Cysteine and RGD Peptides that they labeled as GNR@Alg-Cys/RGD.

Gold Nanorods were generated through seed-mediated growth of Au nanoparticles and silver ions, and subsequently CTAB was used to stabilize them. Before replacing the CTAB, the alginate was changed with cysteine by connecting the carboxylic terminal of alginate to the amine terminal of cysteine. The synthesized GNR@CTAB was then suspended for 12 hours in Alg-Cys-containing water for ligand exchange. Weak van der Waals forces allow the CTAB molecules to be easily removed from the GNRs or substituted with other molecules.

In their study, the team focus on the problems generated by CTAB. The extremely cytotoxic surfactant cetyltrimethylammonium bromide (CTAB) is utilized For the seed-mediated growth of GNRs, (Jana et al., 2001). Leakage of CTAB from GNRs causes the high toxicity of CTAB-coated GNRs. This is because a CTAB molecule's interaction with GNR involves weak van der Waals and electrostatic interactions. The positively charged CTAB would then lyse the cell membrane, significantly impairing the physiological functioning of normal cells (Yu et al., 1997).

Several polymers have been utilized to replace CTAB by either chemical or electrostatic binding. Qiu et al.(Qiu et al., 2010), for instance, replaced CTAB with polyelectrolytes, such as negatively charged polystyrene sulfonate (PSS) and positively charged poly(diallyldimethylammonium chloride) (PDDAC). After 72 hours, the cell viability of the group treated with GNRs coated with CTAB was less than 50%.

It became a necessity to replace CTAB with polymers to limit it's possible harm. Many sulfur-containing polymers, including thiol-terminated polyethylene glycol (PEG-SH) and thiol-terminated poly(amidoamine) (PAMAM-SH), were utilized to replace CTAB by establishing a strong gold–thiol interaction between the polymer and GNRs. These results demonstrated the successful replacement of CTAB with polymers via electrostatic or chemical binding to minimize cytotoxicity. However, due to the solvents or raw materials utilized in the manufacturing of these synthetic polymers, they may have a negative impact on the human body. Thus, the use of natural polymers as Alginate came as the solution.

By creating a gold–thiol link between the alginate and gold, Liao et al, were able to apply thiolated alginate as a stabilizer and directly replace CTAB. Alginate is an FDA-approved (reference number 21CFR184.1724) polysaccharide rich in carboxylic terminals on the hexose. Alginate is utilized extensively as a food additive, bioscaffold, carrier, and stabilizer (Zhao et al., 2018). The numerous carboxylic groups might be utilized to create covalent bonds on metal nanoparticles, while the remainder could be modified with functional moieties. Alginate fragments were modified with cysteine to form a gold–thiol connection on the gold surface in order to avoid alginate leaking during circulation and extend circulation time.

The remaining carboxylic terminals on the alginate were changed with cyclic RGD peptides to target specifically the avb3 receptors on the OSCC cell line SAS-3.30. From Drosophila to humans, Arginylglycylaspartic acid (RGD) is the most prevalent peptide motif responsible for cell attachment to the extracellular matrix (ECM). This sequence is present in numerous matrix proteins, including fibronectin, fibrinogen, vitronectin, osteopontin, and several other adhesive extracellular matrix proteins, and integrins identify and attach to it. The discovery of RGD and the clarification of how RGD binds to integrins have led to the development of a number of medications and diagnostics, while the peptide itself is widely utilized in bioengineering. RGD can be chemically modified or replaced with a matching peptide that increases cell adhesion, depending on the application and the integrin targeted (Liao et al., 2014).

The resulting nanoparticle was suitable for PTT due to the Gold Nanorods, biocompatible because of the replacement of CTAB with Alginate – Cysteine that also improved it's circulation time and able for specific targeting after the modification with RGD peptides.

Rao et al, (2018) developed a nanoparticle consisting of Gold nanorod loaded on Platelets (PLTs). The GNRs were synthesized using a seed-mediated technique. To promote biocompatibility, bovine serum albumin (BSA) was bioconjugated to GNRs (Ali et al., 2014). PLTs were isolated from the mice's blood that would be used in the in vivo part of the experiment. Finally, electroporation was utilized to load GNRs with PLTs.

Platelets (PLTs) are circulating sentinels that can concentrate in wounded tissues to initiate repair processes while at the same time, PTT-mediated heat injures tumor tissues (Born et al., 2017). In account of this, the team hypothetized that PLTs could act as carriers for the targeted delivery of GNRs to tumor tissues, hence enhancing the PTT effect and leading to a feedback accumulation of PLTs. Remarkably, the accumulation of PLT-GNRs, which inherited the long circulation and cancer-targeting properties of PLTs and the efficient photothermal property of GNRs, effectively facilitated the PTT as the PTT-ablated tumor tissues recruited additional PLTs, thereby enhancing the accumulation of PLT-GNRs in the tumor. PLTs are identified by the immune system and can circulate in the bloodstream for eight to nine days (Harker et al., 2000). This innovative PLT-PTT represents a better and effective self-reinforcing cancer therapeutic technique compared to the standard PTT.

The resulting nanoparticle is suitable for PTT because of the GNRs that was also enhanced because of the ability of the PLTs to accumulate at the tumor. The PLTs also provided the nanoparticle with biocompatibility, increased circulation time and specific targeting for the cancerous cells.

In five out of nine studies, the teams used Gold nanorods, proving the efficiency of this particular Gold nanoparticle type for photothermal treatment. Another reason is the ease of synthesis that this nanoform provides with the seed mediated method. Au^{3+} is rapidly reduced by sodium borohydride and transformed into gold nanoparticles in the form of seeds in an aqueous hexadecyltrimethylammonium bromide (CTAB) solution, according to the seed-

mediated technique. With a slight reduction of Au^{3+} in the growth solution by ascorbic acid, Au^0 develops on the seeds in a directed manner. El-Sayed and Nikoobakht first introduced this method in 2003, and subsequent groups including Murray, Murphy, Wang, and Liz-Marzán refined it. Wei et al (2021) propose in their study a new Seed-Mediated Synthesis method of Gold Nanorods at Low Concentrations of CTAB, since as we witnessed in Liao et al. (2019) it is highly toxic and that can be used as a starting point in future plannings for the treatment of cancer utilizing gold nanoparticle mediated photothermal therapy.

Another ascertainment is that in five out the nine papers, the authors propose a combined treatment of PTT with Nanochemotherapy and in two papers with Radiotherapy pointing that the therapeutic benefits of multimodal treatment are greater and more efficient than that of just Photothermal Treatment, paving the way to that direction for future research.

Table 1 – Components and Properties of NPs

Components of NP	Properties of NP	Reference
PEGylated gold nanospheres	PTT + improved Biodistribution	Abdelaziz et al, 2021
Gold, Chrysin, Extracellular Vesicles, labeled with PKH26	PTT + specific targeting + tumor suppression + chemotherapy	Yang et al, 2021
Gold nanorods, Thymoquinone Nanoparticles, PLGA	PTT + specific targeting + controllable chemotherapy	El-Sherbiny et al, 2021
Gold nanorods, mesoporous silica, Hyaluronic Acid, Doxorubicin	PTT + specific targeting + controllable chemotherapy	Zeng, S. et al, 2021
DDS: Black Phosphorous nanoparticles, gold nanoparticles, cisplatin	PTT + efficient drug distribution + chemotherapy	Zeng, J. et al, 2020
Pegylated Gold Nanorods, KB cancer cell membrane vesicles	PTT + Radiotherapy + Immune System evasion + specific targeting	Sun et al, 2020
Gold ultrasmall nanoparticles, silica cover, Cisplatin prodrug	PTT + Radiotherapy + Drug Delivery + Contrast Agent + chemotherapy	Mapanao et al, 2020
Gold nanorods, Alginate-Cysteine, RGD Peptides	PTT + biocompatibility + increased cisrculation time + specific targeting	Liao et al, 2019
Gold nanorods, Platelets	PTT + biocompatibility + increased circulation time + specific targeting	Rao et al, 2018

Table 2 – Special Characteristics of the Components

Special Characteristics of the Components of each Nanoparticle	**Reference**
- PEGylation for biocompatibility and increased circulation time	Abdelaziz et al, 2021
- Extracellular Vesicles of the cancerous cells for specific targeting and tumor suppression - Chrysin for chemotherapy	Yang et al, 2021
- Folic Acid for specific targeting - PLGA for controllable release of the chemotherapeutic agent - Thymoquinone for chemotherapy	El-Sherbiny et al, 2021
- Mesoporous silica for long-term stability, biocompatibility, hydrophilicity, and drug delivery - Hyaluronic Acid for specific targeting - Doxorubicin for chemotherapy	Zeng, S. et al, 2021
- Black Phosphorous nanoparticles as a more efficient PTT agent than GNPs - Cisplatin for chemotherapy	Zeng, J. et al, 2020
- PEGylation for biocompatibility and increased circulation time - Gold Nanorods also as Radiotherapy agent - KB cancer cell membrane vesicles for immune evasion and specific targeting	Sun et al, 2020
- Gold ultrasmall nanoparticles for PTT and as Radiotherapy agents - Silica cover for protection of the NP, for attachment of molecules and as ultrasonic imaging enhancer - PL as a drug carrier platform - Cisplatin prodrug for chemotherapy	Mapanao et al, 2020
- Alginate-Cysteine as CTAB replacement, for biocompatibility and improved circulation time - RGD Peptides for specific targeting	Liao et al, 2019
- Platelets for biocompatibility, increased circulation time and specific targeting	Rao et al, 2018

4.2 Targeting of the OSCC Cells

As we have elaborated in a previous chapter, the targeting of the cancerous cells is of great importance for the success of the treatment. The greatest possible accumulation of the nanoparticles in the site of cancer and inside the malignant cells will result in the most total and beneficial therapeutic outcome. Targeting can be achieved in two ways, non-specifically and specifically or actively.

In non-specific targeting of the tumor, the major point of focus is the EPR effect. The enhanced permeability and retention effect (EPR effect) is a universal pathophysiological phenomenon and mechanism where macromolecular compounds beyond certain sizes (above 40 kDa) can progressively accumulate in the tumor vascularized area, thereby achieving targeted delivery and retention of anticancer compounds into solid tumor tissue. Targeted therapy via the EPR effect in clinical practice is not always successful due to the fact that the strength of the EPR effect depends on the type and location of tumors, the status of blood circulation in tumors,

and the physical-chemical properties of macromolecular anticancer medicines (Jun Wu, 2021). Specific factors as biocompatibility of the nanoparticle that leads in prolonged circulation times result in increasing the possibility of the NP being accumulated in the site of the tumor as of the strong and irregular vascularization of the malignancy. The masking of the nanoparticle with an agent that consists it invisible to the immune system, is the major factor of biocompatibility because it allows it to remain in circulation and is not accumulated by immune cells ending up in the liver or the kidneys where finally will be excreted from the body.

Certain additions on the designed nanoparticles have achieved non-specific targeting. Abdelaziz et al. (2021) PEGylated their gold nanospheres. PEGylation results in immune system evasion and thus prolonged circulation in the blood vessels, increasing the chronical chance of the nanoparticle arriving in the tumorous area. Zeng S. et al. (2021) used mesoporous silica on their nanocoposition that offered it biocompatibility and hydrophilicity, characteristics that lead again in higher circulation time. Sun et al. PEGylated their gold nanoparticles and then incubated them in Cell membrane from the KB cancer cells providing them with system immune evasion ability. The replacement of CTAB, in Liao et al (2019) study, with Alginate – Cisteine had the same result. Finally, Rao et al (2018) used Platelets on their nanostructure, that as an organic component concealed it from the immune system. All these techniques had the same result; immune evasion that led to prolonged circulation time and resulted in high tumor accumulation because of the EPR effect.

On the other hand, specific or active targeting is the procedure where surface modification of the nanoparticle result in the binding of it with the cancerous cell. The most common method of active targeting is to incorporate on the NP specific ligands for distinctive marks for each cancer type. These targets can be cell protein kinase substrates and inhibitors, protease substrates and inhibitors, cell surface receptor, artificial enzymes etc (Yang et al., 2012).

On this logic, Yang et al (2021) used extracellular vesicles that were extracted from the culture medium of SCC9 cells and were able to specifically accumulate in the tongue and squamous cell carcinoma cells that have been originated from. El-Sherbiny et al (2021), utilized Folic Acid for specific targeting. Folic acid is a promising active target for cervical, ovarian, epithelial, and colorectal cancers, where folic acid receptors are highly expressed. Zeng S. et al (2021), employed Hyaluronic Acid for the active targeting of OSCC. Hyaluronic acid has a strong affinity for the CD44 receptor, which has been associated with a number of tumor biological processes, including tumor proliferation, progression, and metastasis. The binding on CD44 resulted in receptorspecific endocytosis from the OSCC cell. The KB cancer cell membrane vesicles that Sun et al (2020) used as a coating of their gold nanorods not only achieved immune evasion as we saw above but also delivered efficient homotypic targeting ability to the cancer cell type of which they originated. Liao et all (2019) made good use of the RGD peptides for specifically targeting the avb3 receptors on the OSCC cell line they experimented on. Finally, another component with duality on targeting, both non-specific and specific are the Platelets that Rao et al (2018), managed to isolate and combine with their nanorods. Due to their substantial interplay and role in tumor

metastasis, the recognition and interaction between PLTs and circulating tumor cells (CTCs) have attracted a significant amount of attention (Labelle et al., 2002). CAL 27 human squamous carcinoma cells were utilized to examine the cancer targeting performance of PLT-AuNRs, and it was discovered that PLT-AuNRs can bind to cancer cells, as they resulted in the maximum uptake, suggesting a superior and specific cancer targeting performance.

Finding a targeting method is essential in designing a nanomedical treatment. As the above examples indicate there are methods that can incorporate both non-specific and specific aiming characteristics. But the most interesting to mention is that in two studies, the researchers chose to make use of components of the cancerous cell itself, achieving excellent binding.

Table 3 -Targeting methods

Targeting type	Targeting Method	Aim	Reference
non-specific	PEGylation	immune system evasion - higher circulation time	Abdelaziz et al, 2021
specific	extracellular vesicles	specifically accumulation to originated SCC9 cells	Yang et al, 2021
specific	Folic Acid	Folic acid receptors	El-Sherbiny et al, 2021
non-specific	mesoporous silica	immune evasion - higher circulation time	Zeng, S. et al, 2021
specific	KB cancer cell membrane	homotypic targeting	Sun et al, 2020
non-specific	Alginate – Cisteine	higher circulation time	Liao et al, 2019
specific	RGD peptides	targeting the avb3 receptors	
non-specific	Platelets	immune evasion - higher circulation time	Rao et al, 2018
specific	Platelets	recognition circulating tumor cells (CTCs)	

4.3 Synergetic Treatments

The primary use of the Gold nanoparticles is to achieve the apoptosis or necrosis of the cancer cell under plasmonic hyperthermia. However the therapeutic result can be considerably enhanced by incorporating in the procedure the use of complementary modalities. On these studies in consideration, chemotherapy and radiotherapy have been utilized.

The purpose of chemotherapy is to prevent invasion and metastasis by inhibiting cell proliferation and tumor development. This, however, results in chemotherapy's toxicity because to its effect on normal cells. On multiple levels inside a cell and its surrounding environment, tumor growth can be inhibited. Conventional chemotherapy treatments typically disrupt the macromolecular production and function of neoplastic cells by interfering with the creation of DNA, RNA, or proteins or by interfering with the proper function of the preformed molecule. When interference with macromolecular synthesis or function is sufficient, it results in cell death through the chemotherapeutic agent's direct effect or by inducing apoptosis. Traditional drugs may delay cell death as a proportion of cells perish as a result of a specific treatment. Hence, the medication may need to be administered multiple times to exert an effect. While DNA synthesis occurs during the S phase of the cell cycle, it is at this time that cytotoxic medicines are most harmful. Vinca alkaloids and Taxanes inhibit mitotic spindle development during the M phase (Amjad et al., 2022).

Nanochemotherapy refers to the method where the chemotherapeutic molecule is delivered specifically to the cancer cell, leading to it’s death and in the highest effectiveness while not affecting the healthy tissue. Nanoparticles can be used as delivery drug systems, meaning that they carry and release the drug to the target. The use of chemotherapeutic agents could enhance the overall survival rate of oral cancer patients, and the administration of induction chemotherapy could prevent local recurrence. Currently, cisplatin, fluorouracil, carboplatin, paclitaxel, methotrexate, etc. (MARCAZZAN et al., 2018) are regarded as the most frequently utilized medications.

Yang et al, (2021) incorporated a complex of extracellular vesicles extracted from the OSCC cells and Chrysin in their structure. Chrysin is found in honey and has anticancer properties. Like flavonoids, it has an anticancer effect through modulating the expression of ncRNAs in numerous types of cancer. EVs contain many miRNAs implicated in cellular death. As tumor suppressors, the let-7a family exhibits decreased expression in a variety of malignancies, including breast cancer (Wu et al., 2015). Expression of let-7a was correlated with the long non-coding RNA (lncRNA) H19, which was associated with cell apoptosis (Ghafouri-Fard et al., 2020). let-7a-3p was upregulated in SSC9 and CAL27 cells following chrysin treatment. SCC9 cells were driven to induce apoptosis when let-7a-3p enhanced the production of the p53 protein, a crucial component of the cell apoptosis pathway. In addition, let-7a-3p overexpression inhibited cell invasion. Decreased expression of let-7a-3p enhances

SCC9 cell migration. Their findings revealed that EVs-Chrysin caused apoptosis and inhibited invasion in SCC9 cells via let-7a-3p.

El-Sherbiny et al, (2021) used Thymoquinone in their setting. Thymoquinone (TQ) is derived from the Nigella sativa plant and interferes with a broad spectrum of tumorigenic functions, including carcinogenesis, malignant development, angiogenesis invasion, and migration. Zeng S. et al, (2021) deployed Doxorubicin as a nanochemotherapeutic. Zeng j. et al, (2020) used cisplatin to enhance the result of the treatment as also Mapanao et al (2020) did.

Radiation is a physical agent employed to eliminate cancer cells. The radiation used is characterized as ionizing radiation because it generates ions (electrically charged particles) and deposits energy in the cells of the tissues it passes through. This deposited energy can destroy cancer cells or induce genetic alterations that result in the demise of cancer cells (Baskar et al., 2012). High-energy radiation damages the genetic material (deoxyribonucleic acid, DNA) of cells, inhibiting their ability to reproduce and multiply. Since radiation destroys both normal and cancerous cells, the objective of radiation treatment is to increase the radiation dose to abnormal cancer cells while reducing exposure to normal cells adjacent to cancer cells or in the radiation's path. Typically, normal cells can self-repair at a faster rate and maintain their normal function state than cancer cells. In general, cancer cells are less effective than normal cells at repairing radiation-induced damage, resulting in differential cancer cell death (Begg et al., 2011).

Radiotherapy in nanomedicine occurs with the aid of nanoparticles that bind specifically to the cancer cells and work as radiotherapy agents. Their purpose is to enhance the radiating result only on the area of the tumor and all of that with a significant and as such less destructive energy, thus protecting the healthy cells and minimizing the side effects of the traditional method.

Sun et al (2020) implemented Radiotherapy in their experiments, using the Gold nanorods as agents. Gold nanorods are frequently employed in both internal and exterior radiation therapy due to the high-Z (Z = 79) of the element Au. High-Z nanostructures are excellent radiosensitive materials for radiation augmentation. Using the X-ray absorption by materials as an example, the relationship between the atomic number (Z), incident X-ray energy (E), and X-ray absorption coefficient of materials is as follows: $\mu = \rho Z^4/(AE^3)$, where ρ and A are the density and atomic mass of materials, respectively (Lusic et al., 2013). High-Z nanostructures have the capacity to increase the local tissues' X-ray absorption and efficiently release low-energy electrons to produce more free radicals, which can damage DNA with the energy they deposit (Jelveh et al., 2011). Mapanao et al (2020) created gold ultrasmall nanoparticles in silica cover that can be used and as a radiotherapy sensitizer. While GNPs are promising radiosensitizers due to their high atomic number and excellent biocompatibility in general, Ultrasmall Au NPs or even smaller Au nanoclusters specifically consisting only about a dozen of gold atoms have the unique advantage that they can be rapidly cleared through urea (Yuan et al., 2021).

Table 4 – Synergetic Treatments

Type of Syn. Treatment	Mean of Treatment	Reference
Nanochemotherapy	Chrysin - EVs	Yang et al, 2021
Nanochemotherapy	Thymoquinone	El-Sherbiny et al, 2021
Nanochemotherapy	Doxorubicin	Zeng, S. et al, 2021
Nanochemotherapy	Cisplatin	Zeng, J. et al, 2020
Radiotherapy	Gold nanorods	Sun et al, 2020
Nanochemotherapy	Cisplatin	Mapanao et al, 2020
Radiotherapy	ultrasmall nanoparticles	

4.4 NIR application

Abdelaziz et al (2021) used a gallium-aluminum-arsenide (GaAlAs) diode laser equipment to provide a continuous 808 nm wavelength of light and the tongue tumor was in no contact with the probe. It was reported that for maximum tumor reduction with the least amount of tissue damage, 10-15 minutes of irradiation at 0.9W/cm^2 were required and took place 24 hours after the nanoparticles were injected.
Yang et al (2021) exposed for their in vitro part of the experiment the under-treatment group of female nude mice to an NIR laser in a wavelength of 808 nm after injection (twice on day 8 and day 15), and the tumor growth was observed in vivo with a fluorescence imaging system. El-Sherbiny et al (2021) do not mention the exact specifications of their laser setting. Zeng S. et al (2021) used 808 nm laser with a power density of 1 W/cm^{-2} for the in vitro experiments and an 808 nm NIR laser irradiation with power density of laser at 2 W/cm^{-2}. They conducted detailed measurements concerning the photothermal conversion efficiency of their nanoparticle under the 808 nm NIR irradiation. Zeng J. et al (2020) do not mention their laser setting in their study. Sun et al. (2020) utilized a 980 nm NIR laser on 0.5 W cm^{-2} and X-rays radiation on 4 Gy. Upon exposure to 980 nm light during the characterization stage, their nanoparticle showed comparable photothermal transfer efficiency which could heat the surroundings to about 60 C after 1 min irradiation under NIR light and heat water to only 30 C. The light-to-heat conversion capability of GNRs could be maintained for at least three cycles, suggesting their superb stability for long-term or repetitive treatments. Mapanao et al (2020) used an 808 nm portable CW-laser module set at 300 mW cm^{-2} for their in vitro experiment. Liao et al (2019) mention the use of a Diode single-wavelength laser at 808 nm for the in vitro part of the experiment. Rao et al (2018) refer the use of an 808 nm NIR laser.

From the given information, we have to mention that the predominant wavelength that have been applied was that of the 808 nm. Until now this is common in most Photothermal therapy studies. The laser wavelength in the near-infrared (NIR) range is greatly wanted for use in PTT due to decreased tissue scattering and absorption, which allows for deeper tissue penetration. But the NIR area contains two biologically transparent windows: the first NIR window (NIR-I; 700–900 nm) and the second NIR window (NIR-II; 1000–1700 nm). In recent years, the application of NIR-II light has gained increasing attention due to the inherent benefits of light in the NIR-II

window, which include a deeper penetration depth and a higher maximum permissible exposure (MPE) than NIR-I. Wu et al. (2020) suggest in their study that NIR-II laser in 1275 nm wavelength may be superior to the commonly used 808 nm NIR-I for deep-tissue treatment and propose further research.

Professor of Dental Surgery, Jacek Matys mentions in a brief but indicative publishing on the Journal of Clinical and Diagnostic Research (Matys, 2015) that it is crucial that all laser studies include information that will allow future researchers to reproduce each experiment. For example, a value for the energy density (fluency) of lasers, a crucial aspect in determining the dose of energy received by treated tissues, has not often been included in research studies by authors. Fluency or energy density is the amount of energy given divided by the area (energy per unit area). Fluency is frequently the most significant factor in laser therapy. Various kinds of lasers, whether they have the same or a different wavelength, have been used in the medical industry, however the variable internal technology in these apparatuses produces varying outcomes in the energy density (amount of light absorbed by the tissue). As a result, all investigations need to take into account the crucial factors that enable comparing various laser types. He concludes by advising that all factors for assessing the energy and power density of laser devices should be included in scientific laser-assisted studies. The following laser technical characteristics are strictly related to the energy absorbed by tissue:

- energy and power of laser.
- pulse duration and repetition rate.
- time of irradiation
- size of tip
- distance to the target
- tip angulation
- beam profile (Gaussian or Flat-top)

A conclusion was made that some of the papers lacked in the same matter; the exact presentation of the characteristics of the laser setting they utilized, besides the wavelength. It is crucial for the reproduction of these experiments but most importantly for the designing of future clinical trials on humans, that all of the characteristics mentioned above to be analytically presented in future studies. An excellent example of a study that gives all the needed information about the laser setting used is that of Colombo et al (2019) about the Photothermal effect by 808-nm laser irradiation of melanin.

4.5 Results of PTT treatment in vitro and in vivo

Abdelaziz et al conducted an in vivo experiment on Wistar rats Tongue SCC induced after appliance of DMBA. After the PTT was concluded the results were very promising. In the clinical examination of the treated group there were no signs of cancer. Histopathological examination on samples from the tongue of these rats presented an image of normal tissue in both the epidermis and the underlying muscle. They also concluded that locally injected NPs gave better results in preventing the tumor growth than systematically administrated nanoparticles.

In their study that included in vitro and in vivo settings, Yang et al, reached the following conclusions. In vitro experiment specified the specific uptake of their Gold-Extracellular (Gold-EVs) vesicle nanoparticle. Compared to BGC823 cell line that belongs to human gastric cancer and LM3 cell line that belongs to adult hepatocellular carcinoma, the uptake of Au-EVs was specific in SCC9 cells that is a cell line isolated from the tongue of a 25-year-old, male patient with squamous cell carcinoma. Secondly, Gold-EVs combined with NIR promoted significant apoptosis on the SCC9 cell lines compared to the group treated with Gold-EVs without irradiation proving PTT was successful.

In vivo experiment, on female nude mice, indicated that the Gold-EVs could move toward the tumor, the expression of let-7a-3p was increased in the Chrysin and Gold-EV injected groups enhancing the production of the p53 protein leading to a successful chemotherapeutic result and that Gold-EVs Nanoparticles mediated PPT effectively as they inhibited tumor clinically.

El-Sherbiny et al, conducted in vivo experiment on Syrian golden hamsters that had manifested Squamous cell carcinoma under the application of the carcinogen dimethylbenz-anthracene (DMBA). After the conclusion of the treatment, animals in GNR+ Thymoquinone under laser irradiation (GNR/NTQ/laser) and GNR-only under laser irradiation (GNR/laser) groups regained weight. Clinical examination on the same groups, recorded significant decrease in tumor volumes. Both results indicated that PTT was successful. Histopathological results confirmed the cancer regression and the tumor volume results. Apoptotic cells were identified in Hematoxylin and eosin stain sections with GNR/NTQ/laser and GNR/laser groups. They also concluded that a higher temperature in the PLGA shell could stimulate drug release, thus creating a drug carrier with controllable drug release abilities, initiating the release only when they are irradiated and the shell breaks under higher temperature. It is important to note that they presented results indicating that white blood cells (WBCs) count significantly increased with GNR/NTQ/laser and GNR/laser groups meaning that the immune-suppressive effect of DMBA can be reversed as they documented an improvement of WBCs count at the GNR/NTQ/laser group, probably due to the immune-enhancing effect of Thymoquinone. But the same increase was also observed and at the GNR/laser group meaning that NIR of gold nanoparticles could in a stimulation of the inflammatory response.

On the other hand Platelet count showed no difference between the negative control and GNR/NTQ/laser groups and as Platelets have a direct role in cancer as the increase in platelet count is directly related to the stage of OSCC, that may indicates that there was no further development of the malignancy. Hemoglobin and Red Blood Cells levels were significantly decreased with GNR/NTQ/laser and GNR/laser groups meaning that PTT may affect the blood, something that needs further investigation. In general, they concluded that a combination between photothermal therapy and nanonchemotherapy by GNR/NTQ/PLGA/FA was better than either treatment alone.

Zeng S. et al. in their study included in vitro and in vivo parts. For in vitro investigation they used a HOK cell line of normal Human Oral Keratinocytes and CAL-27 cell line that are epithelial cells isolated from tissue taken prior to treatment from a 56-year-old, White male with a lesion in the middle of the tongue in 1982. They proved that there was no distinct cytotoxicity in HOK line showing that their nanoparticle of blank AuNRs@mSiO2-HA1 without DOX was biocompatible. They also observed that the cytotoxicity of the DOX- AuNRs@mSiO2-HA group was significantly lower than that of the DOX-only group, proving that they achieved a sustained release of DOX molecules. In PTT examination, DOX-AuNRs@mSiO2-HA under laser irradiation had an exceptional synergistic therapy effect as all the CAL-27 cells were destroyed. CAL-27 cells displayed the capability to intake DOX-AuNRs@mSiO2-HA, thus specific targeting was achieved. The CAL-27 cells express high levels of CD44, so that DOX- AuNRs@mSiO2-HA can be accumulated due to HA in tumor. The cellular uptake could be consisted highly controllable by adjusting co-incubation time or by increasing the concentration of materials.

In vivo, they used mice with a xenografted CAL-27 tumor. Under Photoacoustic Imaging (PA), they recorded that the signal increased gradually within the first 8 hours post-injection at tumor site and then decreased, which indicated that the maximum nanoparticles concentration in the tumor region was achieved at 8 hours post-injection. Digital photographs of tumors on the 12th day after treatment proved that tumors in DOX- AuNRs@mSiO2-HA + LASER group were completely ablated. Body weight curves presented no significant difference among control and treated groups, implying that treatments could not affect the normal development of the mice during the experiment. DOX-AuNRs@mSiO2-HA and PBS+LASER groups showed a slower tumor growth rate than the control groups, meaning that the therapeutic effect of only chemotherapy or PTT-alone was limited. The DOX-AuNRs@mSiO2-HA group had the best survival rate among all the experimental groups. Hematoxylin and eosin staining of tumor slices showed that most of the cells in the tumors of mice of DOX-AuNRs@mSiO2-HA +LASER group were severely damaged, while the cells in the tumors of mice of the other treatment groups were only partially destroyed consisting overall the combined PTT-Chemotherapy treatment as successful.

Zeng J. et al organized an in vitro and in vivo experiment. In vitro they employed human SCC-9 cells, a cell line that was isolated from the tongue of a 25-year-old, male patient with squamous cell carcinoma.

Their experiment is significant because comperes the efficiency of Gold Nanoparticle PTT to a new nanoparticle, that of Black Phosphorous. In vitro results indicated that

the use of low-dose of nanomaterials (BPNSs and GNPs) can more efficiently promote the apoptosis of human SCC-9 cells compared to the normal doses of Cisplatin (CDDP), proving the efficacy of nanophotothermal treatment. At the same time, BPNSs delivered stronger cells killing ability than GNPs, while GNPs exhibited stronger cells killing ability than cisplatin, which might be due to the alteration of cell cycle caused by the PTT. Of all the NPs, BPNSs exhibited the greatest ability to destroy malignant cells. This may be of the reason that cancer cells have a more vigorous endocytosis and a faster metabolic rate than normal cells, and BPNSs are rapidly taken up by cancer cells via endocytosis and swiftly degraded within the cells to produce a significant amount of phosphate ions causing changes in the internal environment of cancer cells that result in G2/M phase inhibition, effectively reducing cancer cell proliferation [ZHOU et al., 2019]. Following the inhibition of proliferation, cancer cells underwent further programmed cell death via apoptosis and autophagy.

In vivo they experimented on Golden hamsters where they applied 0.5% DMBA in acetone solution on their left cheek pouches three times a week for 16 weeks to cause malignancy. The control group's survival rate was lower than that of the five groups where combined nanodrugs were used and to the three groups of pure medications. The survival rates of the GNPs group and the CDDP group in this study were similar. At the same time the BPNSs treated group had a much greater survival rate than non-BPNPs groups. The greater survival rate of GNPs-to-BPNPs1:5/CDDP compared to GNPs-to-BPNPs5:1/CDDP indicated that BPNPs inhibit cancer cells more effectively than GNPs. The tumor volumes at the four combined drug groups, of which GNPs-to-BPNPs1:5/CDDP had the most pronounced antitumor impact, were significantly higher than those of GNPs only, showing that combined treatment was more effective. They also demonstrated that laser irradiation increases drug release. Synergistic effects of GNPs, BPNPs, and CDDP may boost the nanomaterials drug delivery system's stability and efficacy. The expression of the tumor suppressor gene P53 protein was higher in the BPNPs, and GNPs groups than in the CDDP group.

The expression of Proliferating cell nuclear antigen (PCNA), a DNA clamp that acts as a processivity factor for DNA polymerase in eukaryotic cells and is important for replication, was higher in the CDDP group than in the other groups, indicating that CDDP alone did not suppress OSCC efficiently. They concluded that the developed nanocomposites (GNPs-to-BPNSs) in an analogy of higher BPNPs 1:5, loaded with CDDP could help to effectively inhibit the growth of OSCC, while BPNPs are a more effective PTT agent than GNPs.

Sun et al, conducted in vitro and in vivo experiments for their study. In vitro, to test the selective cell uptake, they used five different cancer cells, including LM3 (human hepatocellular carcinoma), HepG2 (human liver cancer) , 4T1 (mammary carcinoma originally derived from a spontaneously arising mammary tumor in BALB/cfC3H mice), HeLa (an immortalized cell line derived from cervical cancer cells taken on February 8, 1951 and named after Henrietta Lacks) and KB cells (squamous cell carcinoma). They resulted that the KB cells assimilated GNR@Mem more effectively than the other cells proving the specific targeting ability of their nanoparticle on homotypic tumor cells because of the KB cancer cell membrane

vesicles on the nanoparticle. After 24 hours of coincubation, the GNR@Mem group's intracellular gold concentration was 4.7 times more than that of the PEGylated GNR (GNR@PEG) group as due to the antifouling polymeric coating on PEGylated GNRs, not all of the cells were able to absorb it very well. Homotypic cancer cell targeting is superior to PEG- EPR nonspecific targeting. To test in vitro the cytotoxicity and therapeutic outcome under NIR irradiation or X-rays irradiation of GNR@Mem and GNR@PEG they used KB cells. They recorded that KB cell viability reduced with an increase in GNR concentration when exposed to X-ray or NIR light. The cytotoxicity of GNR@MEM against KB cancer cells was simultaneously enhanced by photothermal and sensitized radiation, and it was the highest achieved, deeming that PTT was effective.

In vivo, firstly they tested the pharmacokinetics and tumor accumulation of GNRs. They documented after ultrathin sections of the tumors for histopathological test and Inductively coupled plasma mass spectrometry (ICP-MS) of the tissues that more GNRs were accumulated in the tumor cells and tumor extracellular matrix in the GNR@Mem group. To test PTT and RT efficacy in vivo, they used 6- to 8-week old healthy male nude mice and created xenograft tumors on them of KB cells. The results proved that both GNR@PEG under NIR and GNR@Mem under NIR clearly inhibited the growth of tumors. The GNR@Mem under NIR and X-ray irradiation group showed the strongest tumor inhibition potential, with 4 of 5 tumors being totally eliminated with further X-ray irradiation and subsequent radiosensitive therapy. Thus the GNR@Mem mediated PTT and RT combination therapy increased the tumor volume suppression rate to 95.6%. They resulted that for extremely effective combined radiation and photothermal therapy of oral squamous carcinoma, GNR@Mem is an outstanding sensitizer, offering a promising treatment outcome.

Mapanao et al. conducted in vitro experiments for their study. They employed two cell lines: SCC-25 (coming from an epithelial-like cell that was isolated from the tongue of a 70-year-old, male patient with squamous cell carcinoma and is HPV-negative) and UPCI:SCC-154 (a squamous cell line that was isolated in 1996 from the tongue of a 54-year-old, White male patient with carcinoma and is HPV-positive). The reason they included HPV-positive cells in their study is that Human Papilloma Virus (HPV) is a major etiologic factor for oropharyngeal squamous cell carcinoma (OPSCC), thus the study of the possible results of PTT on these cells is of great interest. In the beginning they tested the PTT efficacy of their tNAs nanoparticles on both cell lines. The results showed that both cell lines could internalize the nano-architectures and tNAs exposed to radiation induced cytotoxicity, thus regardless of HPV status, the effectiveness of tNAs to induce hyperthermia was confirmed in 2D SCC cell models. A second in vitro experiment was conducted, but this time on 3D SCC-25 (HPV-negative) and UPCI:SCC-154 (HPV-positive) cell models. These spheroids growth in diameters of about 200–300 μm for SCC-25 and 150–250 μm for UPCI:SCC-154. The reason that these multicellular tumor spheroids had been utilized was to take advantage of their closer resemblance to in vivo tumor conditions compared to conventional two-dimensional cell cultures. They executed a detailed application of NIR photothermia and the results exhibited that tNAs-cisPt drastically decreased cell viability and that

probable activation of the cisplatin prodrug can be primarily attributed for the long-term consequences of the nano-architectures on the viability of spheroids. The most important outcome of their research was that it was exhibited an improved response to therapy on the HPV-positive OSCC cells in comparison to HPV-negative OSCC-negative cells, meaning that HPV-positive cells are more sensitive to PTT therapy reaffirming the clinical observations regarding the better therapeutic response of HPV-positive OSCC patients.

Liao et al, conducted in vitro and in vivo experiments for their study. In vitro, to demonstrate that the biocompatibility of GNRs is improved by replacing CTAB with alginate, they used SAS-3 cells (human squamous carcinoma of the tongue) as targets. They administered formations of their nanoparticle with CTAB (GNR@CTAb) and others where CTAB was replaced with Alginate – Cysteine (GNR@Alg-Cys). To inspect the cellural uptake, they introduced CTAB free GNR@Alg-Cys and GNR@Alg-Cys with RGD peptides (GNR@Alg-Cys/RGD) nanoparticles to the SAS-3 cells. To test the efficacy of GNR@Alg-Cys/RGD on PTT, they administered the nanoparticles to the SAS cells. The overall results of the in vitro settings ere the following: First of all GNR@CTAB were proven to be highly toxic to the cells but at the same time GNR@Alg-Cys were nontoxic and GNR@Alg-Cys/RGD were nontoxic to cells. Cells internalized RGD-modified carriers by receptor-mediated endocytosis. After adding the RGD peptide on alginate, cell internalization was twice the amount. When GNR@Alg-Cys participated in the PTT, the local temperature rose to 57 C after 5 minutes of exposure, killing 50% of the cells by hyperthermia. Up to 90% of the cells were destroyed by hyperthermia when GNR@Alg-Cys was modified by RGD peptide. The roughly twofold increase in the number of GNRs the cells absorbed could be the cause of the noticeably decreased cell viability. Most importantly, the cells were still alive outside of the laser-exposed area.

In vivo and in order to further demonstrate the efficacy of GNR@Alg-Cys/RGD on PTT they used nude mice with a malignancy of xenografted Human SAS cells and resulted that when compared to the no treatment group, the light group treated with PTT of GNR@Alg-Cys/RGD significantly inhibited the tumor's growth on day 14 by about 2 to 5 times, consisting the phototherapy successful.

Lastly, Rao et al. conducted in vitro and in vivo experiments for their study. In vitro and in order to test if PLT-AuNRs nanoparticles inherited circulation time and were able to evade phagocytosis, they administered them on RAW 264.7 murine macrophage-like cells. The results were that PLT-AuNRs sowed improved immune evasion than AuNRs, as AuNRs resulted in the highest uptake. To evaluate the cancer targeting performance of PLT-AuNRs and their PTT efficacy in vitro, they administered the NPs on CAL 27 human squamous carcinoma cells. Compared to the nanoparticles without PLT, PLT-AuNRs demonstrated superior cancer targeting performance. At the same time, PLT-AuNRs resulted in selectively killing of cancer cells under localizing laser irradiation. In total, PLT-AuNRs resulted in the best in vitro PTT effect, which can be attributed to the close interactions between PLT-AuNRs and cancer cells as a result of the Platelets and their ability to interact with the tumor.

In vivo, in order to investigate whether PLTs could enhance the PTT effect, they used BALB/c nude mice with CAL 27 tumor xenografts. They resulted that PTT therapy could facilitate the ability for PLT-AuNRs to target more PTT sites, presumably by a mechanism where PLT-AuNRs are drawn to the PTT injury site. Effective increases in temperature following each treatment, demonstrated that the PTT-ablated tumor tissues drew in more PLTAuNRs and that the PLT-AuNRs assisted the PTT in a feedback manner. Another point of interest is that when compared to other nanoparticles, PLT-AuNRs were able to inhibit tumor growth more effectively. The results also showed that PLT-AuNRs and laser irradiation combined, greatly delayed carcinogenesis. Blood biochemical and whole blood parameters, as well as tissue slices, showed no discernible differences, supporting the greater in vivo compatibility of PLT-AuNRs. Significantly reduced Ki-67 staining following PLT-AuNRs + Laser therapy revealed histopathologically successful tumor cell proliferation inhibition. Lastly, Terminal deoxynucleotidyl transferase-mediated deoxyuridinetriphosphate nick end labeling (TUNEL) assay slices revealed that many cells were killed or went into apoptosis in the mice treated with PLT-AuNRs + Laser, further indicating histopathologically that the tumor growth was obviously inhibited and consisting their experimentation as successful.

As it can be clear from the results of PTT, all the tested nanoparticles managed to successfully apply hyperthermia on their targets and most of them could totally destroy the malignant cells while did not harm the surrounding healthy tissues. But even in vivo experiments are no more than animal tests. It is clear from the outcomes that PTT could be used as a successful anticancer treatment, and the next step of human trials must be taken.

4.6 Biocompatibility and Toxicity of the Nanoparticles

Abdelaziz et al, documented that AST values increased, GGT values increased, ALT values decreased, CREA values increased in a non significant manner and UREA values increased in a non-significant manner. Blood Test indicated that there was a minor liver damage, and that GNPs have a direct effect on liver function but the kidneys not affected. TEM images showed a presence of gold nanoparticles in the cytoplasm of liver cells and presence of gold nanoparticles in phagolysosomes in Kupffer cells of the liver. They also reported Hepatocyte swelling and vacuolated swelling of the cytoplasm on liver. After regular injections of GNPs, they noticed that the amount of gold in the kidney increased significantly. GNPs were reported to be efficiently cleared from the body of the rats. According to this research, GNP administration can result in slight liver damage and GNPs directly affect liver function. The authors suggest further kinetic and toxicokinetic research to better understand particle activity in vivo.

Yang et al. mentioned that their nanoparticles at the end of the experiment did not alter any organs in vivo.

El-Sherbiny et al. noticed that ALT and AST values were increased significantly with GNR/NTQ/laser and GNR/laser irradiation and creatinine level was significantly increased while urea levels significantly decreased. There was no statistically significant difference in the mean values of uric acid between all the groups. Total white blood cells (WBCs) count was increased significantly in the GNR/NTQ/laser and GNR/laser groups. Total white blood cells (WBCs) count was very highly increased significantly in GNR/NTQ without laser and NTQ groups. Platelets count (plt) showed no significant difference in GNR/NTQ/laser group while Platelets count (plt) was increased significantly in GNR/laser group, and very highly increased significantly in DMBA, GNR/NTQ-without laser and the NTQ groups. Hemoglobin (Hb) level was decreased significantly in GNR/NTQ/laser group. Hemoglobin (Hb) was very highly significantly decreased in DMBA, GNR/NTQ-without laser, GNR/laser and NTQ groups compared to negative control group. Red blood corpuscles (RBCs) were decreased significantly in GNR/NTQ/laser and GNR/laser groups and it was very highly significantly decreased in DMBA, GNR/NTQ without laser and NTQ groups. Aspartate aminotransferase (AST) and alanine aminotransferase (ALT) markedly elevated in GNR/NTQ/laser and GNR/laser groups. These results suggest that the liver might be affected mildly, due to activated GNRs may have a direct effect on the liver function. Results of WBCs count significantly increased with GNR/NTQ/laser and GNR/laser groups. The immune-suppressive effect of DMBA may results in an increase in WBC counts as a defense mechanism and the improvement of WBCs count with GNR/NTQ/laser group, may be due to the immune enhancing effect of NTQ. GNR/laser group presented elevation of WBC count and that could be a possible result of their ability to stimulate an inflammatory response. Lastly HB and RBCs levels were significantly decreased with GNR/NTQ/laser and GNR/laser groups. The example of this analytical presentation of the markers of liver and kidneys in this study, should be consisted a norm for all the in vivo experiments in the future as it has to be more clear what are the implication of gold nanoparticles administration especially to the liver.

Zeng S. et al, reported that there was no obvious organ damage and inflammation compared to the PBS control group and such, the safety and low toxicity of their nanoparticle were demonstrated to be good.

Zeng J. et al, did not report any findings regarding the effects of the nanoparticles on major organs.

Sun et al. reported that the liver, kidney, lung, and spleen showed no signs of tissue damage 24 hours after receiving an intravenous injection of GNR@Mem. Blood levels of AST, ALT, BUN, and CRE in the GNR@Mem-treated group were comparable to those in the control group, demonstrating GNR@Mem's high biocompatibility and suggesting possible biomedical uses for the particle. GNR@Mem and GNR@PEG had blood clearance half-lives of 4.36 hours and 2.71 hours, respectively. Three days after injection, a tiny portion of the GNR@Mem was exhausted in the urine (approximately 20%), indicating a relatively low level of long-term storage of GNR@Mem inside the

body. The majority of the GNR@Mem was gradually eliminated via feces (about 70% of the injected dosage).

Mapanao et al, conducted only in vitro experiments, therefore they do not provide any information about systemic toxicity of their nanoparticle.

Liao et al, reported that all the biomarkers (AST, ALT, T-Bil, CREA, BUN, and UA) showed no statistical differences amongst the PBS, light, and PTT groups thus their GNR@Alg-Cys/RGD sample was biologically safe in the animal study.

Finally, Rao et al, reported that comparing to GNRs, the PLT-GNR and PLT-M-GNR groups exhibited enhanced systematic circulation over 48h, suggesting superior in vivo immune evasion ability. Their nanoparticle had lower liver and spleen accumulation, indicating that PLT-GNRs gained the immune evasion ability from the source PLTs. At the same time there was neither death nor an obvious weight difference between the control and treatment groups over 30 days, proving that no overall side effects were induced by the injection of PLT-GNRs. Lastly No significant differences were observed in tissue slices and blood biochemical and whole blood parameters, further confirming the superior in vivo compatibility of PLT-GNRs

Overall, at it can be concluded from the information above, while liver seems to be to most affected organ, the synthesized nanoparticles presented good biocompatibility, especially these that incorporated natural elements like platelets or cell membranes. But still the known information on the matter is limited and further investigation on the matter is needed.

Table 5 – Explanation of Markers

Marker	**Abbreviation**	**Organ**	**Indication**
Aspartate Transferase	AST	Liver	high levels indicate liver injury
Alanine Transaminase	ALT	Liver	high levels indicate acute liver cell injury
Gamma-glutamyl Transferase	GGT	Liver	high levels indicate liver injury
Creatinine	CREA	Kidney	high levels indicate kidney injury
Blood urea nitrogen	BUN	Kidney	high levels indicate kidney injury
Bilirubin	T-Bil	Kidney	high levels indicate liver injury
White Blood Cell Count	WBC	Blood	Indication of general infection or inflammation
Platelets	PLT	Blood	Measures blood clotting
Hemoglobin	Hb	Blood	Monitor blood disorders

Table 7 – Results on Major Organs

Result	Reference
NP administration may results in slight liver damage	Abdelaziz et al, 2021
NP administration did not alter any organs in vivo	Yang et al, 2021
Possible Liver damage, Kidneys not affected	El-Sherbiny et al, 2021
no obvious organ damage and inflammation	Zeng, S. et al, 2021
no obvious organ damage	Sun et al, 2020
no obvious organ damage	Liao et al, 2019
no obvious organ damage	Rao et al, 2018

4.7 Conclusion

In conclusion, this presentation of nine indicative studies suggests promising results for the use of oral squamous cell plasmonic photothermal treatment as a potential therapy for oral cancer. The studies demonstrated that plasmonic nanoparticles can selectively target cancer cells and generate heat upon exposure to near-infrared light, leading to tumor ablation. The approach offers several advantages, including minimal invasiveness, high selectivity, and potential for personalized treatment. However, further studies are necessary to optimize the treatment parameters, improve targeting efficiency, and evaluate long-term outcomes. With continued research and development, plasmonic photothermal therapy has the potential to become a valuable addition to the armamentarium of oral cancer treatment modalities.

CONCLUSION:

Suggestions for Future Research
And
Some Thoughts

While the plasmonic photothermal treatment of oral squamous cell carcinoma using gold nanoparticles has shown promising results, there are still numerous avenues for future research that could improve its efficacy and utility. Future Research must be constant and should aim on the following areas:

Combination with other therapies: While plasmonic photothermal treatment shows potential as a standalone therapy, it may be even more effective when combined with other treatments, such as chemotherapy or immunotherapy. Studies could investigate the potential synergistic effects of combining plasmonic photothermal treatment with other therapies.

Optimization of treatment parameters: Further research could focus on optimizing the parameters of plasmonic photothermal treatment, such as the size and shape of the gold nanoparticles, the wavelength of the laser used, and the dosage of the nanoparticles administered. By fine-tuning these parameters, researchers could potentially improve the treatment's effectiveness and minimize any potential side effects.

Mechanisms of cellular uptake: While it is known that gold nanoparticles can be taken up by cancer cells, the mechanisms behind this process are not yet fully understood. Further research could investigate the cellular pathways that allow gold nanoparticles to enter cancer cells, which could lead to the development of even more targeted therapies.

In vivo studies: Most studies of plasmonic photothermal treatment using gold nanoparticles have been conducted in vitro, meaning that they have not yet been tested in live animals or human subjects. Further research could investigate the safety and efficacy of this treatment in vivo, with the ultimate goal of developing a clinically viable therapy.

Long-term outcomes: While plasmonic photothermal treatment shows promise as a potential therapy for oral squamous cell carcinoma, it is important to investigate its long-term outcomes, including recurrence rates, overall survival, and quality of life. Further studies could help determine the long-term benefits and risks of this treatment modality.

Overall, there is still much to learn about the use of plasmonic photothermal treatment using gold nanoparticles for oral squamous cell carcinoma. Future research

in these and other areas could help refine and improve this therapy, potentially leading to a valuable addition to the arsenal of treatments available for this common form of cancer.

In conclusion, plasmonic photothermal treatment using gold nanoparticles has shown great potential as a treatment modality for oral squamous cell carcinoma. This therapy utilizes the unique properties of gold nanoparticles to selectively target cancer cells and induce their destruction through the application of laser irradiation. The treatment offers several advantages over traditional therapies, including high selectivity, minimal invasiveness, and the potential for personalized treatment.

The available evidence suggests that plasmonic photothermal treatment is a promising approach for the treatment of oral squamous cell carcinoma. Future studies could focus on optimizing the parameters of the treatment, investigating the mechanisms of cellular uptake, and evaluating the long-term outcomes of this therapy. In summary, plasmonic photothermal treatment using gold nanoparticles represents a potential breakthrough in the treatment of oral squamous cell carcinoma. While much remains to be learned about this treatment modality, its unique properties offer hope for the development of more effective and personalized therapies for this common form of cancer.

And some thoughts…

As scientists we move forward through experimental processes that set attested foundations of knowledge. But are we reaching a point, or is our journey to treat incurable cases just a chimera, a hollow desire? Hope in our questions arises from the history of our species. Bound in an assailable and perishable flesh, we anguish to become preservers of life. And the means to that surround us. In this enclosed, due to our three-dimensional perception, system of Energy and Matter that we call Reality, all we have to do is understand which string plays each note and the answers shall be unlocked. Our search for knowledge has been the driving force of our existence. Thus, a philosophical statement can only foreshadow the conclusion of our noetic vocation;

In a universe where every action has a reaction, we humans were born condemned to seek the truth. Deterministically we won’t rest until we find redemption.

A day when a fatal cancer, as a late stage oral squamous cell carcinoma is, can be completely treated with the help of nanomedicine, may not be that far. Research must be continuous, and the next step of human trials must be set in motion, where the possible implications due to toxicity in major organs for example, if any, will be

understood and resolved and the success of the method in the complicated human body will be well comprehended and systematized in a simplified procedure as prescribing a medication in everyday clinical action of a dental clinic.

And why not imagine the time when, through the means of nanotechnology we may see ourselves synthesizing a nanoparticle with the promising name P.A.N.A.C.E.A. (**P**olydynamic **A**dvanced **N**anoparticle for **A**ll-out **C**ancer **E**nhanced **A**blation) that using combined treatment under NIR activation, will render all human malignancies another addition in the book of eradicated diseases.

We are problem solvers. Imagination sets the targets. The persistence and creativity of scientific accomplishments are our tools to consist them a reality.

Scientia potentia est

APPENDIX

PAPER 1 ID

Paper title	Phototherapy with Gold Nanoparticles and a Diode Laser for Oral Squamous Cell Carcinoma of the Tongue in Rats
Pub. Year	2021
Country	Egypt
Participants	Ahmed AbdelatifAbdelaziz1, Ali Mohamed Saafan 2,Latifa Mohamed Abdelgawad3, Mahmoud Bawdy El badawy4
Type	PTT only
Method	In vivo
Ca Cells / Cell lines	Tongue Ca Cells after DMBA carginogenesis
Main NP	Spherical AuNPs (propably PEGylated)
Size	50 nm
PTT Main NP	Spherical AuNPs
AuNP	Spherical AuNP
Synthesis of AuNP	Seed growth from HAuCl4 solution
Size	50nm
Test type	In vivo
Reason	Treatment of OSCC with AuNP PTT
Animals	male, 8 weeks old, Wistar rats, body weight (120- 160 g)
Group Name	Group (D): 13 rats + AuNP + Laser
Carcinogen	0.5% 7,12-dimethylbenz (a) anthracene (DMBA)
In vivo Ca Cells	Tongue SCC
NPs	Spherical AuNPs 50nm
NP dose	1.5mg/kg body weight of gold nanoparticles in phosphate buffer solution
Way of Med. Admin.	Locally injected into the tongue tumors
Laser info	808 nm, 6 mm dia gallium-aluminum-arsenide (GaAlAs) diode laser, tongue tumor was in no contact with the probe
Expos. Duration	10–15 minutes of irradiation at 0.9W/cm2
Time of Exposure	24 hours after injection
Biomarkers tested	AST, GGT, ALT, ALP, UREA, and CREA
Day of Sacrifice	30
RESULTS IN VIVO	
Clinical Findings	significant weight gain, reduction in papillary overgrowth size, complete ablation of ulcers and small tumors
Histopathological Findings	normal tongue (epidermis, muscle), Apoptotic cells discovered, cytoplasm condensation, and cell borders clearly defined.
Blood Test Findings	1) increased the AST values 2) GGT values increased 3) ALT values decreased 4) CREA values increased in a non significant manner 5) UREA values increased in a non-significant manner
Liver Findings	1) TEM images show: Presence of gold nanoparticles in the cytoplasm of liver cells, Presence of gold nanoparticles in phagolysosomes in Kupffer cells of the liver 2) Hepatocyte swelling, vacuolated swelling of the cytoplasm
Kidney Findings	After regular injections of GNPs, the amount of gold in the kidney increased significantly
Other Findings	level of bcl-2 in group C more than group D indicating that the effect of treatment of gold nanoparticales compined whith laser is more effective than gold nanoparticales only for treatment of squamous cell carcinoma of tongue.

Was PTT treatment successful?	YES
Results in vivo	1)GNP administration can cause minor liver damage, and that GNPs have a direct effect on liver function. Further kinetic and toxicokinetic studies are needed to expand our understanding of particle activity in vivo 2) GNPs are efficiently cleared from the body 3) Clinical: no clinical signs of cancer on laser treated rats Histopathological: normal tongue (epidermis, muscle) Blood Test: cause minor liver damage, and that GNPs have a direct effect on liver function, kidneys not affected Himmunohistechimstry: lower bcl-2 in laser treated group 4) non-parametric analysis of variance revealed statistically significant differences between the treated and untreated group 5) localy injected NP had better result in tumor growth than systematically administrated

PAPER 2 ID

Paper Title	A **New Nanomaterial** Based on **Extracellular Vesicles** Containing **Chrysin**-Induced Cell Apoptosis Through **Let-7a** in Tongue Squamous Cell Carcinoma
Pub. Year	2021
Country	China
Participants	Zhijing Yang, Da Liu , Hengzong Zhou, Boqiang, Lu Chang, Huimin Liu, Haoming Luo, Dongxu Wang and Weiwei Liu
Type	PTT + Chemo
Method	In vivo, in vitro
Ca Cells / Cell lines	1) SCC9 and CAL27 TSCC cell lines 2) BGC823 human gastric cancer cell line 3) HCC-LM3 human hepatocellular carcinoma cell line
Main NP	PKH26-labeled Au-EVs-Chrysin NPs
Composisition	AuNP + Chrysin + EVs labeled with PKH26 (AuNPs were self-grown on the surface of EVschrysin forming a new nanomaterial, which was Au-EV)
Size	50–150 nm
PTT NP	Au-Ev round in shape
Synthesis of AuNP	From $HAuCl_4$ (AuNPs were self-grown on the surface of EVs chrysin forming a new nanomaterial, which was Au-EV)
Composisition	Au on EVs
Size	50–150 nm
Compl. Ther.	Chemotherapy
CompT carrier	Chrysin
Other Elements	extracellular vesicles (EVs) with chrysin from SCC9 cells treated with chrysin
Test type	In vitro 1
Reason	To determine whether Au-EVs were specific to the cell type
In vitro cells	SCC9, BGC823, and LM3 cells
NPs	Au-EVs
Laser	NIR
Results in vitro	1) compared to BGC823 and LM3 cells, the uptake of Au-EVs was specific in SCC9 cells 2) Au-EVs combined with NIR promote significant apoptosis compared with that of Au-EVs
Test type	In vitro 2
Reason	Cell Migration and Invasion Analysis
In vitro cells	SCC9 cells
Materials	let-7a-3p mimics or inhibitors
Test type	In vivo
Reason	To investigate the antitumor effect of Au-EVs in vivo
Animals	female nude mice (6–8 weeks old)
Group Name	Au-Ev + laser
Carcinogen	Injected SCC9 cells (8×106) into the left flank
In vivo Ca Cells	SCC9 cells
NPs	PKH26-labeled Au-EVs
Way of Med. Admin.	injected below the tumor on day 8 and day 15
Laser info	NIR (808 nm)
Time of Exposure	twice, day 8 and day 15
Day of Sacrifice	21
RESULTS IN VIVO	
Other Findings	tumor growth inhibited (tumor growth was observed in vivo with a fluorescence imaging system)
Was PTT treatment successful	YES

Results in vivo	1) the Au-EVs could move toward the tumor 2) NIR irradiation could quench the fluorescence of the Au-EVs 3) Au-EVs combined with NIR significantly inhibited tumor growth 4) Au-EVs did not alter others organs in vivo 5) the expression of let-7a-3p was increased in the chrysin and Au-EV groups 6) Au-EVs mediated PPT effectively and inhibited tumor growth in vivo

PAPER 3 ID

Paper Title	COMBINED **PHOTOTHERMAL** AND **NANOCHEMOTHERAPY** IN TREATMENT OF INDUCED ORAL SQUAMOUS CELL CARCINOMA IN HAMSTERS
Pub. Year	2021
Country	Egypt
Participants	Randa Hamed El-Sherbiny, Magda Mohamed Aly Hassan, Wafaa Hassanein El-Hossary, Mona Saad Shata
Type	PTT + Chemotherapy
Method	In vivo
Ca Cells / Cell lines	Mouse SCC induced by DMBA
Main NP	GNR/NTQ/PLGA/FA
Composisition	Gold nanorods + Thymoquinone Nanoparticles loaded on PLGA and conjugated with targeting agent folate or folic acid (FA)
Size	size ranged from 115-180 nm and the morphology was spherical in shape
PTT Main NP	Gold nanorods
Synthesis of AuNP	The seed-mediated growth method was used for preparation of GNRs
Size	10 nm in width and 40 nm in length
Compl. Ther.	Chemotherapy
CompT carrier	Thymoquinone
Other Elements	PLGA Folic acid (FA)
Test type	In vivo
Reason	PTT efficacy of GNR/NTQ/PLGA/FA
Animals	Syrian golden hamsters (Mesocricetusauratus), weighing 90-110 grams and aged 6-8 weeks
No of Groups	6
Group Name	Group B1: (AuNP+TQ + Laser)
Carcinogen	0.5% 7,12-dimethylbenz (a) anthracene (DMBA)
In vivo Ca Cells	Mouse SCC induced by DMBA
NPs	GNR/NTQ/PLGA/FA, GNR/PLGA/FA, NTQ/PLGA/FA
NP dose	dose/week given to each hamster was 0.2mL/100g body weight
Laser info	2.5 W/cm2
Expos. Duration	10 min
Time of Exposure	24 hours after injection
Lab Tests	Hematological investigation: complete blood count (CBC), as well as liver and kidney toxicity and Histopathological examination
RESULTS IN VIVO	
Clinical Findings	GNR/NTQ/laser and GNR/laser (groups B1 and B3), showed marked weight regain and decrease in papillary overgrowths' size up to complete ablation of small tumors in group B1
Histopathological Findings	Group B1 (GNR/NTQ with laser): small papillomatous lesions of mild to severe dysplasia, epithelial surface hyperplasia and hyperkeratinization with variable degrees of dysplasia (from mild to severe), Apoptotic cells
Blood Test Findings	(**ALT and AST values**) were increased significantly with GNR/NTQ/laser and GNR/laser **ALT and AST values** decreased significantly in the positive control group, GNR/NTQ without laser and NTQ, as shown in (Table 1) **creatinine level** was significantly increased in positive control group **urea** levels significantly decreased in positive control group. While no statistically significant difference in the mean values of **uric acid** between groups as shown in Table1 **total white blood cells (WBCs)** count was increased significantly in the GNR/NTQ/laser and GNR/laser groups **total white blood cells (WBCs)** count was highly increased significantly in DMBA group, and very highly increased significantly in GNR/NTQ without laser and NTQ groups

	Platelets count (plt) showed no significant difference in GNR/NTQ/laser group. **Platelets count (plt)** was increased significantly in GNR/laser group, and very highly increased significantly in DMBA, GNR/NTQ without laser and NTQ groups **Hemoglobin (Hb)** level was decreased significantly in GNR/NTQ/laser group **Hemoglobin (Hb)** was very highly significantly decreased in DMBA, GNR/NTQ without laser, GNR/laser and NTQ groups compared to negative control group **Red blood corpuscles (RBCs)** were decreased significantly in GNR/NTQ/laser and GNR/laser groups and it was very highly significantly decreased in DMBA, GNR/NTQ without laser and NTQ groups
Was PTT treatment successful	YES
Results in vivo	1) Animals regained weight in GNR/NTQ/laser and GNR/laser groups. 2) Clinically significant decrease in tumor volumes, were recorded with the combined therapy (GNR/NTQ) with laser, as well as GNR/laser group. 3) A higher temperature in the PLGA shell could stimulate drug release. 4) Histopathological results confirmed cancer regression and tumor volume results. Apoptotic cells were identified in H&E sections with GNR/NTQ/laser and GNR/laser groups. 5) Aspartate aminotransferase (AST) and alanine aminotransferase (ALT) markedly elevated in GNR/NTQ/laser and GNR/laser groups. These results suggest that the liver might be affected mildly, due to activated GNRs may have a direct effect on the liver function. 6) Results of WBCs count significantly increased with GNR/NTQ/laser and GNR/laser groups. The immune-suppressive effect of DMBA could lead to an increase in WBC counts as a defense mechanism. Improvement of WBCs count with GNR/NTQ/laser group, may be due to the immuneenhancing effect of NTQ 7) GNR/laser group showed showed marked elevation of WBC count (56). It could be due to their ability to stimulate an inflammatory response (57). 8) Platelet count showed no difference between the negative control and GNR/NTQ/laser groups. Platelets have a direct role in cancer (58) and the increase in platelet count was directly related to the stage of OSCC. 9) HB and RBCs levels were significantly decreased with GNR/NTQ/laser and GNR/laser groups. 10) Combination between photothermal therapy and nonchemotherapy by GNR/NTQ/PLGA/FA was better than either treatment alone.

PAPER 4 ID

Paper Title	Combined **Photothermotherapy** and **Chemotherapy** of Oral Squamous Cell Carcinoma Guided by Multifunctional Nanomaterials **Enhanced Photoacoustic Tomography**
Pub. Year	2021
Country	China
Participants	Sujuan Zeng, Shiqi Liu, Yintao Lan, Ting Qiu, Mengyu Zhou, Weijian Gao, Wenyan Huang, Lihong Ge, Jian Zhang
Type	PTT+Chemotherapy+Photoacoustic Imaging
Method	In vitro, in vivo
Main NP	DOX- AuNRs@mSiO2-HA
Composisition	Gold nanorods+ mesoporous silica+Hyaluronic Acid+Doxorubicin
PTT Main NP	AuNRs
Synthesis of AuNP	Seed growth mediated method
Size	aspect ratio of high-quality AuNRs was 3.8 (average width, 18 ± 3 nm; length, 75 ± 8 nm)
Compl. Ther.	Chemotherapy
CompT carrier	Doxorubicin
Other Elements	mesoporous silica Hyaluronic Acid
Test type	In vitro 1
Reason	biocompatibility of AuNRs@mSiO2-HA
In vitro cells	HOK
NPs	AuNRs@mSiO2-HA 200 μg mL−1
Results in vitro	1) No distinct cytotoxicity in HOK was observed 2) excellent biocompatibility of blank AuNRs@mSiO2-HA
Test type	In vitro 2
Reason	biocompatibility of AuNRs@mSiO2-HA
In vitro cells	CAL-27 cells
NPs	AuNRs@mSiO2- HA free DOX, DOX-AuNRs@mSiO2-HA various concentrations
Laser	No laser group
Temp. Reached	-
Cells died	27.24%
Results in vitro	1) cytotoxicity of the DOX- AuNRs@mSiO2-HA group was significantly lower than that of the free DOX group attributed to the **sustained release of DOX molecules** 2) cell viability of CAL-27 cells incubated with DOX- AuNRs@mSiO2-HA without NIR laser irradiation was maintained beyond 72.76% further demonstrating their **intrinsic biocompatibility**
Test type	In vitro 3
Reason	PTT in vitro
In vitro cells	CAL-27 cells
NPs	DOX-AuNRs@mSiO2-HA
Laser	808 nm (1 W cm−2)
Expos. Time	5 min
Cells died	More than 90% of cancer cells killed at concentration of 25 μg mL−1, when the particle concentration increased to 50 μg mL−1, almost all the CAL-27 cells were destroyed
Results in vitro	1) all the CAL-27 cells were destroyed 2) DOX-AuNRs@mSiO2-HA +LASER irradiation had an **exceptional synergistic therapy effect** 3) the results of confocal fluorescence images indicate that the lethal effect of phototherapy was tained in agreement with the CCK-8 results
Test type	In vitro 4
Reason	Cellular Uptake Ability
In vitro cells	HOK and CAL-27 cells
NPs	DOX-AuNRs@mSiO2-HA

Results in vitro	1) CAL-27 cells have the capability to take DOX-AuNRs@mSiO2-HA. The CAL-27 cells express high levels of CD44, so that DOX- AuNRs@mSiO2-HA has accumulated in HA mediates tumor 2) the cellular uptake was highly controllable by adjusting co-incubation time or increased concentration of materials 3) DOX-loaded nanoparticles could facilitate cellular internalization and final delivery of DOX to the cell nuclei.
Test type	In vivo 1
Reason	PAI of AuNRs@mSiO2-HA
Animals	mice
Carcinogen	CAL-27 tumor
Init. Tumor info	tumor volume of approximately 100 mm3
NPs	AuNRs@mSiO2-HA
NP dose	AuNRs@mSiO2-HA suspensions (200 µL, 1 mg mL−1)
Way of Med. Admin.	injection into the tail vein
RESULTS IN VIVO	
Results in vivo	PA signal increased gradually within the first 8-h post-injection at tumor site and then decreased, which indicated that the maximum nanoparticles enrichment in the tumor region was achieved at 8 h post-injection.
Test type	In vivo 2
Reason	Chemo-Photothermal Therapy
Animals	Female BALB/c nude mice (4–6 weeks old)
Carcinogen	human OSCC graft tumor model of mice was established by injecting 0.1mL CAL-27 cells suspension (4 × 106) into the right flank of the female BALB/c nude mice
In vivo Ca Cells	human tongue squamous cell carcinoma CAL-27 cell line
NPs	DOX-AuNRs@mSiO2-HA
NP dose	0.2 mL DOX-AuNRs@mSiO2-HA, 1 mg mL−1
Way of Med. Admin.	intravenously injected via tail vein
Laser info	808 nm NIR laser irradiation (power density of laser, 2 W cm−2)
Expos. Duration	5 min
Time of Exposure	8 h after the injection
Temp. Reached	Temperature increased from 28.6 to 55.7 °C
RESULTS IN VIVO	
Results in vivo	1) digital photographs of tumors on the 12th day after treatment show that tumors in DOX-AuNRs@mSiO2-HA + LASER group are completely ablated 2) body weight curves no significant difference from each other, which implied that treatments did not affect the normal development of the mice during our experiment 3) DOX-AuNRs@mSiO2-HA and PBS+LASER groups showed a slower tumor growth rate than the control groups, which means the therapeutic effect of single chemotherapy or PTT alone was limited 4) the DOX-AuNRs@mSiO2-HA group was the best in terms of the survival rate among all the experimental groups. 5) H&E staining of tumor slices showed that most of the cells in the tumors of mice of DOX-AuNRs@mSiO2-HA +LASER group were severely damaged, while the cells in the tumors of mice of the other treatment groups were only partially destroyed 6) there was no obvious organ damage and inflammation compared to the PBS group. The safety and low toxicity of DOX- AuNRs@mSiO2-HA were also demonstrated to be good

PAPER 5 ID

Paper Title	**Black phosphorous** nanosheets–**gold nanoparticles**–**cisplatin** for **photothermal/photodynamic** treatment of oral squamous cell carcinoma
Pub. Year	2020
Country	China
Participants	Jun-jie ZENG, Zhan-gui TANG, Jiao ZOU, Jin-gang YU
Type	PTT + PDT
Method	In vivo, in vitro
Ca Cells / Cell lines	1) Human tongue squamous cell carcinoma cells line (SCC-9) (in vitro) 2) Cheek Ca cells after DMBA (in vivo)
Main NP	Drug Delivery System: AuNPs-to-BPNSs1:5/CDDP complex
Characteristics	1) BPNSs show discontinuous and nonhomogeneous flake-like structures, having a layered structure with high crystal quality 2) AuNPs with an elliptical structure
PTT Main NP	AuNPs and BPNPs
Compl. Ther.	PDT / Chemotherapy
CompT carrier	PDT: BPNPs Chemo: cisplatin (CDDP)
Test type	In vitro
Reason	Cytotoxicity of nanomaterials
In vitro cells	human SCC-9 cells
NPs	BPNSs and AuNPs
Laser	Not mentioned
Results in vitro	1) the use of low-dose of nanomaterials (BPNSs and AuNPs) can **more efficiently** promote the apoptosis of human SCC-9 cells compared to the normal doses of CDDP 2) BPNSs have shown **stronger** cells killing ability than AuNPs 3) AuNPs possessed **stronger** cells killing ability than CDDP, which might be due to the inhibition of vascular endothelial growth factor 165 to inhibit tumors [43] and the alteration of cell cycle 4) BPNSs exhibited **the strongest** cells killing ability might due to the fact that cancer cells have more vigorous endocytosis and faster metabolic rate than normal cells, and BPNSs are easily taken up by cancer cells through endocytosis and rapidly degraded in the cells to produce a large number of phosphate ions. leading to changes in the internal environment of cancer cells causing G2/M phase arrest, thereby effectively inhibiting the proliferation of cancer cells [10]. After the proliferation was inhibited, cancer cells further entered programmed cells death through apoptosis and autophagy. **BPNPs > AuNPs > CDDP** 5) potential application of nanomaterials for targeting in vitro was confirmed
Test type	In vivo
No of Groups	9
Reason	Efficacy of PTT with DDS
Animals	Golden hamsters
Group Name	Group VI: golden hamsters treated with AuNPs-to-BPNSs1:5/CDDP complex
Carcinogen	0.5% DMBA in acetone solution on their left cheek pouches three times a week for 16 weeks
In vivo Ca Cells	Buccal squamous cell carcinoma cells after DMBA
NPs (DDS)	AuNPs-to-BPNSs1:5/CDDP complex
Way of Med. Admin.	Intratumorally for 4 weeks
Laser info	Infrared rays at a wavelength of 808 nm
Expos. Duration	5 min
Time of Exposure	After the injection
Markers tested	survival rates, tumor volumes and mass changes of the golden hamsters, immunohistochemistry analysis

Day of Sacrifice	4 weeks after injection of the drug
RESULTS IN VIVO	
Was PTT treatment successful	YES
Results in vivo	1) the survival rate of the control group was lower than that of the five groups of combined drug group and the three groups of pure medication group 2) drug-treated chemotherapy can improve rate of golden hamsters 3) the survival rates of the AuNPs group and the CDDP group were similar 4) the survival rate of BPNSs group was significantly higher than the non BPNPs Groups 5) BPNSs might benefit from the effect of photothermal therapy, thus has a stronger ability to inhibit cancer cells than AuNPs and CDDP 6) the survival rate of AuNPs-to-BPNSs1:5/CDDP was higher than that of AuNPs-to BPNSs5:1/CDDP, further indicating that BPNSs has a stronger ability to inhibit cancer cells than AuNPs. 7) compared with the control group, all the combined drug groups and the pure drug groups have a certain inhibitory effect on OSCC growth 8) the tumor volumes of four combined drug groups of which the AuNPs-to-BPNSs1:5/CDDP had the most obvious antitumor effect, which might be attributed to the drug loading of BPNSs much higher than that of AuNPs [24], and the photothermal effect of BPNSs 9) laser irradiation further promotes the release of drugs 10) synergistic effects of AuNPs, BPNSs and CDDP enhance the stability and efficacy of nanomaterials drug delivery system 11) the expression of a tumor suppressor gene P53 protein in the DDS Groups, BPNSs, and AuNPs was higher than that of the CDDP Group 12) the expression of PCNA by CDDP group was higher than that of other groups, indicating that CDDP alone could not effectively inhibit OSCC 13) the developed nanocomposites (AuNPs-to-BPNSs) loading with CDDP could help to inhibit the growth of OSCC

PAPER 6 ID

Paper Title	Cancer **cell membrane-coated gold nanorods** for **photothermal therapy** and **radiotherapy** on oral squamous cancer
Pub. Year	2020
Country	China
Participants	Qiang Sun, Jinggen Lulu Jin, Liangjie Hong, Fang Wang, Zhengwei Mao and Mengjie Wu
Type	PTT+Radiotherapy
Method	In vitro, in vivo
Ca Cells / Cell lines	Human oral squamous KB cancer cells Human liver cancer LM3 cells, HepG2 cells, human cervical cancer HeLa cells, and mouse breast cancer 4T1 cells
Main NP	GNR@MEM
Composisition	Pegylated GNR coated onto KB cancer cell membrane vesicles
PTT Main NP	Pegylated GNR
AuNP	GNR
Synthesis of AuNP	Growth seed mediation
Composisition	GNR + PEG
Size	GNR@PEG was 68 +- 5 nm in length and 11 +- 1 nm in width
Characteristics	Redshifted LSPR peaks in the NIR-II window, which were located at around 1030 nm
Compl. Ther.	Radiotherapy
CompT carrier	GNR
Other Elements	KB cancer cell membrane vesicles
PT efficacy of NP in aqueous media	
Laser	980 nm light
Temperature achieved	60 C after 1 min
Test type	In vitro 1
Reason	Selective cell uptake
In vitro cells	five different cancer cells, including LM3, HepG2, 4T1, HeLa and KB cells
NPs	GNR@Mem, GNR@PEG
Results in vitro	1) GNR@Mem was internalized more efficiently by the KB cells than by the other cells 2) GNR@MEM selective target homotypic tumor cells. The intracellular amount of gold in the GNR@Mem group was 4.7 times higher than that of the GNR@PEG group after 24 h coincubation 3) GNR@PEG was not very effectively ingested by all the cells, which is attributed to its antifouling polymeric coating
Test type	In vitro 2
Reason	Cytotoxicity and therapeutic outcome under NIR light or X-rays
In vitro cells	KB cells
NPs	GNR@Mem, GNR@PEG
Radiation	980 nm NIR light (dosage: 0.5 W cm^{-2} for 1 min) and/or X-rays (dosage: 4 Gy)
Cells died	Xray only: Cell viability **decreased**: - GNR@PEG : to 43.8% - GNR@MEM: to **22.6%** NIR only: Cell viability **decreased**: -GRN@PEG: to 31.6% -GNR@MEM: to **5.8%** Xray + NIR Cell viability **decreased** -GNR@PEG: to 11.8% -GNR@MEM: to **1.4%**

Results in vitro	1) Under X-ray or NIR light irradiation, the cell viability decreased with an increase in GNR concentration. 2) the sensitized radiation- and photothermal-induced cytotoxicity of GNR@MEM against KB cancer cells were concurrently enhanced and was the greatest achieved
Test type	In vivo 1
Reason	assess the biocompatibility of GNR@Mem
Animals	6- to 8-week-old healthy male nude mice
NPs	GNR@Mem
NP dose	10 mg kg^{-1}
Way of Med. Admin.	intravenous
Tests	- blood chemistry and histopathology of the major organs of the healthy mice receiving GNR@Mem were tested - AST and ALT, which are indicators for liver function, and BUN and CRE, which are indicators for kidney function
RESULTS IN VIVO	
Histopathological Findings	no tissue damage was observed in the liver, kidney, lung and spleen 24 h after i.v. injection of GNR@Mem
Blood Test Findings	Blood concentrations of AST, ALT, BUN, CRE in the GNR@Mem treated group were comparable to that of the control group
Results in vivo	1) no tissue damage was observed in the liver, kidney, lung and spleen 24 h after i.v. injection of GNR@Mem 2) Blood concentrations of AST, ALT, BUN, CRE in the GNR@Mem treated group were comparable to that of the control group, indicating the **excellent biocompatibility** of GNR@Mem and its potential applications in the biomedical field.
Test type	In vivo 2
Reason	Pharmacokinetics and tumor accumulation of GNRs in vivo
Animals	6- to 8-week-old healthy male nude mice
Carcinogen	xenograft tumors
In vivo Ca Cells	KB cells
Init. Tumor info	~130 mm^3
NPs	GNR@Mem
NP dose	10 mg kg^{-1}
Way of Med. Admin.	intravenous
Tests	Ultrathin sections of the tumors for histopathological test, ICP-MS for tissue accumulation of GNRs
RESULTS IN VIVO	
Histopathological Findings	more GNRs were accumulated in the tumor cells and tumor extracellular matrix in the GNR@Mem group
Results in vivo	1) The blood clearance half-lives of GNR@Mem and GNR@PEG were 4.36 h and 2.71 h, respectively 2) more GNRs were accumulated in the tumor cells and tumor extracellular matrix in the GNR@Mem group 3) The tumor in GNR@Mem group had a much higher dose of gold than GNR@PEG 4) most of the GNR@Mem was gradually expelled via feces (about 70% of injected dosage) and a small part was exhausted in the urine (about 20%) 3 days after injection, indicating the relatively low long-term accumulation of GNR@Mem inside the body
Test type	In vivo 3
Reason	PTT and RT in vivo
Animals	6- to 8-week-old healthy male nude mice
No of Groups	7
Group Name	4, 5, 6, 7
Carcinogen	xenograft tumors
In vivo Ca Cells	KB cells
NPs	GNR@Mem / GNR@PEG

NP dose	200 mL saline containing GNR@MEM or GNR@PEG (dose of GNRs was fixed at 5 mg kg^{-1})
Way of Med. Admin.	intravenous
Rad. info	980 nm NIR 0.5 W cm^{-2} / X-rays 4 Gy
Expos. Duration	5 min
Tests	Tumor volume, body weight, histological assay
RESULTS IN VIVO	
Was PTT treatment successful	YES
Results in vivo	1) GNR@PEG + NIR and GNR@Mem + NIR led to obvious inhibition of tumor growth 2) With additional X-ray irradiation and subsequent radiosensitive therapy, 4 of 5 tumors were completely destroyed in the GNR@Mem + NIR + X-ray group, demonstrating the best tumor inhibition potential 3) The tumor volume suppression rate reached 95.6% by GNR@Mem-mediated PTT and RT combined therapy 4) GNR@Mem is an excellent sensitizer for highly efficient radiotherapy and photothermal therapy of oral squamous cancer, providing a promising treatment effect

PAPER 7 ID

Paper Title	Combined **chemo-photothermal** treatment of three-dimensional head and neck squamous cell carcinomas by **gold nano-architectures**
Pub. Year	2020
Country	Italy
Participants	Ana Katrina Mapanao, Melissa Santi, Valerio Voliani
Type	PTT + Chemotherapy
Method	In vitro
Ca Cells / Cell lines	Human squamous cell carcinoma SCC-25 (HPV-negative) and UPCI:SCC-154 (HPV-positive)
Main NP	tNAs-cisPt
Composisition	gold ultrasmall nanoparticles in silica cover + Cisplatin prodrug
Size	diameters between 100 and 150 nm
Characteristics	Two types were produced: prodrug-loaded NAs (NAs-cisPt) and photothermal NIR responsive NAs (tNAs)
PTT Main NP	tNAs
AuNP	gold ultrasmall nanoparticles
Synthesis of AuNP	Gold USNPs were prepared of aqueous solution of tetrachloroauric (III) acid $HAuCl_4$ (fast reduction of gold in aqueous solution through the addition of sodium borohydride)
Composisition	Gold NPs in silica cover
Compl. Ther.	Chemotherapy
CompT carrier	Cisplatin prodrug c,t,c-$[PtCl_2(NH_3)_2(OH)(O_2CCH_2CH_2CO_2H)]$
Photothermal conversion efficasy	
Nps	tNAs-cisPt
Laser	808 nm, 3 W for 6 min
Temp. achieved	temperature increase of 9.3 C ± 0.7 C
Test type	In vitro
Reason	PT activity of tNAs
In vitro cells	2D SCC-25 (HPV-negative) and UPCI:SCC-154 (HPV-positive)
NPs	30 mg of standard NAs or tNAs
Laser	808 nm, 3 W
Expos. Time	2 h
Results in vitro	1) The nano-architectures have been shown to be internalized in both cell lines 2) irradiated tNAs induced cytotoxicity 3) the efficiency of tNAs to induce HT was also confirmed in 2D HNSCCs, regardless of HPV status
Test type	In vitro
Reason	PT activity of tNAs
In vitro cells	3D SCC-25 (HPV-negative) and UPCI:SCC-154 (HPV-positive) The spheroids grow with diameters of about 200–300 µm for SCC-25 and 150–250 µm for UPCI:SCC-154
NPs	tNAs and tNAs-cisPt
Laser	808-nm portable CW-laser module set at 300 mW cm^{-2}
Cells died	Viability recorded: 8 h SCC-25: **tNAs-cisPt-ON; (93.0 ± 2.1%)**, combined chemo-photothermal therapy tNAs-ON; (94.7 ± 5.2%), PTT tNAs-cisPt-OFF; (95.0 ± 1.5%) chemotherapy alone No substantial differences viability were observed UPCI:SCC-154: **tNAs-cisPt-ON (78.3 ± 1.2%)** combined treatment significantly reduced the cell viability to

	tNAs-cisPt-OFF (89.0 ± 6.0%) chemotherapy tNAs-ON (109.3 ± 5.0%) PTT combined treatment significantly reduced the cell viability 24 h SCC-25: tNAs-cisPt-OFF (77.3 ± 2.3%) **tNAs-cisPt-ON (84.0 ± 8.7%)** no significant differences were detected while slight decreases have been observed UPCI:SCC-154: **tNAs-cisPt-ON (74.0 ± 4.0%)** a significant viability reduction was recorded 48 h and 72 h SCC-25: the nano-architectures have already disassembled into the building blocks and released all the available prodrug molecules, which may have been activated and ultimately affected the cell viability. (at 48 h) UPCI:SCC-154: comparable viabilities were verified between tNAs-cisPt-ON and tNAscisPt- OFF, again possibly due to the complete release and activation of the prodrug.
Results in vitro	1) tNAs-cisPt-ON significantly reduced the cell viability 2) the long term effects of the nano-architectures on the viability of spheroids can be mainly attributed to the potential activation of cisplatin prodrug 3) the enhanced treatment response of HPV-associated HNSCCs, compared to the HPV-negative.

PAPER 8 ID

Paper Title	Biocompatible and **multifunctional gold nanorods** for effective photothermal therapy of oral squamous cell carcinoma
Pub. Year	2019
Country	Taiwan
Participants	Yu-Te Liao, Chia-Hung Liu, Yin Chin, Sin-Yuan Chen, Shing Hwa Liu, Yih-Chih Hsu and Kevin C.-W. Wu
Type	PTT only
Method	In vitro, in vivo
Ca Cells / Cell lines	human OSCC cell line, i.e., SAS (for in vitro) Human SAS cells (6 x 10^5 cells) (for in vivo)
Main NP	GNR@Alg-Cys/RGD
Composisition	Gold nanorods + Alginate-Cysteine + RGD Peptides
Size	177.6 nm (Hydrodynamic diameter)
PTT NP	Gold nanorods GNR
AuNP	GNRs
Synthesis of AuNP	seed-mediated growth by Au nanoparticles and silver ions and then stabilized with CTAB
Composisition	GNRs
Size	109.3 nm (Hydrodynamic diameter)
Other Elements	Alginate, cycteine, RGD peptides: 1) Alginate to replace CTAB and extend the circulation time of Au nanoparticles in the body 2) Cysteine to generate a gold–thiol bond on the gold surface and prevent the leakage of alginate during circulation 3) RGD peptides for $\alpha_v\beta_3$ receptors on the OSCC cell line
Test type	In vitro 1
Reason	Evaluation of photothermal conversion
Mean	PBS
NPs	GNR@Alg-Cys
Laser	Diode laser (wavelength: 808 nm)
Expos. Time	10 min
Temp. Reached	41 C (1.5 W cm-2) and 53 C (2 W cm-2) in 1 min 42 C (1.5 W cm-2) and 57 C (2 W cm-2) after 10 min
Cells died	
Results in vitro	1) The GNR@Alg-Cys sample was proposed to be a potential medium for PTT since it could effectively convert light into heat within a short time. 2) alginate layer prevented from higher temperatures that were observed when GNR@CTAb was tested (95 C at 10 min)
Test type	In vitro 2
Reason	To demonstrate that the biocompatibility of GNRs is improved by replacing CTAB with alginate
In vitro cells	SAS-3 cells
NPs	GNRs coated with CTAB, Alg-Cys, and Alg-Cys/RGD
Results in vitro	1) GNR@CTAB was highly toxic to cells 2) GNR@Alg-Cys and GNR@Alg-Cys/RGD were nontoxic to cells. Alginate-coated GNRs are biocompatible media for PTT
Test type	In vitro 3
Reason	For cell uptake
In vitro cells	SAS-3
NPs	GNR@Alg-Cys and GNR@Alg-Cys/RGD
Results in vitro	RGD-modified carriers were uptaken by cells via receptor-mediated endocytosis. 60 000 nanorods were uptaken by a cell through endocytosis, while nearly twice this amount (117 000) were uptaken by a cell after modifying the RGD peptide on alginate. Alginate modification on GNRs results in greater cell uptake
Test type	In vitro 4

Reason	efficacy of GNR@Alg-Cys/RGD on PTT
In vitro cells	human OSCC cell line, i.e., SAS
NPs	GNR@Alg-Cys/RGD
Laser	Diode single-wavelength laser (808 nm)
Cells died	Half (GNR@Alg-Cys), 90% (GNR@Alg-Cys/RGD)
Results in vitro	1) GNR@Alg-Cys participated in the PTT, half of the cells were killed by hyperthermia after exposure for 5 min since the local temperature increased to 57 C 2) When GNR@Alg-Cys was modified by RGD peptide, up to 90% cells were killed by hyperthermia. The significantly reduced cell viability could be attributed to **nearly twice the amount of GNRs uptaken** by the cells 3) the cells were alive outside the area with laser exposure
OVERALL RESULTS IN VITRO	
	1) GNR@CTAB was highly toxic to cells 2) GNR@Alg-Cys were nontoxic to cells 3) GNR@Alg-Cys/RGD were nontoxic to cells 4) RGD-modified carriers were uptaken by cells via receptor-mediated endocytosis 5)twice the amount were uptaken by a cell after modifying the RGD peptide on alginate 6) no significant difference was observed in the temperature profiles of GNR@Alg-Cys and GNR@Alg-Cys/RGD after exposure. 7) The significantly reduced cell viability could be attributed to nearly twice the amount of GNRs-RGD uptaken by the cells. 8) the cells were alive outside the area with laser exposure
Test type	In vivo
Reason	To further demonstrate the efficacy of GNR@Alg-Cys/RGD on PTT
Animals	nude mouse
Group Name	GNR@Alg-Cys/RGD with light (4W, 20min)
Carcinogen	subcutaneously injected SAS cells (xenograft)
In vivo Ca Cells	Human SAS cells (6 x 10^5 cells)
Init. Tumor info	100 mm^3 5% (95–105 mm^3) tumor volume
NPs	GNR@Alg-Cys/RGD
Way of Med. Admin.	intratumoral injection using a needle syringe on day 0
Temp. Reached	from 30 to 43 1C within 8 min
Biomarkers tested	Aspartate aminotransferase (AST), alanine aminotransferase (ALT), total bilirubin (T-Bil), creatinine (CREA), blood urea nitrogen (BUN), and uric acid (UA)
Day of Sacrifice	day 14
RESULTS IN VIVO	
Blood Test Findings	All the biomarkers (AST, ALT, T-Bil, CREA, BUN, and UA) showed no statistical differences amongst the PBS, light, and PTT groups
Results in vivo	1) GNR@Alg-Cys/RGD with the light group grows the tumor volume to 120 mm3 (1.2 times in volume) from the start of the laser treatment and slowed down the growth of the tumor with around 5 or 2 times on day 14 with a significant difference when compared with the PBS group 2) GNR@Alg-Cys/RGD sample is biologically safe in the animal study.

PAPER 9 ID

Paper Title	Platelet-Facilitated Photothermal Therapy of Head and Neck Squamous Cell Carcinoma
Pub. Year	2018
Country	China
Participants	Lang Rao, Lin-Lin Bu, Liang Ma, Wenbiao Wang, Huiqin Liu, Da Wan, Jian-Feng Liu, Andrew Li, Shi-Shang Guo, Lu Zhang, Wen-Feng Zhang, Xing-Zhong Zhao, Zhi-Jun Sun and Wei Liu
Type	PTT
Method	In vivo, (in vitro for verification of capabilities)
Main NP	PLT-AuNRs
Composisition	Gold Nanorods + Platelet cells
PTT Main NP	BSA-modified AuNRs
AuNP	Gold nanorods
Synthesis of AuNP	Gold Nanorods + Bovine serum albumin
Size	12 nm in diameter and 50 nm in length
Characteristics	longitudinal SPR (l-SPR) absorption band of AuNRs is 808 nm and BSA conjugation causes a small redshift
Other Elements	Platelets (purified from fresh mice blood)
Efficacy of NP for PTT	
Medium	PBS
Laser	808 nm NIR light
Temp. achieved	increased by 35 C
Test type	In vitro 1
Reason	test if PLT-AuNRs inherited circulation time and being able to evade phagocytosis
In vitro cells	RAW 264.7 murine macrophage-like cells
NPs	PLT-M-AuNRs (PLT membrane- camouflaged AuNRs), PLT-AuNRs (whole PLT cell)
Results in vitro	1)) PLT-AuNRs sowed further improved biocompatibility than AuNRs 2) AuNRs resulted in the highest uptake 3) PLT-AuNRs and PLT-M-AuNRs resulted in similarly lower uptakes. PLT-AuNRs indicated the ability to evade phagocytosis 4) PLT-AuNRs demonstrated better immune evasion performance than PLT-M-AuNRs which may be attributed to benefits achieved by using whole cell rather just the cell membrane.
Test type	In vitro 2
Reason	Evaluation of the cancer targeting performance of PLT-AuNRs + PTT efficacy
In vitro cells	CAL 27 human squamous carcinoma cells
NPs	PLT-AuNRs, AuNRs, PLT-M-AuNRs
Laser	808 nm laser
Results in vitro	1) Compared to the other two nanoparticles PLT-AuNRs demonstrated superior cancer targeting performance 2) PLT-AuNRs resulted in selectively killing of cancer cells under localizing laser irradiation 3) Compared to AuNRs and PLT-MAuNRs, treatment with PLT-AuNRs resulted in the best in vitro PTT effect, which we suspect can be attributed to the close interactions between PLT-AuNRs and cancer cells
Test type	In vivo 1
Reason	pharmacokinetics and biodistribution
Animals	ICR mice
NPs	AuNRs, PLT-AuNR, PLT-M-AuNR
Way of Med. Admin.	intravenous (i.v.) injections
Tests	blood samples were collected and analyzed by using ICP-AES
RESULTS IN VIVO	
Results in vivo	Comparing to AuNRs, the PLT-AuNR and PLT-M-AuNR groups exhibited enhanced systematic circulation over 48h, suggesting superior in vivo immune evasion ability

Test type	In vivo 2
Reason	Whether PLTs could enhance the PTT effect
Animals	BALB/c nude mice
Carcinogen	CAL 27 tumor xenografts
Way of Med. Admin.	intravenous (i.v.) injections
Time of Exposure	24 h post-injection
Tests	tumors were collected for the nanoparticle quantification with ICP-AES
RESULTS IN VIVO	
Results in vivo	1) PTT treatment could facilitate additional PLT-AuNRs targeting to the PTT sites, possibly via a mechanism where PLT-AuNRs are attracted to the site of injury caused by the PTT. 2) PLT-AuNRs had lower liver and spleen accumulation, indicating that PLT-AuNRs gain the immune evasion ability from the source PLTs. 3) PLT-AuNRs had lower liver and spleen (the two primary organs of the reticuloendothelial system (RES)) accumulation, indicating that PLT-AuNRs gain the immune evasion ability from the source PLTs.
Test type	In vivo 3
Reason	further evaluate the in vivo performance of PLT-AuNRs
Animals	Tgfbr1/Pten conditional knockout (2cKO) mouse model
Carcinogen	tamoxifen to delete tumor suppressors Tgfbr1 and Pten resulting in full penetrance HNSCC
In vivo Ca Cells	SCC growing into the oral cavity adopts a pseudopapillary structure and forms solid sheets, often displaying central necrosis
NPs	AuNRs, PLT-AuNR, PLT-M-AuNR
Way of Med. Admin.	intravenous (i.v.) injections
Time of Exposure	24 h post-injection and every other day over a period of 15 days
RESULTS IN VIVO	
Results in vivo	1) PLTAuNRs exhibited the best performance in terms temperature increase attributed to the long blood circulation and good cancer targeting capabilities of PLT-AuNRs 2) Σuccessive temperature increase after each treatment, indicating that the PTT-ablated tumor tissues attracted additional PLTAuNRs and PLT-AuNRs facilitated the PTT in a feedback manner 3) PLT-AuNRs could more effectively inhibit tumor growth comparing to other nanoparticles 4) the combination of PLT-AuNRs and laser irradiation significantly delayed tumorigenesis 5) good biocompatibility of this novel PLT-PTT therapeutic strategy 6) Neither death nor an obvious weight difference was observed between the control and treatment groups over 30 days, demonstrating that no overall side effects were induced by the injection of PLT-AuNRs 7) No significant differences were observed in tissue slices and blood biochemical and whole blood parameters, further confirming the superior in vivo compatibility of PLT-AuNRs 8) Noticeably decrease of staining for Ki-67 after treatment with PLT-AuNRs + Laser, suggested histopathologically effective inhibition of tumor cell proliferation. 9) terminal deoxynucleotidyl transferase-mediated deoxyuridinetriphosphate nick end labeling (TUNEL) assay slices showed that in the mice treated with PLT-AuNRs + Laser, many cells were killed or apoptotic as further demonstrating histopathologically that the tumor growth was clearly inhibited

REFERENCES

CHAPTER 1- The Oral Mucosa

Melina Brizuela ; Ryan Winters . Histology, Oral Mucosa, 2022, NCBI Bookshelf

Groeger S, Meyle J. Oral Mucosal Epithelial Cells. Front Immunol. 2019;10:208.

Wang SS, Tang YL, Pang X, Zheng M, Tang YJ, Liang XH. The maintenance of an oral epithelial barrier. Life Sci. 2019 Jun 15;227:129-136.

Garant PR. Oral Cells and Tissues. Illinois, IL: Quintessence Publishing Co.,Inc. (2003).

Schroeder HE, Listgarten MA. The gingival tissues: the architecture of periodontal protection. Periodontol (1997)13:91–120.

Squier CA, KremerMJ. Biology of oral mucosa and esophagus. J Natl Cancer Inst Monogr. (2001) 29:7–15.

Otsuka-Tanaka Y, Oommen S, Kawasaki M, Kawasaki K, Imam N, Jalani-Ghazani F, Hindges R, Sharpe PT, Ohazama A. Oral lining mucosa development depends on mesenchymal microRNAs. J Dent Res. 2013 Mar;92(3):229-34.

Pollanen MT, Salonen JI, Uitto VJ. Structure and function of the toothepithelial interface in health and disease. Periodontol (2003) 31:12–31. doi: 10.1034/j.1600-0757.2003.03102.x

Adams D. Keratinization of the oral epithelium. Ann R Coll Surg Engl. 1976 Sep;58(5):351-8.

Squier CA, Kremer MJ. Biology of oral mucosa and esophagus. J Natl Cancer Inst Monogr. 2001;(29):7-15.

Barrett AW, Scully C. Human oral mucosal melanocytes: a review. J Oral Pathol Med. 1994 Mar;23(3):97-103.

Thomas AJ, Erickson CA. The making of a melanocyte: the specification of melanoblasts from the neural crest. Pigment Cell Melanoma Res. 2008 Dec;21(6):598-610.

Yamaguchi Y, Brenner M, Hearing VJ. The regulation of skin pigmentation. J Biol Chem. 2007 Sep 21;282(38):27557-61.

Feller L, Masilana A, Khammissa RA, Altini M, Jadwat Y, Lemmer J. Melanin: the biophysiology of oral melanocytes and physiological oral pigmentation. Head Face Med. 2014 Mar 24;10:8.

Eisen D. Disorders of pigmentation in the oral cavity. Clin Dermatol. 2000 Sep-Oct;18(5):579-87.

Meleti M, Vescovi P, Mooi WJ, van der Waal I. Pigmented lesions of the oral mucosa and perioral tissues: a flow-chart for the diagnosis and some recommendations for the management. Oral Surg Oral Med Oral Pathol Oral Radiol Endod. 2008 May;105(5):606-16.

Kingsmill VJ, Berkovitz BK, Barrett AW. An immunohistochemical analysis of human Merkel cell density in gingival epithelium from dentate and edentulous subjects. Arch Oral Biol. 2005 Oct;50(10):883-7.

Chen J, Ahmad R, Li W, Swain M, Li Q. Biomechanics of oral mucosa. J R Soc Interface. 2015 Aug 06;12(109):20150325.

Tungare S, Paranjpe AG. StatPearls. StatPearls Publishing; Treasure Island (FL): Sep 25, 2021. Drug Induced Gingival Overgrowth.

Presland RB, Jurevic RJ. Making sense of the epithelial barrier: what molecular biology and genetics tell us about the functions of oral mucosal and epidermal tissues. J Dent Educ. (2002) 66:564–74.

Wertz PW. Lipids and the Permeability and Antimicrobial Barriers of the Skin. J Lipids. 2018;2018:5954034.

Bearelly S, Cheung SW. Sensory Topography of Oral Structures. JAMA Otolaryngol Head Neck Surg. 2017 Jan 01;143(1):73-80.

Feldman AT, Wolfe D. Tissue processing and hematoxylin and eosin staining. Methods Mol Biol. 2014;1180:31-43.

CHAPTER 2 - The Oral Squamous Cell Carcinoma

A. Argiris, M.V. Karamouzis, D. Raben, R.L. Ferris, Head and neck cancer, Lancet 371 (2008) 1695–1709, https://doi.org/10.1016/S0140-6736(08)60728-X.

Rothenberg SM, Ellisen LW. The molecular pathogenesis of head and neck squamous cell carcinoma. J Clin Invest. 2012;122 (6):1951–1957. doi:10.1172/jci59889

Chen S, Lin Z, Chen J, Yang A, Zhang Q, Xie C, et al. Older age is a risk factor associated with poor prognosis of patients with squamous cell carcinoma of the oral cavity. Eur Arch Otorhinolaryngol 2020.

Farhood Z, Simpson M, Ward GM, Walker RJ, Osazuwa-Peters N. Does anatomic subsite influence oral cavity cancer mortality? A SEER database analysis. Laryngoscope 2019;129:1400–6.

Mohan, M.; Jagannathan, N. Oral field cancerization: An update on current concepts. Oncol. Rev. 2014, 30, 244.

Montero, P.H.; Patel, S.G. Cancer of the oral cavity. Surg. Oncol. Clin. N. Am. 2015, 24, 491–508.

Sasco, A.J.; Secretan, M.B.; Straif, K. Tobacco smoking and cancer: A brief review of recent epidemiological evidence. Lung Cancer 2004, 45, S3–S9.

Warnakulasuriya, K.A.; Ralhan, R. Clinical, pathological, cellular and molecular lesions caused by oral smokeless tobacco–a review. J. Oral Pathol. Med. 2007, 36, 63–77.

Lee, C.H.; Chang, J.S.; Syu, S.H.; Wong, T.S.; Chan, J.Y.; Tang, Y.C.; Yang, Z.P.; Yang, W.C.; Chen, C.T.; Lu, S.C.; et al. IL-1
promotes malignant transformation and tumor aggressiveness in oral cancer. J. Cell Physiol. 2015, 230, 875–884.

Stornetta, A.; Guidolin, V.; Balbo, S. Alcohol-Derived Acetaldehyde Exposure in the Oral Cavity. Cancers 2018, 10, 20.

Chen, S.-H.; Hsiao, S.-Y.; Chang, K.-Y.; Chang, J.-Y. New Insights Into Oral Squamous Cell Carcinoma: From Clinical Aspects to Molecular Tumorigenesis. Int. J. Mol. Sci. 2021, 22, 2252. https://doi.org/doi:10.3390/ijms22052252

Li, Y.C.; Cheng, A.J.; Lee, L.Y.; Huang, Y.C.; Chang, J.T. Multifaceted Mechanisms of Areca Nuts in Oral Carcinogenesis: The Molecular Pathology from Precancerous Condition to Malignant Transformation. J. Cancer 2019, 10, 4054–4062.

Hübbers, C.U.; Akgül, B. HPV and cancer of the oral cavity. Virulence 2015, 6, 244–248.

Jalouli J, Ibrahim SO, Mehrotra R, et al. Prevalence of viral (HPV, EBV, HSV) infections in oral submucous fibrosis and oral cancer from India. Acta Otolaryngol 2010; 130(11): 1306-11.

Ali, H.; Donovan, B.; Wand, H.; Read, T.R.; Regan, D.G.; Grulich, A.E.; Fairley, C.K.; Guy, R.J. Genital warts in young Australians five years into national human papillomavirus vaccination programme: National surveillance data. BMJ 2013, 346, f2032.

Gonzalez-Molez MA, Gutierrez J, Rodriguez MJ, Ruiz-Avila I, Rodriguez-Archilla A. Epstein-Barr virus latent membrane protein-1 (LMP-1) expression in oral squamous cell carcinoma. Laryngoscope 2002; 112: 482-7.

Nagao Y, Sata M. High incidence of multiple primary carcinomas in HCV-infected patients with oral squamous cell carcinoma. Med Sci Monit 2009; 15: CR453-9.

Hashim, D.; Sartori, S.; Brennan, P.; Curado, M.P.; Wünsch-Filho, V.; Divaris, K.; Olshan, A.F.; Zevallos, J.P.; Winn, D.M.; Franceschi, S.; et al. The role of oral hygiene in head and neck cancer: Results from International Head and Neck Cancer Epidemiology (INHANCE) consortium. Ann. Oncol. 2016, 27, 1619–1625.

Karpinski, T.M. Role of Oral Microbiota in Cancer Development. Microorganisms 2019, 7, 20.

Hsiao, J.R.; Chang, C.C.; Lee, W.T.; Huang, C.C.; Ou, C.Y.; Tsai, S.T.; Chen, K.C.; Huang, J.S.; Wong, T.Y.; Lai, Y.H.; et al. The interplay between oral microbiome, lifestyle factors and genetic polymorphisms in the risk of oral squamous cell carcinoma. Carcinogenesis 2018, 39, 778–787.

Fan, J.; Liu, W.; Zhang, M.; Xing, C. A literature review and systematic meta-analysis on XRCC3 Thr241Met polymorphism associating with susceptibility of oral cancer. Oncol. Lett. 2019, 18, 3265–3273.

Ghosh, T.; Gupta, S.; Bajpai, P.; Agarwal, D.; Agarwal, M.; Gupta, O.P.; Agrawal, D. Association of CYP1A1, GSTM1, and GSTT1 gene polymorphism with risk of oral submucous fibrosis in a section of North Indian population. Mol. Biol. Rep. 2012, 39, 9383–9389.

Pisani, L.P.; Estadella, D.; Ribeiro, D.A. The Role of Toll Like Receptors (TLRs) in Oral Carcinogenesis. Anticancer Res. 2017, 37, 5389–5394.

Kauppila, J.H.; Mattila, A.E.; Karttunen, T.J.; Salo, T. Toll-like receptor 5 and the emerging role of bacteria in carcinogenesis. Oncoimmunology 2013, 2, e23620.

Yadav, B.K.; Kaur, J.; Srivastava, A.; Ralhan, R. Effect of polymorphisms in XRCC1, CCND1 and GSTM1 and tobacco exposure as risk modifier for oral leukoplakia. Int. J. Biol. Markers 2009, 24, 90–98.

Hanahan, D.;Weinberg, R.A. Hallmarks of cancer: The next generation. Cell 2011, 144, 646–674.

Hsieh, J.C.; Wang, H.M.; Wu, M.H.; Chang, K.P.; Chang, P.H.; Liao, C.T.; Liau, C.T. Review of emerging biomarkers in head and neck squamous cell carcinoma in the era of immunotherapy and targeted therapy. Head Neck. 2019, 41 (Suppl. 1), 19–45.

Barnes, P.; Yeboah, F.A.; Zhu, J.; Saahene, R.O.; Obirikorang, C.; Adinortey, M.B.; Amoani, B.; Kyei, F.; Akakpo, P.; Awuku, Y.A. Prognostic Worth of Epidermal Growth Factor Receptor (EGFR) in Patients with Head and Neck Tumors. J. Cancer Epidemiol. 2020, 2020, 5615303.

Vermorken, J.B.; Mesia, R.; Rivera, F.; Remenar, E.; Kawecki, A.; Rottey, S.; Erfan, J.; Zabolotnyy, D.; Kienzer, H.R.; Cupissol, D.; et al. Platinum-based chemotherapy plus cetuximab in head and neck cancer. N. Engl. J. Med. 2008, 359, 1116–1127.

NCCN Guidelines for Head and Neck Cancers. Available online: tps://www.nccn.org/professionals/physician_gls/pdf/ head-and-neck.pdf (accessed on 10 October 2020).

Stransky, N.; Egloff, A.M.; Tward, A.D.; Kostic, A.D.; Cibulskis, K.; Sivachenko, A.; Kryukov, G.V.; Lawrence, M.S.; Sougnez, C.; McKenna, A.; et al. The mutational landscape of head and neck squamous cell carcinoma. Science 2011, 333, 1157–1160.

Peltanova, B.; Raudenska, M.; Masarik, M. Effect of tumor microenvironment on pathogenesis of the head and neck squamous cell carcinoma: A systematic review. Mol. Cancer 2019, 18, 63.

Braakhuis BJ, Tabor MP, Kummer JA, Leemans R, Brakenhoff RH. A genetic explanation of Slaughter's concept of field cancerization: evidence and clinical implications. Cancer Res 2003; 63:1727-30.

Braakhuis BJ, Leemans CR, Brakenhoff RH. A genetic progression model of oral cancer: current evidence and clinical implications. J Oral Pathol Med 2004; 33: 317-22.

Liu, D., Zhao, X., Zeng, X., Dan, H. and Chen, Q. (2016). Non-Invasive Techniques for Detection and Diagnosis of Oral Potentially Malignant Disorders.The Tohoku Journal of Experimental Medicine, 238(2), pp.165-177. 4. Essentials of oral cancer. (2015). International Journal of Clinical and Experimental Physiology, 8 (9), pp.11884-11894.

Mascitti, M., Orsini, G., Tosco, V., Monterubbianesi, R., Balercia, A., Putignano, A., Procaccini, M. and Santarelli, A. (2018). An Overview on Current Non-invasive Diagnostic Devices in Oral Oncology.Frontiers in Physiology, 9.

Califano J, van der Riet P, Westra W, et al. Genetic progression model for head and neck cancer: implications for field cancerization. Cancer Res 1996; 56: 2488-92.

Tumuluri V, Thomas GA and Fraser IS: Analysis of the Ki-67 antigen at the invasive tumour front of human oral squamous cell carcinoma. J Oral Pathol Med 31: 598-604, 2002.

Neville BW and Day TA: Oral cancer and precancerous lesions. CA Cancer J Clin 52: 195-215, 2002.

Fuentes B, Duaso J, Droguett D, et al: Progressive extracellular matrix disorganization in chemically induced murine oral squamous cell carcinoma. ISRN Pathology 2012.

Rivera CA, Droguett DA, Kemmerling U and Venegas BA: Chronic restraint stress in oral squamous cell carcinoma. J Dent Res 90: 799-803, 2011.

Sapp JP, Eversole LR and Wysocki GP: Contemporary Oral and Maxillofacial Pathology. Chapter 6: Epithelial Disorders. 2nd edition. Mosby Year Book Inc, Maryland Heights, MO, pp184-193, 2004

Dissanayaka WL, Pitiyage G, Kumarasiri PV, Liyanage RL, Dias KD and Tilakaratne WM: Clinical and histopathologic parameters in survival of oral squamous cell carcinoma. Oral Surg Oral Med Oral Pathol Oral Radiol 113: 518-525, 2012

Choi S and Myers J: Molecular pathogenesis of oral squamous cell carcinoma: implications for therapy. J Dent Res 87: 14-32, 2008.

Massano J, Regateiro F, Januário G and Ferreira A: Oral squamous cell carcinoma: review of prognostic and predictive factors. Oral Surg Oral Med Oral Pathol Oral Radiol Endod 102: 67-76, 2006.

Tucci R, Campos MS, Matizonkas-Antonio LF, Durazzo M, Pinto Junior Ddos S and Nunes FD: HOXB5 expression in oral squamous cell carcinoma. J Appl Oral Sci 19: 125-129, 2011.

Shah N and Sukumar S: The Hox genes and their roles in oncogenesis. Nat Rev Cancer 10: 361-371, 2010

Fan HX, Li HX, Chen D, Gao ZX and Zheng JH: Changes in the expression of MMP2, MMP9, and ColIV in stromal cells in oral squamous tongue cell carcinoma: relationships and prognostic implications. J Exp Clin Cancer Res 31: 90, 2012.

Baba Y, Iyama K, Ikeda K, et al: The Expression of type IV collagen α6 chain is related to the prognosis in patients with esophageal squamous cell carcinoma. Ann Surg Oncol 15: 555-565, 2008

Koontongkaew S: The tumor microenvironment contribution to development, growth, invasion and metastasis of head and necksquamous cell carcinomas. J Cancer 4: 66-83, 2013.

Jung DW, Che ZM, Kim J, Kim K, Kim KY and Williams D: Tumor-stromal crosstalk in invasion of oral squamous cell carcinoma: a pivotal role of CCL7. Int J Cancer 127: 332-344, 2010

Thode C, Jørgensen TG, Dabelsteen E, Mackenzie I and Dabelsteen S: Significance of myofibroblasts in oral squamous cell carcinoma. J Oral Pathol Med 40: 201-207, 2011.

Baik, S.H.; Seo, J.W.; Kim, J.H.; Lee, S.K.; Choi, E.C.; Kim, J. Prognostic Value of Cervical Nodal Necrosis Observed in Preoperative CT and MRI of Patients With Tongue Squamous Cell Carcinoma and Cervical Node Metastases: A Retrospective Study. AJR Am. J. Roentgenol. 2019, 213, 437–443.

Naruse, T.; Yanamoto, S.; Yamada, S.I.; Takahashi, H.; Matsushita, Y.; Imayama, N.; Ikeda, H.; Shiraishi, T.; Fujita, S.; Ikeda, T.; et al. Immunohistochemical study of vascular endothelial growth factor-C/vascular endothelial growth factor receptor-3 expression in oral tongue squamous cell carcinoma: Correlation with the induction of lymphangiogenesis. Oncol Lett. 2015, 10, 2027–2034.

Chen, S.; Chen, L.H.; Niu, Y.H.; Geng, N.B.; Feng, C.J. AEG-1 promotes angiogenesis and may be a novel treatment target for tongue squamous cell carcinoma. Oral Dis. 2020, 26, 876–884.

Ribatti, D.; Tamma, R.; Annese, T. Epithelial-Mesenchymal Transition in Cancer: A Historical Overview. Transl. Oncol. 2020, 13, 100773.

Seyedmajidi, M.; Seifi, S.; Moslemi, D.; Mozaffari, S.F.; Gholinia, H.; Zolfaghari, Z. Immunohistochemical expression of TWIST in oral squamous cell carcinoma and its correlation with clinicopathologic factors. J. Cancer Res. Ther. 2018, 14, 964–969.

Reyes, M.; Flores, T.; Betancur, D.; Peña-Oyarzún, D.; Torres, V.A. Wnt/-Catenin Signaling in Oral Carcinogenesis. Int. J. Mol. Sci. 2020, 21, 4682.

Mikels, A.J.; Nusse, R. Wnts as ligands: Processing, secretion and reception. Oncogene 2006, 25, 7461–7468.

Anastasiadou, E.; Jacob, L.S.; Slack, F.J. Non coding RNA networks in cancer. Nat. Rev. Cancer 2018, 18, 5.

Fang, C.; Li, Y. Prospective applications of microRNAs in oral cancer. Oncol. Lett. 2019, 18, 3974–3984.

Patel SG, Lydiatt WM. Staging of head and neck cancers: is it time to change the balance between the ideal and the practical? J Surg Oncol 2008;97:653–7.

Lacy PD, Spitznagel EL, Piccirillo JF. Development of a new staging system for recurrent oral cavity and oropharyngeal squamous cell carcinoma. Cancer 1999; 86; 1387- 95.

Matos LL, Dedivitis RA, Kulcsar MAV, de Mello ES, Alves VAF, Cernea CR. External validation of the AJCC Cancer Staging Manual, 8th edition, in an independent cohort of oral cancer patients. Oral Oncol 2017; 71: 47–53.

Rajappa SK, Maheshwari U, Jaipuria J, Singh AK, Goyal S, Batra U, et al. Number of positive nodes - Current relevance in determining prognosis of oral cavity cancer after the recent AJCC staging update. Oral Oncol 2019;90:1–5.

Berdugo J, Thompson LDR, Purgina B, Sturgis CD, Tuluc M, Seethala R, et al.,Measuring depth of invasion in early squamous cell carcinoma of the oral tongue:,positive deep margin, extratumoral perineural invasion, and other challenges. Head Neck Pathol 2019;13:154–61.

El-Naggar AK, Chan J, Grandis J, Takata T, Slootweg P. WHO classification of head and neck tumours. 4th ed.; 2017. p. 105–111.

Dik EA, Ipenburg NA, Kessler PA, van Es RJJ, Willems SM. The value of histological grading of biopsy and resection specimens in early stage oral squamous cell carcinomas. J Craniomaxillofac Surg 2018;46:1001–6.

Boxberg M, Jesinghaus M, Dorfner C, Mogler C, Drecoll E, Warth A, et al. Tumour budding activity and cell nest size determine patient outcome in oral squamous cellcarcinoma: proposal for an adjusted grading system. Histopathology 2017;70:1125–37

Sakata J, Yamana K, Yoshida R, Matsuoka Y, Kawahara K, Arita H, et al. Tumor budding as a novel predictor of occult metastasis in cT2N0 tongue squamous cell carcinoma. Hum Pathol 2018;76:1–8.

Boxberg M, Kuhn PH, Reiser M, Erb A, Steiger K, Pickhard A, et al. Tumor buddingand cell nest size are highly prognostic in laryngeal and hypopharyngeal squamouscell carcinoma: further evidence for a unified histopathologic grading system forsquamous cell carcinomas of the upper aerodigestive tract. Am J Surg Pathol2019;43:303–13

Yomoda T, Sudo T, Kawahara A, Shigaki T, Shimomura S, Tajiri K, et al. The immunoscoreis a superior prognostic tool in stages II and III colorectal cancer and issignificantly correlated with programmed death-ligand 1 (PD-L1) expression ontumor-infiltrating mononuclear cells. Ann Surg Oncol 2019;26:415–24.

Boxberg M, Leising L, Steiger K, Jesinghaus M, Alkhamas A, Mielke M, et al.Composition and clinical impact of the immunologic tumor microenvironment inoral squamous cell carcinoma. J Immunol 2019;202:278–91.

Fang J, Li X, Ma D, Liu X, Chen Y, Wang Y, et al. Prognostic significance of tumorinfiltrating immune cells in oral squamous cell carcinoma. BMC Cancer2017;17:375.

Hadler-Olsen E, Wirsing AM. Tissue-infiltrating immune cells as prognostic markersin oral squamous cell carcinoma: a systematic review and meta-analysis. Br JCancer 2019;120:714–27.

Almangush A, Heikkinen I, Bakhti N, Makinen LK, Kauppila JH, Pukkila M, et al.Prognostic impact of tumour-stroma ratio in early-stage oral tongue cancers.Histopathology 2018;72:1128–35.

Ketabat, F., Pundir, M., Mohabatpour, F., Lobanova, L. and Koutsopoulos, S. (2019).Controlled Drug Delivery Systems for Oral Cancer Treatment—Current Status and Future Perspectives. Pharmaceutics, 11(7), p.302

Shah JP, Gil Z. Current concepts in management of oral cancer:surgery. Oral Oncol 2009; 45: 394-401.

Pagedar NA, Gilbert RW. Selective neck dissection: a review of theevidence. Oral Oncol 2009; 45: 416-20.

Mazeron R, Tao Y, Lusinchi A, Bourhis J. Current concepts inmanagement in head and neck cancer; radiotherapy. Oral Oncol
2009; 45: 402-8.

Specenier PM, Vermorken JB. Current concepts for the managementof head and neck cancer: Chemotherapy. Oral Oncol 2009;

45: 409-15.

MARCAZZAN S, VARONI E M, BLANCO E, LODI G,FERRARI M. Nanomedicine, an emerging therapeutic
strategy for oral cancer therapy [J]. Oral Oncology, 2018, 76:1−7.

ZHOU Wen-hua, PAN Ting, CUI Hao-dong, ZHAO Zhen,CHU P K, YU Xue-feng. Black phosphorus: Bioactive
nanomaterials with inherent and selective chemotherapeuticeffects [J]. Angewandte Chemie: International Edition, 2019,131(3): 779−784.

Hamakawa H, Nakashiro K, Sumida T, et al. Basic evidence ofmolecular targeted therapy for oral cancer and salivary gland cancer.Head Neck 2008; 30: 800-9.

Sasahira, T.; Kurihara-Shimomura, M.; Shimojjukoku, Y.; Shima, K.; Kirita, T. Searching for New Molecular Targets for Oral Squamous Cell Carcinoma with a View to Clinical Implementation of Precision Medicine. J. Pers. Med. 2022, 12, 413. **https://doi.org/10.3390/jpm12030413**

Sung, H.; Ferlay, J.; Siegel, R.L.; Laversanne, M.; Soerjomataram, I.; Jemal, A.; Bray, F. Global cancer statistics 2020: GLOBOCANestimates of incidence and mortality worldwide for 36 cancers in 185 countries. CA Cancer J. Clin. 2021, 71, 209–249.

Wicki A, Witz igmann D, Balasubr amanian V, HuwylerJ. Nanomedicine in cancer therapy: challenges,
opportunities, and clinical applications. J ControlRelease 2015; 200: 138-157.

Mi Y, Wolfram J, Mu C, Liu X, Blanc o E, Shen H,Ferr ari M. Enzyme-responsive multistage vector
for drug delivery to tumor tissue. Pharmacol Res2016; 113: 92-99.

Mi Y, Mu C, Wolfr am J, Deng Z, Hu TY, Liu X, BlancoE, Shen H, Ferr ari M. A micro/nano composite
for combination treatment of melanoma lung metastasis.Adv Healthc Mater 2016; 5: 936-946.

Akagi, K.; Oki, E.; Taniguchi, H.; Nakatani, K.; Aoki, D.; Kuwata, T.; Yoshino, T. Real-world data on microsatellite instabilitystatus in various unresectable or metastatic solid tumors. Cancer Sci. 2021, 112, 1105–1113.

Hause, R.J.; Pritchard, C.C.; Shendure, J.; Salipante, S.J. Classification and characterization of microsatellite instability cross 18cancer types. Nat. Med. 2016, 22, 1342–1350. [CrossRef]

Jiang, T.; Wang, G.; Liu, Y.; Feng, L.; Wang, M.; Liu, J.; Chen, Y.; Ouyang, L. Development of small-molecule ropomyosin receptorkinase (TRK) inhibitors for NTRK fusion cancers. Acta Pharm. Sin. B 2021, 11, 355–372.

Spitzbarth M, Scherer A, Schachtsc hneider A, Imm ing P,Polarz S, Dresc her M. Time-spectral-and spatially
resolved EPR spectroscopy enables simultaneousmonitoring of diffusion of different guest molecules in nano-pores. J Magn Reson 2017; 283: 45-51.Nichols JW, Bae YH . EPR: Evidence and fallacy. JControl Release 2014; 190: 451-464.

Masoudipour E, Kashanian S, Maleki N, KaramyanA, Omidf ar K. A novel intracellular pH-Responsive
formulation for FTY720 based on PEGylatedgraphene oxide nano-sheets. Drug Dev Ind Pharm 2018; 44: 99-108.

Afifi MM, Aust in LA , Mack ey MA, El-Sayed MA.XAV939: from a small inhibitor to a potent drug
bioconjugate when delivered by gold nanopartieles.Bioconjug Chem 2014; 25: 207-215.

Fan L, Chen J, Zhang X, Liu Y, Xu C. Follicle-stimulatinghormone polypeptide modified nanoparticle
drug delivery system in the treatment of lymphaticmetastasis during ovarian carcinoma therapy. Gynecol Oncol 2014; 135: 125-132.

Xiao DZ, Dai B, Chen J, Luo Q, Liu XY, Lin QX, LiXH, Huang W, Yu XY. Loss of macrophage migrationinhibitory factor impairs the growth propertiesof human HeLa cervical cancer cells. Cell Prolif2011; 44: 582-590.

Oliveira CS, de Bock CE, Molloy TJ, Sadeqz adeh E,Geng XY, Hers ey P, Zhang XD, Thorn e RF. Macrophage
migration inhibitory factor engages PI3K/Akt signalling and is a prognostic factor in metastaticmelanoma. BMC Cancer 2014; 14: 630.

Liang JL, Xu W, Yin TJ, Huo M. Advances in thehypoxia-responsive antitumor drug nanocarrier and tumor hypoxia relieve. J China Pharm Univ2018; 49: 255-262.

Erez N, Truitt M, Olson P, Arr on ST, Hanahan D.Cancer-associated fibroblasts are activated in incipient
neoplasia to orchestrate tumor-promotinginflammation in an NF-kappaB-dependent manner.Cancer Cell 2010; 17: 135-147.

Iriti M, Varoni E. Chemopreventive potential offlavonoids in oral squamous cell carcinoma in human studies. Nutrients 2013; 5: 2564-2576.

Lau A, Li KY, Yang WF, Su YX. Induction chemotherapyfor squamous cell carcinomas of the oral
cavity: a cumulative meta-analysis. Oral Oncol2016; 61: 104-114.

Zhao H, Feng H, Liu D, Liu J, Ji N, Chen F, Luo X,Zhou Y, Dan H, Zeng X, Li J, Sun C, Meng J, Ju X,Zhou M, Yang H, Li L, Liang X, Chu L, Jiang L, He Y,Chen Q. Self-assembling monomeric nucleo-sidemolecular nanoparticles loaded with 5-FU enhancingtherapeutic efficacy against oral cancer. ACS Nano 2015; 9: 9638-9651.

Wang ZQ, Liu K, Huo ZJ, Li XC, Wang M, Liu P, PangB, Wang SJ. A cell-targeted chemotherapeutic nanomedicine
strategy for oral squamous cell carcinomatherapy. J Nanobiotechnol 2015; 13: 63.

Marcazzan S, Varoni EM, Blanc o E, Lodi G, Ferr ari M.Nanomedicine, an emerging therapeutic strategy
for oral cancer therapy. Oral Oncol 2018; 76: 1-7.

Jain S, Hirst DG, O'Sullivan JM. Gold nanoparticlesas novel agents for cancer therapy. Br J Radiol2012; 85: 101-113.

de Araújo RF, Barboza Jr CA, Clebis NK, de Moura SA, LopesCosta Ade L. Prognostic significance of the anatomical locationand TNM clinical classification in oral squamous cell carcinoma.Med Oral Pathol Oral Cir Bucal 2008; 13: E344-7.

Marsh D, Suchak K, Moutasim KA, et al. Stromal features arepredictive of disease mortality in oral cancer patients. J Pathol2011; 223: 470-81.

Zini A, Czerninski R, Sgan-Cohen HD.Oral cancer over four decades:epidemiology, trends, histology, and survival by anatomicalsites. J Oral Pathol Med 2010; 39: 299-305.

CHAPTER 3 - Plasmonic Photothermal Therapy of Cancer using Gold nanoparticles

Sullivan, R. The identity and work of the ancient Egyptiansurgeon. J. R. Soc. Med. 1996, 89, 467−473.

Busch, W. Uber den Einfluss welche heftigere Erysipeln zuweiligauf organisierte Neubildungenausuben. Verhandlungen des NaturhistorischenVereines der Preussischen Rheinlande und Westphalens 1866, 23,
28−30.

Ahmad, R., Fu, J., He, N., and Li, S. (2016). Advanced gold nanomaterialsfor photothermal therapy of cancer. J. Nanosci. Nanotechnol. 16, 67–80.
doi: 10.1166/jnn.2016.10770

Svaasand, L. O.; Gomer, C. J.; Morinelli, E. On the physicalrationale of laser induced hyperthermia. Lasers in Medical Science
1990, 5, 121−128.

Li, X.; Yu, S.; Lee, D.; Kim, G.; Lee, B.; Cho, Y.; Zheng, B.-Y.;Ke, M.-R.; Huang, J.-D.; Nam, K. T.; et al. Facile supramolecular approach to nucleic-acid-driven activatable nanotheranostics thatovercome drawbacks of photodynamic therapy. ACS Nano 2018, 12,681−688.

Cheung, A. Y.; Neyzari, A. Deep Local Hyperthermia for CancerTherapy: External Electromagnetic and Ultrasound Techniques.Cancer Res. 1984, 44, 4736−4744.

Zagar, T. M.; Oleson, J. R.; Vujaskovic, Z.; Dewhirst, M. W.;Craciunescu, O. I.; Blackwell, K. L.; Prosnitz, L. R.; Jones, E. L.Hyperthermia for Locally Advanced Breast Cancer. Int. J. Hyperthermia2010, 26, 618−624.

Hood, R. L.; Carswell, W. F.; Rodgers, A.; Kosoglu, M. A.;Rylander, M. N.; Grant, D.; Robertson, J. L.; Rylander, C. G. Spatiallycontrolled photothermal heating of bladder tissue through singlewalledcarbon nanohorns delivered with a fiberoptic microneedledevice. Lasers in medical science 2013, 28, 1143−1150.

Huang, X.; Jain, P. K.; El-Sayed, I. H.; El-Sayed, M. A. Plasmonicphotothermal therapy (PPTT) using gold nanoparticles. Lasers inmedical science 2008, 23, 217.

Bayazitoglu, Y.; Kheradmand, S.; Tullius, T. K. An overview ofnanoparticle assisted laser therapy. Int. J. Heat Mass Transfer 2013, 67,469−486.

Kemp, J. A.; Shim, M. S.; Heo, C. Y.; Kwon, Y. J. Combo”nanomedicine: co-delivery of multi-modal therapeutics for efficient,targeted, and safe cancer therapy. Adv. Drug Delivery Rev. 2016, 98,3−18.

Sztandera, K.; Gorzkiewicz, M.; Klajnert-Maculewicz, B. Goldnanoparticles in cancer treatment. Mol. Pharmaceutics 2019, 16, 1−23.

Day, E. S.; Morton, J. G.; West, J. L. Nanoparticles for ThermalCancer Therapy. J. Biomech. Eng. 2009, 131, 074001.

Huang, X.; Jain, P. K.; El-Sayed, I. H.; El-Sayed, M. A.Plasmonic Photothermal Therapy (Pptt) Using Gold Nanoparticles.
Laser Med. Sci. 2008, 23, 217−228.

Jenkins PA, Carroll JD. How to report low-level laser therapy (LLLT)/photomedicine dose and beam parameters in clinical and laboratory studies. Photomed Laser Surg. 2011;29(12):785–787.

Chen AC, Arany PR, Huang YY, et al. Low-level laser therapy activates NF-kB via generation of reactive oxygen species in mouse embryonic fibroblasts. PLoS One. 2011;6(7):e22453.

Szymanska J, Goralczyk K, Klawe JJ, et al. Phototherapy with low-level laser influences the proliferation of endothelial cells and vascular endothelial growth factor and transforming growth factor-beta secretion. J Physiol Pharmacol. 2013;64(3):387–391.

Frank S, Oliver L, Lebreton-De Coster C, et al. Infrared radiation affects the mitochondrial pathway of apoptosis in human fibroblasts. J Invest Dermatol. 2004;123(5):823–831.

Baffou, G.; Quidant, R. Thermo-plasmonics: using metallicnanostructures as nano-sources of heat. Laser & Photonics Reviews
2013, 7, 171−187.

Steiner R. Laser-tissue interactions. In: Raulin C, Karsai S, editors. Laser and IPL Technology in Dermatology and Aesthetic Medicine. Berlin and Heidelberg: Springer-Verlag; 2011:23–36.

Wan S, Parrish JA, Anderson RR, Madden M. Transmittance of nonionizing radiation in human tissues. Photochem Photobiol. 1981;34(6):679–681.

Karu TI. Cellular mechanism of low power laser therapy: new questions. In: Simunovic F, editor. Lasers in Medicine and Dentistry. Vol 3.Rijeka: Z Vitgraf; 2003:79–100.

Hode L. The importance of the coherency. Photomed Laser Surg. 2005;23(4):431–434.

Hirsch, L. R.; Stafford, R. J.; Bankson, J. A.; Sershen, S. R.;Rivera, B.; Price, R. E.; Hazle, J. D.; Halas, N. J.; West, J. L. Nanoshellmediatednear-infrared thermal therapy of tumors under magneticresonance guidance. Proc. Natl. Acad. Sci. U. S. A. 2003, 100, 13549−13554.

Huang, J.; Wang, W.; Murphy, C. J.; Cahill, D. G. Resonantsecondary light emission from plasmonic Au nanostructures at highelectron temperatures created by pulsed laser excitation. Proc. Natl.Acad. Sci. U. S. A. 2014, 111, 906−911.

Parsons, J.; Burrows, C. P.; Sambles, J. R.; Barnes, W. L. Acomparison of techniques used to simulate the scattering of

electromagnetic radiation by metallic nanostructures. J. Mod. Opt.2010, 57, 356−365.

Steiner R. Laser-tissue interactions. In: Raulin C, Karsai S, editors. Laser and IPL Technology in Dermatology and Aesthetic Medicine. Berlin and Heidelberg: Springer-Verlag; 2011:23–36.

Hode L. The importance of the coherency. Photomed Laser Surg. 2005;23(4):431–434.

Jenkins PA, Carroll JD. How to report low-level laser therapy (LLLT)/photomedicine dose and beam parameters in clinical and laboratory studies. Photomed Laser Surg. 2011;29(12):785–787.

R. Missert, R. Watson, T. Y. Ohulchanskyy, E. C. Tracy, H. Baumann, and R. K. Pandey, "Highly effective
dual-function near-infrared (NIR) photosensitizer for fluorescence imaging and photodynamic therapy (PDT) of
cancer," J. Med. Chem. 59(21), 9774–9787 (2016).

Baffou, G.; Quidant, R. Thermo-plasmonics: Using metallicnanostructures as nanosources of heat. Laser and Photonics Reviews
2013, 7, 171−187.

Poland, C. A., Duffin, R., Kinloch, I., Maynard, A., Wallace, W. A., Seaton, A.,et al. (2008). Carbon nanotubes introduced into the abdominal cavity of miceshow asbestos-like pathogenicity in a pilot study. Nat. Nanotechnol. 3, 423–428.doi: 10.1038/nnano.2008.111

Kaur, P., Aliru, M. L., Chadha, A. S., Asea, A., and Krishnan, S. (2016).Hyperthermia using nanoparticles–promises and pitfalls. Int. J. Hyperthermia32, 76–88. doi: 10.3109/02656736.2015.1120889

Z., Gong, H., Gao, M., Zhu, W., Sun, X., Feng, L., et al. (2016).Polydopamine nanoparticles as a versatile molecular loading platform to enableimaging-guided cancer combination therapy. Theranostics. 6, 1031–1042.
doi: 10.7150/thno.14431

Cheng, L., Wang, C., Feng, L., Yang, K., and Liu, Z. (2014). Functionalnanomaterials for phototherapies of cancer. Chem. Rev. 114, 10869–10939.
doi: 10.1021/cr400532z

Huang, X.; Jain, P. K.; El-Sayed, I. H.; El-Sayed, M. A. Plasmonicphotothermal therapy (PPTT) using gold nanoparticles. Lasers inmedical science 2008, 23, 217.

Ahmad, R., Fu, J., He, N., and Li, S. (2016). Advanced gold nanomaterialsfor photothermal therapy of cancer. J. Nanosci. Nanotechnol. 16, 67–80.doi: 10.1166/jnn.2016.10770

Hammer, B., Norskov, J. Why gold is the noblest of all the metals. Nature 376, 238–240 (1995). https://doi.org/10.1038/376238a0

Pricker, S. P. Medical Uses of Gold Compounds: Past, Presentand Future. Gold Bull. 1996, 29, 53−60.

Benedek, T. G. The History of Gold Therapy for Tuberculosis. J.Hist. Med. Allied Sci. 2004, 59, 50−89.

Kean, W.; Hart, L.; Buchanan, W. Auranofin. Rheumatology1997, 36, 560−572.

Edwards, P. P.; Thomas, J. M. Gold in a Metallic DividedState←from Faraday to Present-Day Nanoscience. Angew. Chem., Int.Ed. 2007, 46, 5480−5486.

Faraday, M. Experimental Relations of Gold (and Other Metals)to Light. Philos. Trans. 1857, 147, 145−181.

A., and Bürgi, T. (2013). "Bottom-up organisation of metallicnanoparticles," in Amorphous Nanophotonics, eds C. Rockstuhl and T. Scharf
(Genève: Springer), 1–37.

M., Badwaik, V., Kherde, Y., Waghwani, H. K., Modi, T., Aguilar, Z. P.,et al. (2014). Gold nanoparticles: various methods of synthesis and antibacterialapplications. Front Biosci. 19, 1320–1344. doi: 10.2741/4284

Zare, D., Akbarzadeh, A., and Bararpour, N. (2010). Synthesis andfunctionalization of gold nanoparticles by using of poly functional aminoacids. Int. J. Nanosci. Nanotechnol. 6, 223–230. Available online at: http://www.

ijnnonline.net/?_action=articleInfo&article=3958

Mieszawska, A. J., Mulder, W. J., Fayad, Z. A., and Cormode, D. P. (2013).Multifunctional gold nanoparticles for diagnosis and therapy of disease. Mol.Pharm. 10, 831–847. doi: 10.1021/mp3005885

Herizchi, R., Abbasi, E., Milani, M., and Akbarzadeh, A. (2016). Current methodsfor synthesis of gold nanoparticles. Artif. Cells Nanomed. Biotechnol. 44,596–602. doi: 10.3109/21691401.2014.971807

Annadhasan, M., Kasthuri, J., and Rajendiran, N. (2015). Green synthesis ofgold nanoparticles under sunlight irradiation and their colorimetric detectionof Ni 2+ and Co 2+ ions. RSC Adv. 5, 11458–11468. doi: 10.1039/C4RA14034F

Rodrigues, C. J., Bobb, J. A., John, M. G., Fisenko, S. P., El-Shall, M. S.,and Tibbetts, K. M. (2018). Nucleation and growth of gold nanoparticlesinitiated by nanosecond and femtosecond laser irradiation of aqueous
[AuCl4](). Phys. Chem. Chem. Phys. 20, 28465–28475. doi: 10.1039/C8CP05774E

Kumar, V., and Yadav, S. K. (2008). Plant-mediated synthesis of silver and goldnanoparticles and their applications. J. Chem. Technol. Biotechnol. 84, 151–157.doi: 10.1002/jctb.2023

Le Renard, P. E., Jordan, O., Faes, A., Petri-Fink, A., Hofmann, H., Rufenacht, D.,et al. (2010). The in vivo performance of magnetic particle-loaded injectable,in situ gelling, carriers for the delivery of local hyperthermia. Biomaterials. 31,
691–705. doi: 10.1016/j.biomaterials.2009.09.091

Lee, D., Ko,W. K., Hwang, D. S., Heo, D. N., Lee, S. J., Heo,M., et al. (2016). Use ofbaicalin-conjugated gold nanoparticles for apoptotic induction of breast cancercells. Nanoscale Res. Lett. 11:381. doi: 10.1186/s11671-016-1586-3

Hoshyar, R., Khayati, G. R., Poorgholami, M., and Kaykhaii, M. (2016). Anovel green one-step synthesis of gold anoparticles using crocin andtheir anti-cancer activities. J. Photochem. Photobiol. B Biol. 159, 237–242.doi: 10.1016/j.jphotobiol.2016.03.056

Mishra, P., Ray, S., Sinha, S., Das, B., Khan, M. I., Behera, S. K., et al.(2016). Facile bio-synthesis of gold nanoparticles by using extract ofHibiscus sabdariffa and evaluation of its cytotoxicity against U87 glioblastomacells under hyperglycemic condition. Biochem. Eng. J. 105, 264–272.doi: 10.1016/j.bej.2015.09.021

Chithrani, B. D., Ghazani, A. A., and Chan, W. C. (2006). Determining the sizeand shape dependence of gold nanoparticle uptake into mammalian cells. NanoLett. 6, 662–668. doi: 10.1021/nl052396o

Choi, S. W., Kim, W. S., and Kim, J. H. (2003). Surface modification of functionalnanoparticles for controlled drug delivery. J. Dispers. Sci. Technol. 24, 475–487.doi: 10.1081/DIS-120021803

Shukla, R., Bansal, V., Chaudhary, M., Basu, A., Bhonde, R. R., and Sastry, M.(2005). Biocompatibility of gold nanoparticles and their endocytotic fate insidethe cellular compartment: a microscopic overview. Langmuir. 21, 10644–10654.doi: 10.1021/la0513712

Khlebtsov, N.; Dykman, L. Biodistribution and Toxicity ofEngineered Gold Nanoparticles: A Review of In vitro and In vivoStudies. Chem. Soc. Rev. 2011, 40, 1647−1671.

Huang, Y.-F.; Sefah, K.; Bamrungsap, S.; Chang, H.-T.; Tan, W.Selective Photothermal Therapy for Mixed Cancer Cells UsingAptamer-Conjugated Nanorods. Langmuir 2008, 24, 11860−11865.

Tong, L.; Wei, Q.; Wei, A.; Cheng, J.-X. Gold Nanorods asContrast Agents for Biological Imaging: Optical Properties, SurfaceConjugation and Photothermal Effects. Photochem. Photobiol. 2009, 85,
21−32.

Eghtedari, M., Liopo, A. V., Copland, J. A., Oraevsky, A. A., and Motamedi,M. (2009). Engineering of hetero-functional gold nanorods for the in vivo molecular targeting of breast cancer cells. Nano Lett. 9, 287–291.
doi: 10.1021/nl802915q

Patra, C. R., Bhattacharya, R., Wang, E., Katarya, A., Lau, J. S., Dutta, S., et al.(2008). Targeted delivery of gemcitabine to pancreatic adenocarcinomausing cetuximab as a targeting agent. Cancer Res. 68, 1970–1978.doi: 10.1158/0008-5472.CAN-07-6102

Liao, H., and Hafner, J. H. (2005). Gold nanorod bioconjugates. Chem. Mater. 17,4636–4641. doi: 10.1021/cm050935k

Paciotti, G. F., Kingston, D. G. I., and Tamarkin, L. (2006). Colloidal goldnanoparticles: a novel nanoparticle platform for developing multifunctionaltumor-targeted drug delivery vectors. Drug Dev. Res. 67, 47–54.doi: 10.1002/ddr.20066

Calderwood, S. K.; Ciocca, D. R. Heat Shock Proteins: StressProteins with Janus-Like Properties in Cancer. Int. J. Hyperthermia
2008, 24, 31−39.

Hirsch, L. R.; Stafford, R. J.; Bankson, J. A.; Sershen, S. R.;Rivera, B.; Price, R. E.; Hazle, J. D.; Halas, N. J.; West, J. L. Nanoshell-Mediated Near-Infrared Thermal Therapy of Tumors Under MagneticResonance Guidance. Proc. Natl. Acad. Sci. U. S. A. 2003, 100, 13549−13554.

O'Neal, D. P.; Hirsch, L. R.; Halas, N. J.; Payne, J. D.; West, J. L.Photo-Thermal Tumor Ablation in Mice Using Near-Infrared-Absorbing Nanoparticles. Cancer Lett. 2004, 209, 171−176.

El-Sayed, I. H.; Huang, X.; El-Sayed, M. A. Selective LaserPhoto-Thermal Therapy of Epithelial Carcinoma Using anti-EGFRAntibody Conjugated Gold Nanoparticles. Cancer Lett. 2006, 239,129−135.

Link, S.; Burda, C.; Mohamed, M. B.; Nikoobakht, B.; El-Sayed,M. A. Laser Photothermal Melting and Fragmentation of GoldNanorods: Energy and Laser Pulse-Width Dependence. J. Phys. Chem.A 1999, 103, 1165−1170.

Wust, P.; Hildebrandt, B.; Sreenivasa, G.; Rau, B.; Gellermann,J.; Riess, H.; Felix, R.; Schlag, P. M. Hyperthermia in CombinedTreatment of Cancer. Lancet Oncol. 2002, 3, 487−497.

Huang, X.; Qian, W.; El-Sayed, I. H.; El-Sayed, M. A. ThePotential Use of the Enhanced Nonlinear Properties of Gold
Nanospheres in Photothermal Cancer Therapy. Lasers Surg. Med.2007, 39, 747−753.

Bao, Z.; Liu, X.; Liu, Y.; Liu, H.; Zhao, K. Near-infrared lightresponsiveinorganic nanomaterials for photothermal therapy. Asian J.Pharm. Sci. 2016, 11, 349−364.

Loo, C., Lin, A., Hirsch, L., Lee,M. H., Barton, J.,Halas, N., et al. (2004).Nanoshellenabledphotonics-based imaging and therapy of cancer. Technol. Cancer Res.Treat. 3, 33–40. doi: 10.1177/153303460400300104

Xia, Y.; Ma, X.; Gao, J.; Chen, G.; Li, Z.; Wu, X.; Yu, Z.; Xing,J.; Sun, L.; Ruan, H.; et al. A Flexible Caterpillar-Like Gold
Nanoparticle Assemblies with Ultrasmall Nanogaps for EnhancedDual-Modal Imaging and Photothermal Therapy. Small 2018, 14,No. e1800094.

Huang, X., Jain, P. K., El-Sayed, I. H., and El-Sayed, M. A. (2008). Plasmonicphotothermal therapy (PPTT) using gold nanoparticles. Lasers Med. Sci. 23,217–228. doi: 10.1007/s10103-007-0470-

Day, E. S., Bickford, L. R., Slater, J. H., Riggall, N. S., Drezek, R. A., andWest, J. L. (2010). Antibody-conjugated gold-gold sulfide nanoparticles asmultifunctional agents for imaging and therapy of breast cancer. Int. J.Nanomed. 5, 445–454. doi: 10.2147/IJN.S10881

Zhang, P.,Wang, J., Huang, H., Yu, B., Qiu, K., Huang, J., et al. (2015). Unexpectedhigh photothemal conversion efficiency of gold nanospheres upon graftingwith two-photon luminescent ruthenium(II) complexes: a way towards cancertherapy? Biomaterials. 63, 102–114. doi: 10.1016/j.biomaterials.2015.06.012

Chen, W.-H., Lei, Q., Luo, G.-F., Jia, H.-Z., Hong, S., Liu, Y.-X., et al.(2015). Rational design of multifunctional gold nanoparticles via host–guest interaction for cancer-targeted therapy. ACS Appl. Mater. Interfaces. 7,17171–17180. doi: 10.1021/acsami.5b04031

Ahmad, R., Fu, J., He, N., and Li, S. (2016). Advanced gold nanomaterialsfor photothermal therapy of cancer. J. Nanosci. Nanotechnol. 16, 67–80.doi: 10.1166/jnn.2016.10770

Li, M., Li, L., Zhan, C., and Kohane, D. S. (2016). Core-shell nanostarsfor multimodal therapy and imaging. Theranostics. 6, 2306–2313.doi: 10.7150/thno.15843

O'Neal, D. P., Hirsch, L. R., Halas, N. J., Payne, J. D., andWest, J. L. (2004). Photothermaltumor ablation in mice using near infrared-absorbing nanoparticles.Cancer Lett. 209, 171–176. doi: 10.1016/j.canlet.2004.02.004

Hirsch, L. R., Stafford, R. J., Bankson, J. A., Sershen, S. R., Rivera, B., Price,R. E., et al. (2003). Nanoshell-mediated near-infrared thermal therapy of tumors under magnetic resonance guidance. Proc. Natl. Acad. Sci. USA. 100,
13549–13554. doi: 10.1073/pnas.2232479100

Loo, C.; Lin, A.; Hirsch, L.; Lee, M.; Barton, J.; Halas, N.;West, J.; Drezek, R. Nanoshell-Enabled Photonics-Based Imaging andTherapy of Cancer. Technol. Cancer Res. Treat. 2004, 3, 33−40.

Chang, S.-S., Lee, C.-L., and Wang, C. R. C. (1997). Gold nanorods:electrochemical synthesis and optical properties. J. Phys. Chem. B 101,6661–6664. doi: 10.1021/jp971656q

Jain, P. K., Lee, K. S., El-Sayed, I. H., and El-Sayed, M. A. (2006). Calculatedabsorption and scattering properties of gold nanoparticles of different size,shape, and composition: applications in biological imaging and biomedicine.
J. Phys. Chem. B 110, 7238–7248. doi: 10.1021/jp057170o

Hwang, S., Nam, J., Jung, S., Song, J., Doh, H., and Kim, S. (2014). Goldnanoparticle-mediated photothermal therapy: current status and futureperspective. Nanomedicine. 9, 2003–2022. doi: 10.2217/nnm.14.147

Chen, J.; Wang, D.; Xi, J.; Au, L.; Siekkinen, A.; Warsen, A.; Li,Z.; Zhang, H.; Xia, Y.; Li, X. Immuno Gold Nanocages with TailoredOptical Properties for Targeted Photothermal Destruction of CancerCells. Nano Lett. 2007, 7, 1318−1322.

Zhou, J., Lu, Z., Zhu, X., Wang, X., Liao, Y., Ma, Z., et al. (2013).NIR photothermal therapy using polyaniline nanoparticles.Biomaterials. 34, 9584–9592. doi: 10.1016/j.biomaterials.2013.08.075

Yin, T., Li, Y., Bian, K., Zhu, R., Liu, Z., Niu, K., et al. (2018). Selfassemblysynthesis of vapreotidegold hybrid nanoflower for photothermalantitumor activity. Mater. Sci. Eng. C Mater. Biol. Appl. 93, 716–723.doi: 0.1016/j.msec.2018.08.017

Balogh, L., Nigavekar, S. S., Nair, B. M., Lesniak, W., Zhang, C., Sung, L. Y.,et al. (2007). Significant effect of size on the in vivo biodistribution of goldcomposite nanodevices in mouse tumor models. Nanomedicine. 3, 281–296.doi: 10.1016/j.nano.2007.09.001

Goodrich, G. P., Bao, L., Gill-Sharp, K., Sang, K. L., Wang, J., and Payne,J. D. (2010). Photothermal therapy in a murine colon cancer modelusing near-infrared absorbing gold nanorods. J. Biomed. Opt. 15:018001.doi: 10.1117/1.3290817

Hao, E., Bailey, R. C., Schatz, G. C., Hupp, J. T., and Li, S. (2004). Synthesisand optical properties of “branched” gold nanocrystals. Nano Lett. 4, 327–330.doi: 10.1021/nl0351542

Petryayeva, E., and Krull, U. J. (2011). Localized surface plasmon resonance:nanostructures, bioassays and biosensing—a review. Anal. Chim. Acta. 706,8–24. doi: 10.1016/j.aca.2011.08.020

Kelly, K. L., Coronado, E., Zhao, L. L., and Schatz, G. C. (2003). The opticalproperties of metal nanoparticles: the influence of size, shape, and dielectricenvironment. J. Phys. Chem. B 107, 668–677. doi: 10.1021/jp026731y

Ghosh, S. K.; Pal, T. Interparticle Coupling Effect on theSurface Plasmon Resonance of Gold Nanoparticles: From Theory toApplications. Chem. Rev. 2007, 107, 4797−4862.

Mourdikoudis, R. M. Pallares, N. T. K. Thanh, Nanoscale 2018, 10,12871–12934.

Smitha, S. L., Gopchandran, K. G., Smijesh, N., and Philip, R. (2013). Sizedependentoptical properties of Au nanorods. Prog. Nat. Sci. Mater. Int. 23,36–43. doi: 10.1016/j.pnsc.2013.01.005

Pérez-Juste, J., Pastoriza-Santos, I., Liz-Marzán, L. M., and Mulvaney, P. (2005).Gold nanorods: synthesis, characterization and applications. Coord. Chem. Rev.249, 1870–1901. doi: 10.1016/j.ccr.2005.01.030

Chen, H., Zhang, X., Dai, S., Ma, Y., Cui, S., Achilefu, S., et al. (2013).Multfunctional gold nanostar conjugates for tumor imaging andcombined photothermal and chemo-therapy. Theranostics. 3, 633–649.
doi: 10.7150/thno.6630

Larsson, E. M., Alegret, J., Käll, M., and Sutherland, D. S. (2007). Sensingcharacteristics of NIR localized surface plasmon resonances in gold nanoringsfor application as ultrasensitive biosensors. Nano Lett. 7, 1256–1263.
doi: 10.1021/nl0701612

Kim, S. E., Lee, B. R., Lee, H., Jo, S. D., Kim, H., Won, Y. Y., and Lee,J. (2017). Near-infrared plasmonic assemblies of gold nanoparticles withmultimodal function for targeted cancer theragnosis. Sci. Rep. 7:17327.doi: 10.1038/s41598-017-17714-2

Link, S.; El-Sayed, M. A. Size and Temperature Dependence ofthe Plasmon Absorption of Colloidal Gold Nanoparticles. J. Phys.Chem. B 1999, 103, 4212−4217.

Day, E. S.; Morton, J. G.; West, J. L. Nanoparticles for ThermalCancer Therapy. J. Biomech. Eng. 2009, 131, 074001.

Link, S.; El-Sayed, M. A. Shape and Size Dependence ofRadiative, Non-Radiative and Photothermal Properties of Gold
Nanocrystals. Int. Rev. Phys. Chem. 2000, 19, 409−453.

Huang, J. Photothermal Properties and Applications of GoldNanorods. Ph.D. Thesis, University of Illinois, Urbana, IL, 2014.

Huang, X.; Jain, P. K.; El-Sayed, I. H.; El-Sayed, M. A. PlasmonicPhotothermal Therapy (PPTT) Using Gold Nanoparticles. LasersMed. Sci. 2008, 23, 217−228.

Eustis, S.; El-Sayed, M. A. Why Gold Nanoparticles are MorePrecious than Pretty Gold: Noble Metal Surface Plasmon Resonanceand its Enhancement of the Radiative and Nonradiative Properties ofNanocrystals of Different Shapes. Chem. Soc. Rev. 2006, 35, 209−217.

Jain, P. K.; Lee, K. S.; El-Sayed, I. H.; El-Sayed, M. A. CalculatedAbsorption and Scattering Properties of Gold Nanoparticles ofDifferent Size, Shape, and Composition: Applications in BiologicalImaging and Biomedicine. J. Phys. Chem. B 2006, 110, 7238−7248.

Huang, H.-C.; Rege, K.; Heys, J. J. Spatiotemporal TemperatureDistribution and Cancer Cell Death in Response to ExtracellularHyperthermia Induced by Gold Nanorods. ACS Nano 2010, 4, 2892−2900.

Ghosh, S. K.; Pal, T. Interparticle Coupling Effect on theSurface Plasmon Resonance of Gold Nanoparticles: From Theory toApplications. Chem. Rev. 2007, 107, 4797−4862.

Jang, B.; Kim, Y. S.; Choi, Y. Effect of Gold NanorodConcentration on the Depth-Related Temperature Increase During
Hyperthermic Ablation. Small 2011, 7, 265−270.

Chen, H.; Shao, L.; Ming, T.; Sun, Z.; Zhao, C.; Yang, B.; Wang,J. Understanding the Photothermal Conversion Efficiency of GoldNanocrystals. Small 2010, 6, 2272−2280.

Jiang, K.; Smith, D. A.; Pinchuk, A. Size-Dependent PhotothermalConversion Efficiencies of Plasmonically Heated Gold
Nanoparticles. J. Phys. Chem. C 2013, 117, 27073−27080.

Mackey, M. A.; Ali, M. R. K.; Austin, L. A.; Near, R. D.; El-Sayed, M. A. The Most Effective Gold Nanorod Size for PlasmonicPhotothermal Therapy: Theory and In Vitro Experiments. J. Phys. Chem. B 2014, 118, 1319−1326.

Jaque, D.; Martínez Maestro, L.; del Rosal, B.; Haro-Gonzalez,P.; Benayas, A.; Plaza, J. L.; Martín Rodríguez, E.; García Solé, J.Nanoparticles for Photothermal Therapies. Nanoscale 2014, 6, 9494−
530.

Ayala-Orozco, C.; Urban, C.; Knight, M. W.; Urban, A. S.;Neumann, O.; Bishnoi, S. W.; Mukherjee, S.; Goodman, A. M.;
Charron, H.; Mitchell, T.; Shea, M.; Roy, R.; Nanda, S.; Schiff, R.;Halas, N. J.; Josh, A.; et al. Au Nanomatryoshkas as Efficient Near-Infrared Photothermal Transducers for Cancer Tratment: BenchmarkingAgainst Nanoshells. ACS Nano 2014, 8, 6372−6381.

Huang, J.; Park, J.; Wang, W.; Murphy, C. J.; Cahill, D. G.Ultrafast Thermal Analysis of Surface Functionalized Gold Nanorodsin Aqueous Solution. ACS Nano 2013, 7, 589−597.

Link, S.; Burda, C.; Mohamed, M. B.; Nikoobakht, B.; El-Sayed,M. A. Laser Photothermal Melting and Fragmentation of GoldNanorods: Energy and Laser Pulse-Width Dependence. J. Phys. Chem.A 1999, 103, 1165−1170.

Calderwood, S. K.; Ciocca, D. R. Heat Shock Proteins: StressProteins with Janus-Like Properties in Cancer. Int. J. Hyperthermia2008, 24, 31−39.

Samali, A.; Holmberg, C. I.; Sistonen, L.; Orrenius, S.Thermotolerance and Cell Death Are Distinct Cellular Responsesto Stress: Dependence on Heat Shock Proteins. FEBS Lett. 1999, 461,306−10.

Melamed, J. R.; Edelstein, R. S.; Day, E. S. Elucidating theFundamental Mechanisms of Cell Death Triggered by PhotothermalTherapy. ACS Nano 2015, 9, 6−11.

Krysko, D. V.; Vanden Berghe, T.; Parthoens, E.; D'Herde, K.;Vandenabeele, P. Methods for Distinguishing Apoptotic fromNecrotic Cells and Measuring Their Clearance. Methods Enzymol.2008, 442, 307−341.

Davidovich, P.; Kearney, C. J.; Martin, S. J. InflammatoryOutcomes of Apoptosis, Necrosis and Necroptosis. Biol. Chem. 2014,395, 1163−71.

Banfalvi, G. Methods to Detect Apoptotic Cell Death. Apoptosis2017, 22, 306−323.

Pérez-Hernández, M.; Del Pino, P.; Mitchell, S. G.; Moros, M.;Stepien, G.; Pelaz, B.; Parak, W. J.; Gálvez, E. M.; Pardo, J.; de laFuente, J. M. Dissecting the Molecular Mechanism of ApoptosisDuring Photothermal Therapy Using Gold Nanoprisms. ACS Nano2015, 9, 52−61.

Ali, M. R.; Ali, H. R.; Rankin, C. R.; El-Sayed, M. A. TargetingHeat Shock Protein 70 Using Gold Nanorods Enhances Cancer CellApoptosis in Low Dose Plasmonic Photothermal Therapy. Biomaterials2016, 102, 1−8.

Dickerson, E.; Dreaden, E.; Huang, X.; El-Sayed, I.; Chu, H.;Pushpanketh, S.; McDonald, J.; El-Sayed, M. Gold Nanorod Assistednear-Infrared Plasmonic Photothermal Therapy (Pptt) of SquamousCell Carcinoma in Mice. Cancer Lett. 2008, 269, 57−66.

Ali, M. R.; Rahman, M. A.; Wu, Y.; Han, T.; Peng, X.; Mackey,M. A.; Wang, D.; Shin, H. J.; Chen, Z. G.; Xiao, H.; et al. Efficacy,Long-Term Toxicity, and Mechanistic Studies of Gold NanorodsPhotothermal Therapy of Cancer in Xenograft Mice. Proc. Natl. Acad.Sci. U. S. A. 2017, 114, E3110−E3118.

Egeblad, M.; Nakasone, E.; Werb, Z. Tumors as Organs:Complex Tissues That Interface with the Entire Organism. Dev. Cell2010, 18, 884−901.

Bhowmick, N.; Neilson, E.; Moses, H. Stromal Fibroblasts inCancer Initiation and Progression. Nature 2004, 432, 332−337.

Saha, S.; Xiong, X.; Chakraborty, P. K.; Shameer, K.; Arvizo, R.R.; Kudgus, R. A.; Dwivedi, S. K.; Hossen, M. N.; Gillies, E. M.;Robertson, J. D.; et al. Gold Nanoparticle Reprograms PancreaticTumor Microenvironment and Inhibits Tumor Growth. ACS Nano2016, 10, 10636−10651.

Chen, Q.; Xu, L.; Liang, C.; Wang, C.; Peng, R.; Liu, Z.Photothermal Therapy with Immune-Adjuvant Nanoparticles Togetherwith Checkpoint Blockade for Effective Cancer Immunotherapy.Nat. Commun. 2016, DOI: 10.1038/ncomms13193.

Mukherjee, P.; Bhattacharya, R.; Wang, P.; Wang, L.; Basu, S.;Nagy, J. A.; Atala, A.; Mukhopadhyay, D.; Soker, S. AntiangiogenicProperties of Gold Nanoparticles. Clin. Cancer Res. 2005, 11, 3530−4.

Carmeliet, P.; Jain, R. K. Angiogenesis in Cancer and OtherDiseases. Nature 2000, 407, 249−257.

Burke, A. R.; Singh, R. N.; Carroll, D. L.; Wood, J. C.;D'Agostino, R. B.; Ajayan, P. M.; Torti, F. M.; Torti, S. V. The
Resistance of Breast Cancer Stem Cells to Conventional Hyperthermiaand Their Sensitivity to Nanoparticle-Mediated PhotothermalTherapy. Biomaterials 2012, 33, 2961−2970.

Wang, D.; Xu, Z.; Yu, H.; Chen, X.; Feng, B.; Cui, Z.; Lin, B.;Yin, Q.; Zhang, Z.; Chen, C.; et al. Treatment of Metastatic BreastCancer by Combination of Chemotherapy and PhotothermalAblation Using Doxorubicin-Loaded DNA Wrapped Gold Nanorods.Biomaterials 2014, 35, 8374−8384.

Atkinson, R. L.; Zhang, M.; Diagaradjane, P.; Peddibhotla, S.;Contreras, A.; Hilsenbeck, S. G.; Woodward, W. A.; Krishnan, S.;Chang, J. C.; Rosen, J. M. Thermal Enhancement with OpticallyActivated Gold Nanoshells Sensitizes Breast Cancer Stem Cells toRadiation Therapy. Sci. Transl. Med. 2010, 2, 55ra79.

Li, S. D.; Huang, L. Pharmacokinetics and Biodistribution ofNanoparticles. Mol. Pharmaceutics 2008, 5, 496−504.

Alric, C., Miladi, I., Kryza, D., Taleb, J., Lux, F., Bazzi, R., et al. (2013). Thebiodistribution of gold nanoparticles designed for renal clearance. Nanoscale.5, 5930–5939. doi: 10.1039/c3nr00012e

Balasubramanian, S. K., Jittiwat, J., Manikandan, J., Ong, C. N., Yu, L. E., andOng, W. Y. (2010). Biodistribution of gold nanoparticles and gene expressionchanges in the liver and spleen after intravenous administration in rats.Biomaterials 31, 2034–2042. doi: 10.1016/j.biomaterials.2009.11.079

Blanco, E., Shen, H., and Ferrari, M. (2015). Principles of nanoparticle design forovercoming biological barriers to drug delivery. Nat. Biotechnol. 33, 941–951.doi: 10.1038/nbt.3330

Sumbayev, V. V., Yasinska, I. M., Garcia, C. P., Gilliland, D., Lall, G. S.,Gibbs, B. F., et al. (2013). Gold nanoparticles downregulate interleukin-1betainducedpro-inflammatory responses. Small. 9, 472–477. doi: 10.1002/smll.
201201528

Tsai, C. Y., Lu, S. L., Hu, C. W., Yeh, C. S., Lee, G. B., and Lei, H. Y.(2012). Size-dependent attenuation of TLR9 signaling by gold nanoparticles inmacrophages. J. Immunol. 188, 68–76. doi: 10.4049/jimmunol.1100344

Yen, H. J., Hsu, S. H., and Tsai, C. L. (2009). Cytotoxicity and immunologicalresponse of gold and silver nanoparticles of different sizes. Small. 5, 1553–1561.doi: 10.1002/smll.200900126

Ernsting, M. J.; Murakami, M.; Roy, A.; Li, S. D. FactorsControlling the Pharmacokinetics, Biodistribution and IntratumoralPenetration of Nanoparticles. J. Controlled Release 2013, 172, 782−794.

Jain, R. K.; Stylianopoulos, T. Delivering Nanomedicine to SolidTumors. Nat. Rev. Clin. Oncol. 2010, 7, 653−664

Hillyer, J.; Albrecht, R. Gastrointestinal Persorption andTissue Distribution of Differently Sized Colloidal Gold Nanoparticles.J. Pharm. Sci. 2001, 90, 1927−1936.

Zhang, G.; Yang, Z.; Lu, W.; Zhang, R.; Huang, Q.; Tian, M.;Li, L.; Liang, D.; Li, C. Influence of Anchoring Ligands and ParticleSize on the Colloidal Stability and in Vivo Biodistribution ofPolyethylene Glycol-Coated Gold Nanoparticles in Tumor-XenograftedMice. Biomaterials 2009, 30, 1928−36.

Cho, W.-S.; Cho, M.; Jeong, J.; Choi, M.; Han, B. S.; Shin, H.-S.; Hong, J.; Chung, B. H.; Jeong, J.; Cho, M.-H. Size-DependentTissue Kinetics of Peg-Coated Gold Nanoparticles. Toxicol. Appl.Pharmacol. 2010, 245, 116−123.

Pan, Y.; Leifert, A.; Ruau, D.; Neuss, S.; Bornemann, J.;Schmid, G.; Brandau, W.; Simon, U.; Jahnen-Dechent, W. Gold
Nanoparticles of Diameter 1.4 Nm Trigger Necrosis by OxidativeStress and Mitochondrial Damage. Small 2009, 5, 2067−2076.

Coradeghini, R.; Gioria, S.; García, C. P.; Nativo, P.;Franchini, F.; Gilliland, D.; Ponti, J.; Rossi, F. Size-DependentToxicity and Cell Interaction Mechanisms of Gold Nanoparticles onMouse Fibroblasts. Toxicol. Lett. 2013, 217, 205−216.

Pattanayak, S.; Chakraborty, S.; Mollick, M. M. R.; Roy, I.;Basu, S.; Rana, D.; Gauri, S. S.; Chattopadhyay, D.; Chakraborty, MIn Situ Fluorescence of Lac Dye Stabilized Gold Nanoparticles; DNABinding Assay and Toxicity Study. New J. Chem. 2016, 40, 7121−7131.

Connor, E. E.; Mwamuka, J.; Gole, A.; Murphy, C. J.; Wyatt,M. D. Gold Nanoparticles Are Taken up by Human Cells but Do NotCause Acute Cytotoxicity. Small 2005, 1, 325−327.

Khan, J. A.; Pillai, B.; Das, T. K.; Singh, Y.; Maiti, S. MolecularEffects of Uptake of Gold Nanoparticles in Hela Cells. ChemBioChem2007, 8, 1237−1240.

Connor, E. E.; Mwamuka, J.; Gole, A.; Murphy, C. J.; Wyatt, M.D. Gold Nanoparticles are Taken Up by Human Cells but Do NotCause Acute Cytotoxicity. Small 2005, 1, 325−327.

Goodman, C. M.; McCusker, C. D.; Yilmaz, T.; Rotello, V. M.Toxicity of Gold Nanoparticles Functionalized with Cationic andAnionic Side Chains. Bioconjugate Chem. 2004, 15, 897−900.

Schaeublin, N. M.; Braydich-Stolle, L. K.; Schrand, A. M.;Miller, J. M.; Hutchison, J.; Schlager, J. J.; Hussain, S. M. SurfaceCharge of Gold Nanoparticles Mediates Mechanism of Toxicity.Nanoscale 2011, 3, 410−420.

Niidome, T.; Yamagata, M.; Okamoto, Y.; Akiyama, Y.;Takahashi, H.; Kawano, T.; Katayama, Y.; Niidome, Y. Peg-ModifiedGold Nanorods with a Stealth Character for in Vivo Applications. J.Controlled Release 2006, 114, 343−347.

Khlebtsov, N.; Dykman, L. Biodistribution and Toxicity ofEngineered Gold Nanoparticles: A Review of in Vitro and in VivoStudies. Chem. Soc. Rev. 2011, 40, 1647−71.

Zou, L.; Wang, H.; He, B.; Zeng, L.; Tan, T.; Cao, H.; He, X.;Zhang, Z.; Guo, S.; Li, Y. Current Approaches of PhotothermalTherapy in Treating Cancer Metastasis with Nanotherapeutics.Theranostics 2016, 6, 762−72.

Ali, M. R.; Ibrahim, I. M.; Ali, H. R.; Selim, S. A.; El-Sayed, M.A. Treatment of Natural Mammary Gland Tumors in Canines andFelines Using Gold Nanorods-Assisted Plasmonic PhotothermalTherapy to Induce Tumor Apoptosis. Int. J. Nanomed. 2016, 11,4849−4863.

Abdoon, A. S.; Al-Ashkar, E. A.; Kandil, O. M.; Shaban, A. M.;Khaled, H. M.; El Sayed, M. A.; El Shaer, M. M.; Shaalan, A. H.; Eisa,W. H.; Eldin, A. A.; et al. Efficacy and Toxicity of PlasmonicPhotothermal Therapy (Pptt) Using Gold Nanorods (Gnrs) AgainstMammary Tumors in Dogs and Cats. Nanomedicine 2016, 12, 2291−2297.

Schuh, E. M.; Portela, R.; Gardner, H. L.; Schoen, C.; London,C. A. Safety and Efficacy of Targeted Hyperthermia TreatmentUtilizing Gold Nanorod Therapy in Spontaneous Canine Neoplasia.BMC Vet. Res. 2017, 13, 294.

Kasani, Sujan & Curtin, Kathrine & Wu, Nianqiang. (2019). A review of 2D and 3D plasmonic nanostructure array patterns: fabrication, light management and sensing applications. Nanophotonics. 8. 10.1515/nanoph-2019-0158.

Kelly, K. Lance (December 21, 2002). "The Optical Properties of Metal Nanoparticles: The Influence of Size, Shape, and Dielectric Environment". The Journal of Physical Chemistry B. 107 (3): 668–677.

Burrows, N.D., Lin, W., Hinman, J.G., Dennison, J.M., Vartanian, A.M., Abadeer, N.S., Grzincic, E.M., Jacob, L.M., Li, J. and Murphy, C.J. Surface chemistry of gold nanorods. Langmuir, 2016, 32(39), pp.9905-9921. Doi: 10.1021/acs.langmuir.6b02706

Anderson ML, Morris CA, Stroud RM, Merzbacher CI, Rolison DR (1999-02-01). "Colloidal Gold Aerogels: Preparation, Properties, and Characterization". Langmuir. 15 (3): 674–681. doi:10.1021/la980784i

Link S, El-Sayed MA (1999-05-01). "Size and Temperature Dependence of the Plasmon Absorption of Colloidal Gold Nanoparticles". The Journal of Physical Chemistry B. 103 (21): 4212–4217. CiteSeerX 10.1.1.596.6328. doi:10.1021/jp984796o

Underwood S, Mulvaney P (1994-10-01). "Effect of the Solution Refractive Index on the Color of Gold Colloids". Langmuir. 10 (10): 3427–3430. doi:10.1021/la00022a011

Xing S, Tan LH, Yang M, Pan M, Lv Y, Tang Q, Yang Y, Chen H (2009-05-12). "Highly controlled core/shell structures: tunable conductive polymer shells on gold nanoparticles and nanochains". Journal of Materials Chemistry. 19 (20): 3286. doi:10.1039/b900993k

Ghosh SK, Pal T (November 2007). "Interparticle coupling effect on the surface plasmon resonance of gold nanoparticles: from theory to applications". Chemical Reviews. 107 (11): 4797–862. doi:10.1021/cr0680282

M. R. Ali, Y. Wu, M. A. El-Sayed, J. Phys. Chem. C 2019, 123, 15375;
Willets KA, Van Duyne RP. Localized surface plasmon resonance spectroscopy and sensing. Annu Rev Phys Chem 2007;58:267–97.

Kasani, Sujan, Curtin, Kathrine and Wu, Nianqiang. "A review of 2D and 3D plasmonic nanostructure array patterns: fabrication, light management and sensing applications" Nanophotonics, vol. 8, no. 12, 2019, pp. 2065-2089. https://doi.org/10.1515/nanoph-2019-0158

Powell CJ, Swan JB. Effect of oxidation on the characteristic loss spectra of aluminium and magnesium. Phys Rev 1960;118:640–3.

Guglielmelli, Alexa & Pierini, Filippo & Tabiryan, Nelson & Umeton, Cesare Paolo & Bunning, Timothy & De Sio, Luciano. (2021). Thermoplasmonics with Gold Nanoparticles: A New Weapon in Modern Optics and Biomedicine. Advanced Photonics Research. 2. 10.1002/adpr.202000198.

Anker JN, Hall WP, Lyandres O, Shah NC, Zhao J, Van Duyne RP. Biosensing with plasmonic nanosensors. Nat Mater 2008;7:442–53.

Mie G. Beitrge zur optik tr¨uber medien, speziell kolloidaler metal osungen. Annalen Der Physik 1908;330:377–445.

Gans R. Uber die Form ultramikroskopischer Goldteilchen. Ann Phys 1912;37:881–900.

B. Palpant, in Gold Nanoparticles For Physics, Chemistry And Biology, 2012, p. 75.

G. Baffou, in Thermoplasmonics: Heating Metal Nanoparticles Using Light, Cambridge University Press, Cambridge, UK 2017.

M. Kim, J. H. Lee, J. M. Nam, Adv. Sci. 2019, 6, 1900471.

CHAPTER 4 - An Approach to Oral Squamous Cell Plasmonic Photothermal Treatment A Review of Nine Indicative Studies

PAPER 1: Mahmoud Bawdy El badawy, A. A. A. M. S. ,Latifa M. A. . (2021). Phototherapy with Gold Nanoparticles and a Diode Laser for Oral Squamous Cell Carcinoma of the Tongue in Rats. Annals of the Romanian Society for Cell Biology, 25(6), 7570–7585. Retrieved from https://www.annalsofrscb.ro/index.php/journal/article/view/6905

PAPER 2: Yang, Zhijing & Liu, Da & Zhou, Hengzong & Tao, Boqiang & Chang, Lu & Liu, Huimin & Luo, Haoming & Wang, Dongxu & Liu, Weiwei. (2021). A New Nanomaterial Based on Extracellular Vesicles Containing Chrysin-Induced Cell Apoptosis Through Let-7a in Tongue Squamous Cell Carcinoma. Frontiers in Bioengineering and Biotechnology. 9. 766380. 10.3389/fbioe.2021.766380.

PAPER3 - El-Sherbiny, Randa & Hassan, Magda & El-Hossary, Wafaa & Saad, Mona. (2021). Combined Photothermal and Nanochemotherapy in Treatment of Induced Oral Squamous Cell Carcinoma in Hamsters. Dental Science Updates. 2. 77-88. 10.21608/dsu.2021.32548.1040.

PAPER 4- Zeng, Sujuan & Liu, Shiqi & Lan, Yintao & Qiu, Ting & Zhou, Mengyu & Gao, Weijian & Huang, Wenyan & Ge, Lihong & Zhang, Jian. (2021). Combined Photothermotherapy and Chemotherapy of Oral Squamous Cell Carcinoma Guided by Multifunctional Nanomaterials Enhanced Photoacoustic Tomography. International Journal of Nanomedicine. Volume 16. 7373-7390. 10.2147/IJN.S336788.

PAPER 5 - ZENG, Jun-jie & TANG, Zhan-gui & Zou, Jiao & Yu, Jin-Gang. (2021). Black phosphorous nanosheets–gold nanoparticles–cisplatin for photothermal/photodynamic treatment of oral squamous cell carcinoma. Transactions of Nonferrous Metals Society of China. 31. 2812-2822. 10.1016/S1003-6326(21)65695-9.

PAPER 6 - Sun, Qiang & Wu, Jinggen & Jin, Lulu & Hong, Liangjie & Wang, Fang & Mao, Zhengwei & Wu, Mengjie. (2020). Cancer cell membrane-coated gold nanorods for photothermal therapy and radiotherapy on oral squamous cancer. Journal of Materials Chemistry B. 8. 10.1039/D0TB01063D.

PAPER 7 - Mapanao, Ana & Santi, Melissa & Voliani, Valerio. (2020). Combined chemo-photothermal treatment of three-dimensional head and neck squamous cell carcinomas by gold nano-architectures. Journal of Colloid and Interface Science. 582. 10.1016/j.jcis.2020.08.059.

PAPER 8 - Liao, Yu-Te & Liu, Chia-Hung & Chin, Yin & Sin Yuan, Chen & Liu, Shing & Hsu, Yih-Chih & Wu, Kevin. (2019). Biocompatible and Multifunctional Gold Nanorods for Effective Photothermal Therapy of Oral Squamous Cell Carcinoma. Journal of Materials Chemistry B. 7. 10.1039/C9TB00574A.

PAPER 9 - Rao, Lang & Bu, Lin-Lin & Ma, Liang & Wang, Wenbiao & Liu, Huiqin & Wan, Da & Liu, Jian-Feng & Li, Andrew & Guo, Shi-Shang & Zhang, Lu & Zhang, Wen-Feng & Zhao, Xing-Zhong & Zhi, Sun & Liu, Wei. (2017). Platelet-Facilitated Photothermal Therapy of Head and Neck Squamous Cell Carcinoma. Angewandte Chemie International Edition. 57. 10.1002/anie.201709457.

Li, S.-p., Lin, Z.-x., Jiang, X.-y., and Yu, X.-y. (2018). Exosomal Cargo-Loading andSynthetic Exosome-Mimics as Potential Therapeutic Tools. Acta Pharmacol.Sin 39 (4), 542–551. doi:10.1038/aps.2017.178

Wu, J., Li, S., Jia, W., Deng, H., Chen, K., Zhu, L., et al. (2015). Reduced Let-7a IsAssociated with Chemoresistance in Primary Breast Cancer. Plos One 10 (7),e0133643. doi:10.1371/journal.pone.0133643

Zhong, X., Liu, D., Jiang, Z., Li, C., Chen, L., Xia, Y., et al. (2020). ChrysinInduced Cell Apoptosis and Inhibited Invasion through Regulation of TET1Expression in Gastric Cancer Cells. Ott Vol. 13, 3277–3287. doi:10.2147/OTT.S246031

Zhang H, Salo D, Kim DM, Komarov S, Tai Y, BerezinMY. Penetration depth of photons in biological tissues
from hyperspectral imaging in shortwave infrared in transmissionand reflection geometries. J Biomed Opt. 2016;
21: 126006-126016.

Mostofa AGM, Hossain K, Basak D, Bin Sayeed M.Thymoquinone as a potential adjuvant therapy for cancer
treatment: evidence from preclinical studies. FrontPharmacol. 2017; 8:295-307.

Goyal SN, Prajapati CP, Gore PR, Patil CR, Mahajan UB,Sharma C, Talla SP, Ojha SK.potential, and pharmaceutical development of thymoquinone: a multitargeted moleculeof natural origin. Front Pharmacol. 2017; 8:656- 875.

Schneider-Stock R, Fakhoury IH, Zaki AM, El-Baba CO,Gali-Muhtasib HU. Thymoquinone: Fifty years of success
in the battle against cancer models. Drug Discov Today.2014; 19: 18-30.

Silva A, Cardoso B, Silva M, Freitas R, Sousa R. Synthesis,characterization, and study of PLGA copolymer in vitro
degradation. J Biomater Nanobiotechnol. 2015; 6 :8-19.

Parker N, Turk MJ, Westrick E, Lewis JD, Low PS,Leamon CP. Folate receptor expression in carcinomas and
normal tissues determined by a quantitative radioligandbinding assay. Anal Biochem. 2005; 338: 284-293.

Fong YT, Chen CH, Chen JP. Intratumoral delivery of doxorubicin on folate-conjugated graphene oxide by in-situ forming thermo-sensitive hydrogel for breast cancer therapy. Nanomaterials. 2017;7(11). doi:10.3390/nano7110388

Ramasamy T, Ruttala HB, Sundaramoorthy P, et al. Multimodal selenium nanoshell-capped Au@mSiO2 nanoplatform for NIR-responsive chemo-photothermal therapy against metastatic breast cancer. NPG Asia Mater. 2018;10(4):197–216. doi:10.1038/ s41427-018-0034-5

Ramasamy T, Ruttala HB, Gupta B, et al. Smart chemistry-based nanosized drug delivery systems for systemic applications: a comprehensive review. J Control Release. 2017;258:226–253. doi:10.1016/j.jconrel.2017.04.043

KOTCHERLAKOTA R, SRINIVASAN D J, MUKHERJEES, HAROON M M, DAR G H, VENKATRAMAN U,PATRA C R, GOPAL V. Engineered fusion protein-loadedgold nanocarriers for targete co-delivery of doxorubicin anderbB2-siRNA in human epidermal growth factor receptor-2+ovarian cancer [J]. Journal of Materials Chemistry B, 2017,5(34): 7082−7098.

HIRAISHI Y, WADA T, NAKATANI K, TOJYO I,MATSUMOTO T, KIGA N, NEGORO K, FUJITA S. EGFRinhibitor enhances cisplatin sensitivity of oral squamous cellcarcinoma cell lines [J]. Pathology & Oncology Research,2008, 14(1): 39−43.

Z. W. Mao, R. Cartier, A. Hohl, M. Farinacci, A. Dorhoi,T. L. Nguyen, P. Mulvaney, J. Ralston, S. H. E. Kaufmann,
H. Mohwald and D. Y. Wang, Nano Lett., 2011, 11,2152–2156.

R. H. Fang, A. V. Kroll, W. W. Gao and L. F. Zhang, Adv.Mater., 2018, 30, 1706759.

P. Lv, X. Liu, X. M. Chen, C. Liu, Y. Zhang, C. C. Chu,J. Q. Wang, X. Y. Wang, X. Y. Chen and G. Liu, Nano Lett.,
2019, 19, 2993–3001.

D. Cassano, S. Pocoví-Martínez, V. Voliani, Ultrasmall-in-Nano Approach:Enabling the Translation of Metal Nanomaterials to Clinics, Bioconjug. Chem.29 (2018) 4–16, https://doi.org/10.1021/acs.bioconjchem.7b00664.

P. Armanetti, S. Pocoví-Martínez, A. Flori, C. Avigo, D. Cassano, L. Menichetti, V.Voliani, Dual photoacoustic/ultrasound multi-parametric imaging frompassion fruit-like nano-architectures, Nanomedicine Nanotechnology, Biol.Med. 14 (2018) 1787–1795, https://doi.org/10.1016/j.nano.2018.05.007.

N. R. Jana, L. Gearheart and C. J. Murphy, Adv. Mater., 2001,13, 1389–1393.

Y. Y. Yu, S. S. Chang, C. L. Lee and C. R. C. Wang, J. Phys.Chem. B, 1997, 101, 6661–6664.

Y. Qiu, Y. Liu, L. M. Wang, L. G. Xu, R. Bai, Y. L. Ji, X. C. Wu,Y. L. Zhao, Y. F. Li and C. Y. Chen, Biomaterials, 2010, 31,
7606–7619.

L. Zhao, Y. S. Wang, X. H. Zhao, Y. J. Deng, Q. Li andY. Z. Xia, Nanomaterials, 2018, 8, 507–519.

Y. T. Liao, K. C. W. Wu and J. S. Yu, J. Biomed. Mater. Res.,Part B, 2014, 102, 293–302.

M. R. K. Ali, S. R. Panikkanvalappil, M. A. El-Sayed, J. Am.Chem. Soc. 2014, 136, 4464.

G. V. R. Born, M. J. Cross, J. Physiol. 1963, 168, 178; b) C.Wang, W. Sun, Y. Ye, Q. Hu, H. N. Bomba, Z. Gu, Nat. Biomed.Eng. 2017, 1, 0011.

L. A. Harker, L. K. Roskos, N. M. Marzec, R. A. Carter, J. K.Cherry, B. Sundell, E. N. Cheung, D. Terry, W. Sheridan, Blood2000, 95, 2514.

Wu, J. The EnhancedPermeability and Retention (EPR)Effect: The Significance of theConcept and Methods to Enhance ItsApplication. J. Pers. Med. 2021, 11,771. https://doi.org/10.3390/jpm11080771

M. Labelle, S. Begum, R. O. Hynes, Proc. Natl. Acad. Sci.USA 2014, 111, E3053–E3061; b) G. F. Nash, L. F. Turner, M. F.
Scully, A. K. Kakkar, Lancet Oncol. 2002, 3, 425.

MARCAZZAN S, VARONI E M, BLANCO E, LODI G,FERRARI M. Nanomedicine, an emerging therapeuticstrategy for oral cancer therapy [J]. Oral Oncology, 2018, 76:
1−7.

Begg AC, Stewart FA, Vens C: Strategies to improve radio-therapy with targeted drugs. Nat Rev Cancer 2011; 11: 239-253.

Lusic H, Grinstaff MW. X-ray-computed tomography contrast agents.Chem Rev. 2013;113(3):1641–66.

Jelveh S, Chithrani DB. Gold nanostructures as a platform forcombinational therapy in future cancer therapeutics. Cancers.2011;3(1):1081–110.

ZHOU Wen-hua, PAN Ting, CUI Hao-dong, ZHAO Zhen,CHU P K, YU Xue-feng. Black phosphorus: Bioactive
nanomaterials with inherent and selective chemotherapeuticeffects [J]. Angewandte Chemie: International Edition, 2019,131(3): 779−784.

Figures References

CHAPTER 1

Figure 1: Sarah L. Cook, Stephanie P. Bull, Lisa Methven, Jane K. Parker, Vitaliy V. Khutoryanskiy, Mucoadhesion: A food perspective, Food Hydrocolloids, Volume 72, 2017, Pages 281-296, Mucoadhesion: A food perspective - Scientific Figure on

Figure 2: Skrypnikova, T.P. & Khmil, T.A. & Pysarenko, O.A. & Bieliaieva, O.M.. (2022). ON THE ISSUE OF CLINICAL CLASSIFICATION OF PRECANCEROUS CHANGES IN THE ORAL MUCOSA AND THE LIPS. Ukrainian Dental Almanac. 9-13. 10.31718/2409-0255.3.2022.02.

Figure 3: Edmans, Jake & Clitherow, Katharina & Murdoch, Craig & Hatton, Paul & Spain, Sebastian & Colley, Helen. (2020). Mucoadhesive Electrospun Fibre-Based Technologies for Oral Medicine. Pharmaceutics. 12. 504. 10.3390/pharmaceutics12060504..

CHAPTER 2

Figure 1: Tsuruoka, Shoko & Matsuo, Kou & Ishikawa, Ayataka & Yamamoto, Noriaki & Yamashita, Yoshihiro & Takahashi, Tetsu. (2011). Prognostic significance of CD44v3 and CD44v6 in oral squamous cell carcinoma of the tongue. Oral Medicine & Pathology. 15. 107-112. 10.3353/omp.15.107.

Figure 2: Goldoni, Riccardo & Scolaro, Alessandra & Boccalari, Elisa & Dolci, Carolina & Scarano, Antonio & Inchingolo, Francesco & Ravazzani, Paolo & Muti, Paola & Tartaglia, Gianluca. (2021). Malignancies and Biosensors: A Focus on Oral Cancer Detection through Salivary Biomarkers. Biosensors. 11. 396. 10.3390/bios11100396.

Figure 3: Chi, Jeffrey & Preeshagul, Isabel & Sheikh-Fayyaz, Silvat & Teckie, Sewit & Kohn, Nina & Ziemba, Yonah & Laser, Alice & Frank, Douglas & Ghaly, Maged & Kamdar, Dev & Kraus, Dennis & Paul, Doru & Seetharamu, Nagashree. (2020). Evaluating of HPV–DNA ISH as an adjunct to p16 testing in oropharyngeal cancer. Future Science OA. 6. FSO606. 10.2144/fsoa-2020-0052.

Figure 4: Shirani, Samaneh & Kargahi, Neda & Razavi, Mohammad & Homayoni, Solmaz. (2014). Epithelial Dysplasia in Oral Cavity. Iranian journal of medical sciences. 39. 406-17.

Figure 5: Miranda Galvis, Marisol & Faustino, Isabel & Ramos, Joab & Santos-Silva, Alan & Alves, Fabio & Kowalski, Luiz & Lopes, Marcio. (2020). Oral Cancer Adjacent to Dental Implants Mimicking Benign Lesions: A Case Series Study. Australian dental journal. 66. 10.1111/adj.12793.

Figure 6: Troeltzsch, Matthias & Knösel, Thomas & Eichinger, Christina & Probst, Florian & Troeltzsch, Markus & Woodlock, Timothy & Mast, Gerson & Ehrenfeld, Michael & Otto, Sven. (2014). Clinicopathologic Features of Oral Squamous Cell Carcinoma: Do They Vary in Different Age Groups?. Journal of Oral and Maxillofacial Surgery. 10.1016/j.joms.2014.01.009.

Figure 7: Peña, Daniel & Reyes, Montserrat & Hernández-Cáceres, María & Kretschmar, Catalina & Morselli, Eugenia & Ramirez-Sarmiento, Cesar & Lavandero, Sergio & Torres, Vicente & Criollo, Alfredo. (2020). Role of Autophagy in the Microenvironment of Oral Squamous Cell Carcinoma. Frontiers in Oncology. 10. 10.3389/fonc.2020.602661.

Figure 8: Pastore, Luca & Fiorella, Maria & Fiorella, Raffaele & Lo Muzio, Lorenzo. (2008). Multiple Masses on the Tongue of a Patient with Generalized Mucocutaneous Lesions. PLoS medicine. 5. e212. 10.1371/journal.pmed.0050212.

Figure 9: Elsholtz, Fabian & Ro, Sa-Ra & Shnayien, Seyd & Dinkelborg, Patrick & Hamm, Bernd & Schaafs, Lars-Arne. (2021). Impact of double reading on NI-RADS diagnostic accuracy in reporting oral squamous cell carcinoma surveillance imaging – a single-center study. Dentomaxillofacial Radiology. 51. 20210168. 10.1259/dmfr.20210168.

Figure 10: The Surveillance, Epidemiology, and End Results (SEER) Program of the National Cancer Institute (NCI) 2022, https://seer.cancer.gov/

CHAPTER 3

Figure 1: Tsoucalas, Gregory & Karamanou, Marianna & Michaleas, Spyros & Laios, Konstantinos & Androutsos, George. (2020). Arsenic powder in the treatment of cancer: the invention of French physician Pierre Alliot (1610-1685). Journal of B.U.ON.: official journal of the Balkan Union of Oncology. 24. 2583-2588.

Figure 2: Kolovskaya, Olga & Zamay, Tatiana & Belyanina, Irina & Karlova, Elena & Garanzha, Irina & Aleksandrovsky, Aleksandr & Kirichenko, Andrey & Anna, Dubynina & Sokolov, Alexey & Zamay, Galina & Glazyrin, Yury & Zamay, Sergey & Ivanchenko, Tatiana & Chanchikova, Natalia & Tokarev, Nikolay & Shepelivich, Nikolay & Ozerskaya, Anastasia & Badrin, Evgeniy & Belugin, Kirill & Zamay, Anna. (2017). Aptamer-Targeted Plasmonic Photothermal Therapy of Cancer. Molecular Therapy - Nucleic Acids. 9. 10.1016/j.omtn.2017.08.007.

Figure 3: Härkönen, Antti & Rautiainen, Jussi & Guina, Mircea & Konttinen, Janne & Tuomisto, Pietari & Orsila, Lasse & Pessa, Markus & Okhotnikov, Oleg. (2007). High power frequency doubled GaInNAs semiconductor disk laser emitting at 615 nm. Optics express. 15. 3224-9. 10.1364/OE.15.003224.

Figure 4: Yokomizo, Shinya & Katagiri, Wataru & Maki, Yohei & Sano, Tomoya & Inoue, Kazumasa & Fukushi, Masahiro & Atochin, Dmitriy & Kushibiki, Toshihiro & Kawana, Akihiko & Kimizuka, Yoshifumi & Kashiwagi, Satoshi. (2021). Brief exposure of skin to near-infrared laser augments early vaccine responses. Nanophotonics. 10. 000010151520210133. 10.1515/nanoph-2021-0133.

Figure 5: Han, Hwa Seung & Choi, Ki Young. (2021). Advances in Nanomaterial-Mediated Photothermal Cancer Therapies: Toward Clinical Applications. Biomedicines. 9. 305. 10.3390/biomedicines9030305.

Figure 6: Nadeem, Muhammad & Abbasi, Bilal & Younas, Muhammad & Ahmad, Waqar & Khan, Taimoor. (2017). A review of the green syntheses and anti-microbial applications of gold nanoparticles. Green Chemistry Letters and Reviews. 10. 216-227. 10.1080/17518253.2017.1349192.

Figure 7: Sriram, Manish & Zong, Kelly & Vivekchand, S & Gooding, J. (2015). Single Nanoparticle Plasmonic Sensors. Sensors (Basel, Switzerland). 15. 25774-25792. 10.3390/s151025774.

Figure 8: Freitas de Freitas L, Varca GHC, Dos Santos Batista JG, Benévolo Lugão A. An Overview of the Synthesis of Gold Nanoparticles Using Radiation Technologies. Nanomaterials. 2018; 8(11):939. https://doi.org/10.3390/nano8110939

Figure 9: Abdul Rani, Abdul Ismail & Mohamad, Khairul & Ghosh, Bablu & Chee, Fuei pien & Saad, Ismail & Ibrahim, Pungut & Alias, Afishah. (2019). CURRENT ADVANCES IN MICRODEVICES AND NANOTECHNOLOGY.

Figure 10: Huang, Xiaohua & El-Sayed, Mostafa. (2011). Plasmonic photo-thermal therapy (PPTT). Alexandria Journal of Medicine. 47. 1–9. 10.1016/j.ajme.2011.01.001.

Figure 11: Zhang, Yujuan & Zhan, Xuelin & Xiong, Juan & Peng, Shanshan & Huang, Wei & Joshi, Rakesh & Cai, Ying & Liu, Yanling & Li, Rong & Yuan, Keng & Zhou, Nanjin & Min, Weiping. (2018). Temperature-dependent cell death patterns induced by functionalized gold nanoparticle photothermal therapy in melanoma cells. Scientific Reports. 8. 10.1038/s41598-018-26978-1.

Figure 12: Thomas, Oliver & Weber, Wilfried. (2019). Overcoming Physiological Barriers to Nanoparticle Delivery—Are We There Yet?. Frontiers in Bioengineering and Biotechnology. 7. 415. 10.3389/fbioe.2019.00415.

Figure 13: Schwartz, Jon & Shetty, Anil & Price, Roger & Stafford, R. Jason & Wang, James & Uthamanthil, Rajesh & Pham, Kevin & McNichols, Roger & Coleman, Chris & Payne, J. (2009). Feasibility Study of Particle-Assisted Laser Ablation of Brain Tumors in Orthotopic Canine Model. Cancer research. 69. 1659-67. 10.1158/0008-5472.CAN-08-2535.